SURFACE TO SUBSURFACE CORRELATION OF NATURAL FRACTURES IN PALEOZOIC ROCKS IN SELECTED AREAS OF CENTRAL AND NORTH-CENTRAL TEXAS

By

MATTHEW RUSSELL GARRISON

Bachelor of Science, Geology

Texas A & M University

College Station, Texas

2005

Submitted to the Faculty of the
Graduate College of the
Oklahoma State University
in partial fulfillment of
the requirements for
the Degree of
MASTER OF SCIENCE
May, 2007

SURFACE TO SUBSURFACE CORRELATION OF NATURAL FRACTURES IN PALEOZOIC ROCKS IN SELECTED AREAS OF CENTRAL AND NORTH-CENTRAL TEXAS

Thesis Approved:

Dr. Ibrahim Cemen
Thesis Adviser

Dr. Surinder Sahai

Dr. Jim Puckette

Dr. A. Gordon Emslie
Dean of the Graduate College

AKNOWLEDGEMENTS

Many people were instrumental in the successful completion of this thesis; without their support, this thesis may never have been completed. First and foremost, I would like to thank my committee chair, Dr. Ibrahim Cemen. His work ethic and dedication to his job as well as the people around him have taught me many valuable life lessons that I will always remember. I wish to thank my other committee members, Dr. Jim Puckette, for always being their to lend an ear and offer invaluable advice and Dr. Surinder Sahai, who always kept an open door policy and was willing to help in any way he could.

I would also like to thank EOG Resources, Inc. for funding this project and providing the well data necessary for the subsurface correlation. Specifically, I would like to thank David Trice, Exploration Manager of the Fort Worth Division and Bill Thomas, Executive Vice President and General Manager of the Fort Worth Division. Also from EOG Resources, I would like to thank Mike Cooksey, who wished simply to be addressed as "Cooker - The Drafting God," for scanning in the geologic maps which were used in portions of this research.

Bo Henk, Chief Geologist at Matador Resources and adjunct professor at Texas Christian University in Fort Worth, Texas graciously volunteered his time to seek out the localities studied in this thesis. I am also grateful for his expertise that he offered in the early stages of writing this thesis. I would like to thank him personally for always taking

time to give back to the science, which has given so much to us.

From Oklahoma State University, I would like to offer my sincere thanks to Dr. Anna Cruse who became a wonderful friend in the last year of my stay at the university. Her willingness to help any time the situation warranted it was greatly appreciated, even if all she could do was simply lend an ear. Additionally, I would like to thank Sandy Earls - who works harder then most to facilitate the day-to-day life within this department. Without her selfless hard work and dedication to the students and her job, little if any would ever get accomplished. Thank you, Sandy. Also, I would like to thank my colleague John Tackett, who saved me from endless hours of digitizing my geologic maps by showing me the beautiful simplicity of GIS. John's seemingly endless patience and understanding was much appreciated in the final days and hours before the deadline of this thesis. I am grateful to Onur Ataman, another graduate colleague, who spent an entire week in the field with me during the data collection phase of this thesis. Although there were times when Onur may not have understood the words I was trying to say, no translation is needed when describing *"friend."*

To the land owners of the localities studied in this thesis, in particular, Mr. and Mrs. Richard Archer and Ms. Laura White, thank you for allowing me to access the rocks on your land. Your kindness was greatly appreciated and essential to the overall picture of this thesis.

Special thanks are extended to my friends Lance Murphy and Daniel (Danny) Ramirez. Thanks for always being there to offer encouragement and support. Thanks for always reminding me to remain focused on the end result: a life outside of academia.

I would like to thank my parents Robert and Loretta Garrison, and my sister Katy.

Thank you for never allowing me to accept less then my personal best, and always being there for me in the good times...and the bad. Finally, thank you for never missing an important event in my life and for teaching all of life's lessons to me - even though I may have had to sit through some lessons more then once.

Last but not least, I would like to thank my loving wife Ashley for her endless love and dedication to our relationship. Success in graduate school would not have been possible for me if there was not support at home. She labored for hours over the formatting of this thesis so that it would meet the standards of the Graduate College. Thank you for putting up with the misfortune of being the wife of a geology graduate student.

This thesis is dedicated to my family.

Without you, none of this would be possible.

"From knowledge acquired by personal initiative, arises the desire for more knowledge."

E.O. Wilson

TABLE OF CONTENTS

LIST OF TABLES

LIST OF FIGURES

Figure ..... Page

Figure ..... Page

LIST OF PLATES

CHAPTER I

INTRODUCTION

Statement of Purpose

The Fort Worth basin in north-central Texas contains one of the largest natural gas producing fields in North America. This basin is one of several foreland basins formed during the Ouachita Orogeny. In recent years, gas production within the basin has been coming from the Mississippian age Barnett Shale. Natural fractures play a vital role in the movement of fluids such as oil and gas, and are also a critical controlling factor in the adequate distribution of hydraulic fracture treatments when completing horizontal wells. It is for these reasons that research into the complexity of these fracture systems, by observing them in surface exposures, would be beneficial.

Few outcrops of the Barnett Shale exist in Texas, and those that do are poorly preserved. A detailed fracture analysis leading to the correct interpretation of fracture orientations cannot be conducted on Barnett outcrops. Fractures are preserved in subsurface sections of the Barnett, and are imaged on Formation Micro Imaging (FMI) logs in the Barnett Shale within the basin. However, Paleozoic limestone units exist across large areas in north-central and central Texas. These limestone units are better preserved in outcrop because limestone tends to be more resistant to weathering in the arid and semi-arid climate conditions of Texas. The tectonic forces that created the fracture systems within the Barnett also affected underlying older units, such as

the Honeycut (Lower Ordovician), and overlying Marble Falls (Lower Pennsylvanian) and Winchell (Upper Pennsylvanian) limestone units (Figure 1). It is hypothesized that these limestone units should display fracture patterns that are similar to fracture patterns preserved in subsurface sections of the Barnett Shale.

This thesis also demonstrates that the proximity to major geologic structures such as the Llano Uplift, as well as minor structures such as local faults or folds can have a dramatic effect on the orientations of fracture sets. In addition, this thesis seeks to prove that lithology of a particular rock unit can effect fracture intensity, as well as fracture orientation.

Finally, this study will attempt to correlate the fractures observed in outcrop to fracture patterns observed in wells that were logged horizontally with FMI logs. Log datasets for two wells with FMIs were donated by EOG Resources, Inc. for the correlation. One set is from a well in Palo Pinto County, the second is for a well drilled in Erath County.

This surface to subsurface correlation, which is not believed to have been documented in any other publication, will help in understanding the complexity and regional extent of fracture systems formed by the Ouachita Orogeny, as well as those that formed as a result of the opening of the Gulf of Mexico.

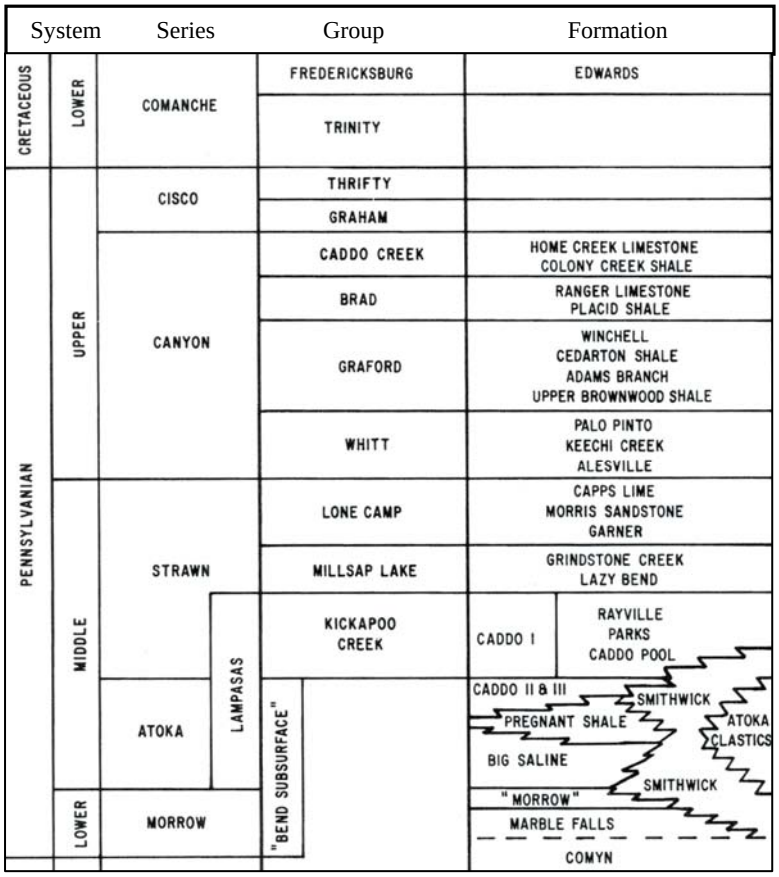

Figure 1: Generalized stratigraphic nomenclature of north-central and central Texas. Modified from Flippin (1982)

Study Area

Four localities (Figure 2) were chosen to constrain how fracture orientations would be affected by proximity to geologic structures such as the Llano Uplift, the Bend Arch, the Lampasas Arch, and the Southern Oklahoma Aulacogen. These geologic structures create stress fields proximal to them that are different from the regional stress field resulting from events such as the Ouachita Orogeny.

The first locality is Possum Kingdom Lake, located in Palo Pinto County. This location was chosen to investigate the effect of tectonic forces acting on the western edge of the Fort Worth Basin. The Winchell Limestone crops out along the shoreline of Possum Kingdom Lake, and provided adequate exposures for measuring fractures.

The second location chosen is the Lake Brownwood spillway, 7.5 miles north of the town of Brownwood, Texas. Deformation at this outcrop should reflect the effects of tectonic forces felt within the foreland of the Ouachita orogenic belt, but outside of the foreland basin. This location was affected by its proximity to the Bend Arch, and the removal of overburden during the construction of the spillway, providing a test of the influences of local stresses. The Winchell limestone is exposed throughout the spillway and there were adequate exposures for fracture analysis.

The Bend River locality is located on the northern rim of the Llano Uplift, located along the Colorado River, 0.7 miles southwest of the town of Bend, Texas. This locality was chosen to determine the effect of the Llano Uplift on fracture orientation. The core of the Llano Uplift consists entirely of pre-Cambrian basement rock. During the orogeny, the uplift acted as a stable buttress, creating an entirely different stress field proximal to it. At this locality, the boundary between the Marble

Falls Limestone and the Smithwick Shale is present. The Marble Falls and a lower carbonate member of the Smithwick contained fractures adequate for measurement.

The fourth locality is the Archer Ranch, located on the southeastern edge of the Llano Uplift; 4.3 miles east of the town of Johnson City, Texas. This locality was chosen for its unique location because it offered an opportunity to demonstrate how fracture orientations may have change as the Ouachita thrust belt wrapped around the uplift. The Honeycut, Stribling, and Marble Falls formations are present at this locality, with the Honeycut and Marble Falls limestone units containing fractures adequate for measurement.

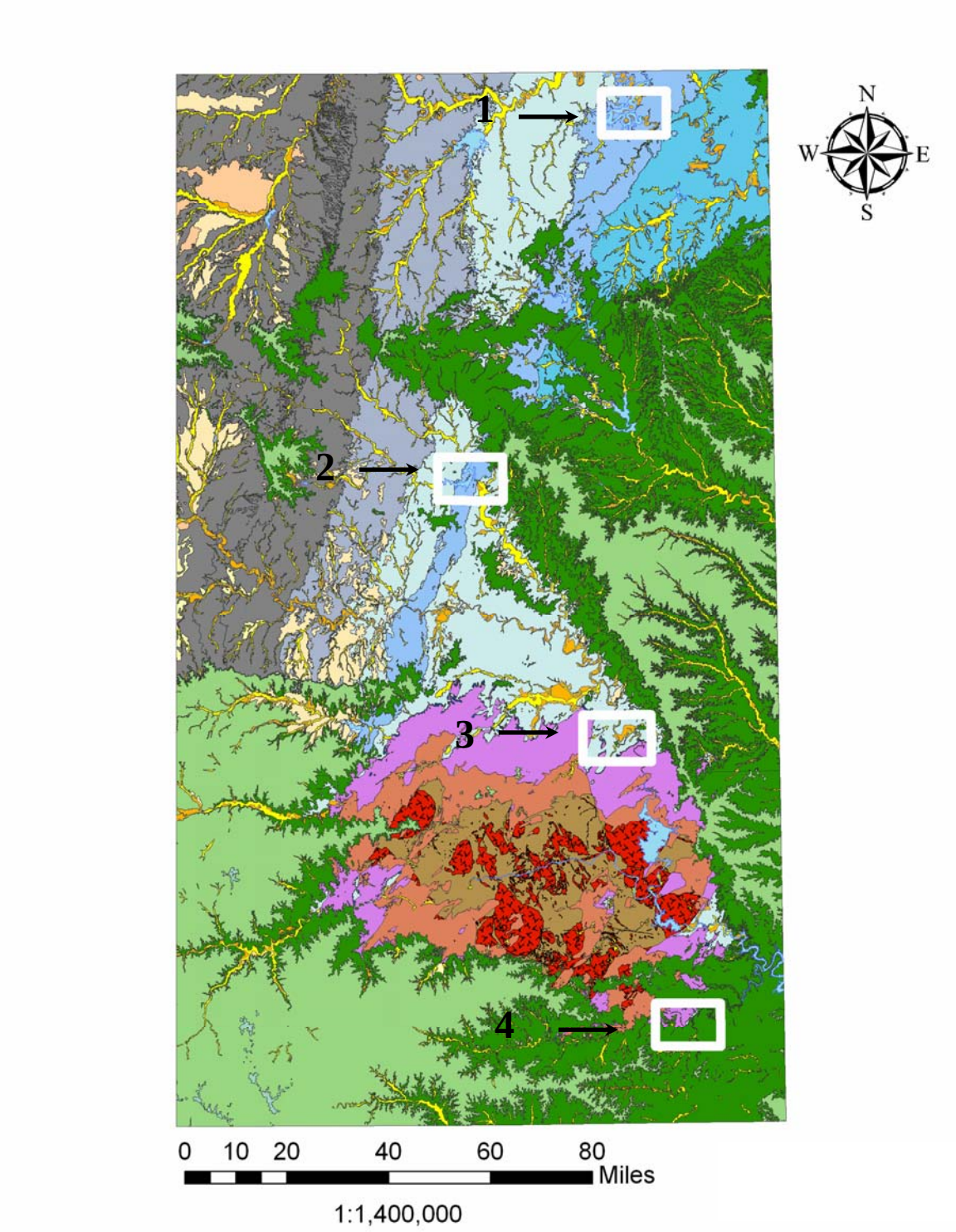

Figure 2: The location of the study area within central and north-central Texas. Individual localities chosen for measurement are highlighted in white boxes: (1) Possum Kingdom; (2) Brownwood Spillway; (3) Bend River; (4) Archer Ranch. Map digitized after Renfro et al. (1979).

Methodology

The geology of each locality was described using a combination of published literature and visual examination of the outcrops. Hand-held GPS units, geologic maps made by the Texas Bureau of Economic Geology, and United States Geological Survey (USGS) topographic sheets were utilized in determining the exact position for each locality. Fracture orientations were measured using a Brunton transit, along scanlines, which were oriented perpendicular to the strike of the fracture sets. Fractures were described based on the presence or absence of mineral fill, crosscutting relationships, plumose markings, strike, and dip. Data collected was compiled and displayed in rose diagrams created using Rock Works ® software package. Maps were digitized using ArcGIS. The geologic maps of Texas were purchased through the Texas Natural Resources Information System (TNRIS) and were based on the original 1:250,000 Geologic Atlas of Texas published by the Texas Bureau of Economic Geology.

FMI logs are used by geologists in industry to determine basic properties of the rock by displaying a resistivity image of the inside of the borehole wall. Fracture intensities are measured by counting the number of fractures seen per unit length of the wellbore. Orientations, strike, dip, and mineral fill of fractures are measured by service companies using proprietary software.

Implications of Research

Understanding unconventional reservoirs such as the Barnett Shale, which need hydraulic fracture treatments to release hydrocarbons, is a primary task confronting the next generation of petroleum geologists. A solid understanding of the natural fracture systems is essential for successful completion and production in the Barnett Shale, as well as other unconventional plays.

FMI logs provide information about the strike, dip, and intensity of fractures, but cannot provide information as to the behavior of fractures beyond the borehole wall. Analysis of surface exposures will increase knowledge of the behavior of fractures over great distances, and will show the crosscutting relationships between fractures that are not adequately described from analysis of FMI logs.

This thesis concentrates on fracture systems in Paleozoic limestones and shales across several counties in north-central and central Texas. This work will provide a basic understanding of the genesis of natural fractures caused by tectonic forces (both compressional and extensional). Fractures behavior and interactions seen in the surface, will be used as an analogue to predict fracture behavior in the subsurface.

CHAPTER II

REVIEW OF LITERATURE

Origin of Fractures in Rock

The term 'fracture' is used to describe a surface in a material, across which there has been a loss of continuity and, therefore, strength (Van Der Pluijm and Marshak, 2004). This definition applies to surfaces ranging in size from the molecular level to tens of kilometers. A joint is a planar, tensile opening-mode fracture with little or no displacement parallel to the fracture plane (Narr and Suppe, 1991). In sedimentary rocks, joints are generally perpendicular to bedding and occur in conjunction with parallel fractures, forming a joint set (Narr and Suppe, 1991).

Fractures are the product of brittle deformation, which occurs when stress exerted on a rock body exceeds the strength of molecular bonds within rock minerals. Brittle deformation only occurs when stresses exceed a critical point of elasticity, and thus only after a rock has already undergone some elastic and/or plastic strain (Van Der Pluijm and Marshak, 2004). Stress imposed on a rock can be initiated by any number of mechanisms, including: compressional forces, extensional forces, tensile forces, desiccation cracking, and shear forces.

Fractures record the orientations of regional and local tectonic forces at the time of formation (Nelson, 2001). In many cases, fractures have similar orientations to large-scale tectonic features, such as faults. This relationship is due to the fact that

the same stresses that caused the fracturing also caused the through-going faults. The fracture swarms, when they exist, predate the through-going fault and acts as a process zone conditioning the rock mass for the eventual fault offset (Nelson, 2001). Several authors have demonstrated this fault-fracture relationship: Stearns (1964), Yamaguchi (1965), Norris (1966), Stearns (1968a, 1968b, 1972), Skehan (1968), Friedman (1969, 1975), Tchalenko and Ambraseys (1970), Stearns and Friedman (1972), and Freund (1974).

Fractures begin where there is a flaw in the rock, such as open pores, preexisting microcracks, irregularities on a bedding plane, inclusions (pebble, fossil, or concretion), or primary sedimentary structures, such as sole marks or ripples. Once a fracture initiates, its growth is subject to the three principal stresses (σ_1, σ_2, σ_3), which act on the rock at the time of deformation. Three configurations of fracture growth in response to principal stresses are: Mode I, Mode II, and Mode III displacement (Figure 3).

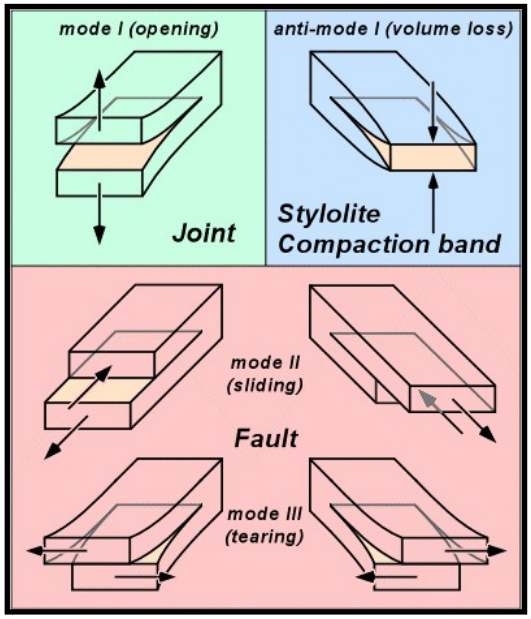

Figure 3: Diagram depicting fractures caused by Modes I, II, and III displacements, from (Lacazette, A., 2001).

During Mode I opening, a crack opens perpendicular to the fracture surface. These fractures are often called tensile fractures, or joints. They form parallel to the principal plane of stress that contains the σ_1 and σ_2 directions (i.e., perpendicular to σ_3), and can grow without changing orientation (Van Der Pluijm and Marshak, 2004). Pollard and Aydin (1988) suggest that the term "joint" be restricted to those sets of fractures with field evidence for dominantly opening mode displacements.

In Mode II displacement, rock on one side of the fracture surface moves slightly in the direction parallel to the fracture surface; perpendicular to the fracture front. This displacement resembles strike slip motion in faults, and these are often termed 'sliding-mode' fractures (Van Der Pluijm and Marshak, 2004). In Mode III displacement, rock on one side of the fracture moves parallel to the fracture surface,

in a direction parallel to the fracture front (Van Der Pluijm and Marshak, 2004). This movement is described as a tearing motion acrss the fracture surface.

Fracture Arrays

Systematic joints are planar joints that comprise a family in which all the joints are parallel or subparallel to one another, and maintain roughly the same average spacing over the region of observation (Van Der Pluijm and Marshak, 2004). Nonsystematic joints have an irregular spatial distribution, do not parallel neighboring joints, and tend to be nonplanar (Van Der Pluijm and Marshak, 2004). Non-systematic joints may terminate at other joints (Figure 4).

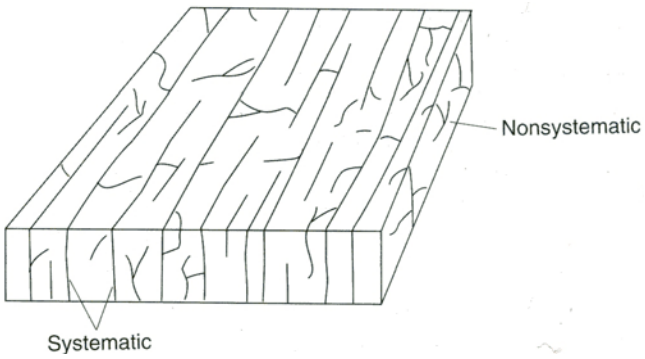

Figure 4: Systematic and Nonsystematic jointing patterns, taken from Van Der Pluijm and Marshak (2004).

A joint set is defined as a group of systematic joints. Two or more joint sets that intersect at fairly constant angles comprise a joint system, and the angle between two joint sets in a joint system is the dihedral angle (Van Der Pluijm and Marshak, 2004). If the two systems in a set are mutually perpendicular (~90^o) they are called orthogonal fracture sets. If the two systems in a set intersect at angles approximately 30^o or 45^o they are called conjugate fracture sets. The terms orthogonal and conjugate denote geometry of the fracture sets, and not the mode or timing (Van Der Pluijm and Marshak, 2004).

Cross-Cutting Relationships Between Fracture Sets

The relative ages of two sets of nonparallel joints can be determined by studying the manner in which they interact on the outcrop. For example, if joint B terminates at its intersection with joint A, then joint B is younger, because a propagating fracture cannot cross a free surface (Figure 5; Van Der Pluijm and Marshak, 2004).

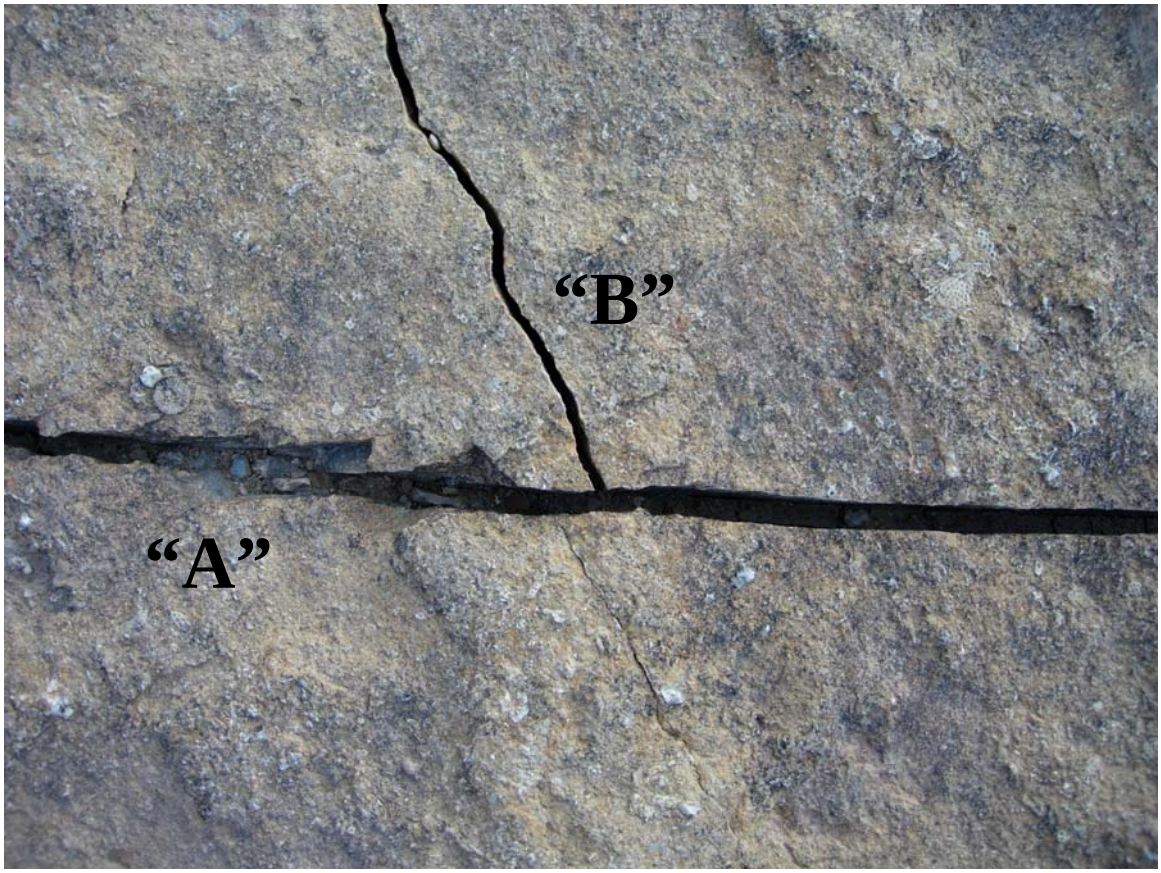

Figure 5: An example of crosscutting relationships when one fracture acts as a free surface

However, this relationship is not always easy to establish, because a younger joint’s orientation can also change if it approaches an older joint that behaves like a

free surface. The stress field associated with a pre-existing joint can affect the growth of neighboring joints, especially if the distance between them is small with respect to their lengths (Pollard et al., 1982). Pollard and Segall (1987) call the zone surrounding a joint the 'exclusion' zone. The distance to which stress relief (or stress perturbation) extends from a joint is also termed its 'mechanical interaction distance' (Olson, 2004). Pre-existing joints will perturb the stress field, thereby mechanically influencing any new joints, enhancing or hindering propagation as well as modifying the opening distribution (Pollard et al. 1982, Olson and Pollard, 1989, 1991).

This influence arises because at, or near a free surface, a Mode I fracture must be either parallel or perpendicular to the surface so as to maintain perpendicularity to σ_3 (Van Der Pluijm and Marshak, 2004). Near a free surface, the local stress field differs from the remote stress field. If an older joint "A" acts as a free surface, then the younger joint "B" will curve in the vicinity of joint A to become parallel with the local principal plane of stress adjacent to joint "A" (Van Der Pluijm and Marshak, 2004). The curvature of the younger joint depends on the remote stress field (Van Der Pluijm and Marshak, 2004). If the local σ_3 adjacent to the older joint is parallel to the walls of the older joint, then the younger joint curves in such a manner to intersect the first joint at nearly 90^o. This relationship is called hooking or a J junction (Figure 6).

Figure 6: An example of a J-Junction, where a younger joint curves into the older joint acting as a free surface. Picture from the Bend River locality.

A third crosscutting relationship between joints in outcrops occurs when two nonparallel joints appear to be mutually cross cutting. In this case, it is extremely difficult to confidently distinguish the relative ages of the fractures. This relationship arises in one of three ways (Van Der Pluijm and Marshak, 2004). First, the earlier joint did not act as a free surface, which can occur when joints are filled, or whose faces are tightly held together by stress. Second, the intersection of two younger joints at the same point on an older joint is simply coincidental. Finally, the crosscutting relationship can be an illusion, whereby within the body of the outcrop,

the older joint terminated, and the younger joint simply grew around it (Van Der Pluijm and Marshak, 2004).

Fracture Spacing in Sedimentary Rocks

Fracture spacing is the average distance between adjacent members of a joint set, measured perpendicular to the surface of the joints. Many factors affect fracture intensity, such as lithology, bed thickness, porosity, grain size, and structural position. Variations in one or more of these factors can cause fractures within the same unit to be either “closely spaced” or “widely spaced,” referring to high and low fracture intensities, respectively.

The percentage of brittle or ductile minerals in the rock matrix can dramatically affect fracture intensity (Figure 7). Rocks with higher fracture intensities have higher percentages of brittle minerals such as: quartz, feldspar, dolomite, and sometimes calcite. Rocks with similar brittle mineral composition, but higher clay content will be more ductile. This means they can absorb higher levels of stress, yielding a lower fracture intensity

Figure 7: Mechanical stratigraphy caused by a change in lithologic components

The thickness and porosity of a particular rock unit can also affect fracture intensity. If all other rock parameters and loading conditions are equal, thinner beds will fracture at a closer spacing than thicker beds (Nelson, 2001). Rock strength also decreases with increasing porosity, although the relationship is not linear (Nelson, 2001). Generally speaking, in rocks of similar composition and fabric, a lower porosity will lead to closer-spaced, more numerous fractures than those with higher porosity (Nelson, 2001).

No quantitative relationship has been documented showing the effect of grain size on fracture spacing (Nelson, 2001). In well-sorted clastic rocks, decreasing grain size increases compressive and tensile strength of the rock (Gallagher, 1976; Ramez and Mosalamy, 1969); this would lead to a higher fracture density. This increase in strength is apparently due to an increase in specific surface energy (a surface-to-volume function) as the grain diameter becomes smaller (Brace, 1961). However, the relationship between grain size and fracture intensity is not easy to quantify because intervals that are fine grained are typically also thinner than coarse-grained intervals (Nelson, 2001).

The effect of structural positioning also affects fracture spacing. Rocks exhibit increased fracture intensity with increased strain (Nelson, 2001). Price (1966) concluded that a rock with relatively high-calculated strain energy would have more frequent fractures than a rock of equal thickness with relatively low calculated strain energy.

Fractures Related to Regional Deformation

During a collisional orogenic event, compressive tectonic stress may affect rocks over a broad region, including the continental interior (Van Der Pluijm and Marshak, 2004). Nelson (2001) defines regional fractures as those that exhibit relatively little change in orientation, show no evidence of offset across the fracture plane, are perpendicular to major bedding surfaces, and typically will have variations in orientation of $15^{o} – 20^{o}$ over ~80-100 miles.

Joints from natural hydrofracturing often form on the foreland margins of orogens during orogeny (Van Der Pluijm and Marshak, 2004). It is believed that fluid movement within the rock occurs syntectonically with the orogenic event. Joints in the foreland of thrust belts typically contain mineral fill, which is believed to have formed at temperatures and fluid pressures found at a depth of several kilometers; and thus, they are not a consequence of the recent cracking of rocks in the near surface (Van Der Pluijm and Marshak, 2004). During an orogenic event, the maximum horizontal stress is approximately perpendicular to the trend of the orogen, and as a result, joints that form by syntectonic hydrofracturing strike perpendicular to the trend of the orogen (Van Der Pluijm and Marshak, 2004). Secondary sets of joints with different orientations can be related to the same orogenic event because the stress state may change over the course of the orogenic event. These secondary fracture sets may not be oriented perpendicular to the first fracture set, or to local structures formed by the initial stress state of the orogen (Van Der Pluijm and Marshak, 2004).

CHAPTER III

GEOLOGIC SETTING

The Ouachita Orogeny

The Ouachita Orogeny began in the early-mid Pennsylvanian, as the North American craton collided with South America and Africa during the closing of the Iapetus Ocean, and subsequent formation of Pangaea. Surface representations of this major collisional event are scarce and limited to southeastern Oklahoma and west Texas. Most geologic evidence lies in the subsurface as part of the Ouachita fold-thrust belt. The belt is approximately 2100 km, extending from the subsurface of Mississippi to the Marathon region of Texas, and is mostly buried beneath the Mesozoic and Tertiary sediments composing the Gulf Coastal Plain (Figure 8; Viele, 1989)

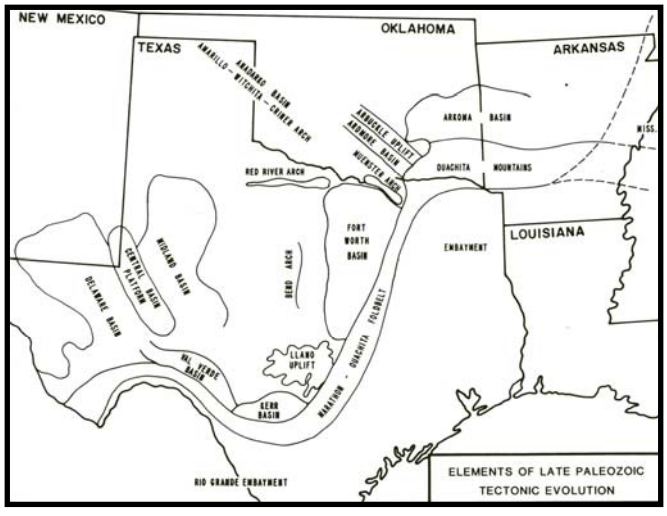

Figure 8: Map showing structural features associated with the Ouachita Orogeny. From Walper (1982)

In the mid Pre-Cambrian, the opening of the Iapetus Ocean separated Laurentia from Gondwana and Baltica (Figure 9). The southern margin of North America was a passive margin during the early Paleozoic time. Two aulacogens were critical in the geologic development of this area: the Southern Oklahoma aulacogen, and the Reelfoot aulacogen beneath the Mississippi embayment. These aulacogens were active in the mid Cambrian, and were re-activated in the Pennsylvanian due to compression that resulted in a series of uplifts along the border between Texas and Oklahoma.

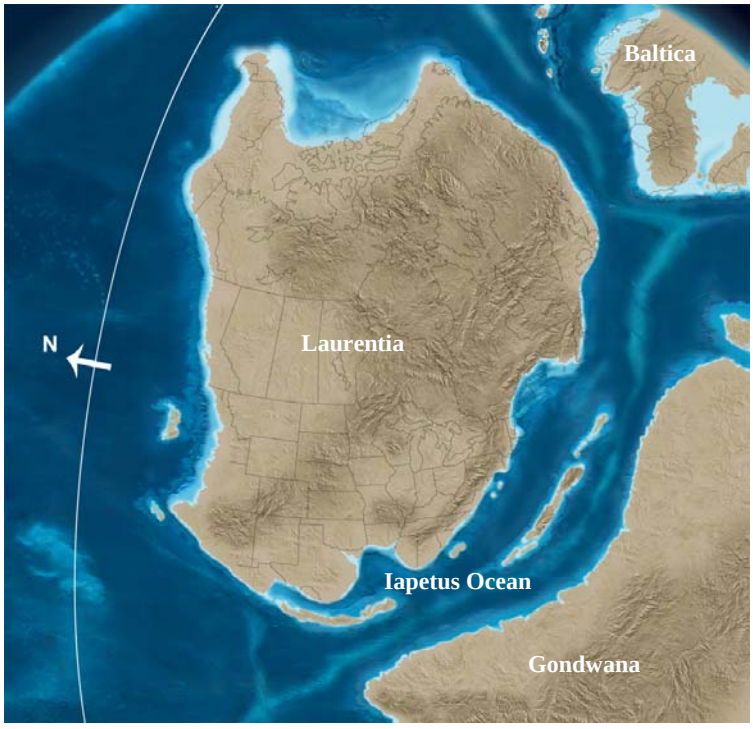

Figure 9: Mid Pre-Cambrian opening of the Iapetus ocean and separation of Laurentia from Gondwana and Baltica modified from Blakey, 2006

Within the Ouachita embayment, located between the Southern Oklahoma and Reelfoot aulacogens, deep-water sediments were deposited from the Late Cambrian through the Ordovician. The aulacogens existed as topographically low coastal re-

entrants by the time of the collision. Active river systems flowed into these low features, and drained into the Iapetus ocean basin. Consequently, the mouths of these aulacogens are sources of large deltaic packages (Walper, 1982)

The passive margin setting prevailed until the late Ordovician, when it changed from a passive to an active margin as the Iapetus Ocean closed (Walper and Miller, 1985). The North American craton was subducted beneath an off-shore island arc and the accreted wedge of the subduction complex created slope-rise deposits along the shelf margin. These deposits were structurally imbricated and thrust over the coeval shelf carbonates on the continental margin (Walper & Miller, 1985). The orogeny ended diachronously in the Late Pennsylvanian in the Ouachita Mountains, Early Permian in the Marathon region, and Late Permian in Sonora, indicating an oblique convergence of Gondwana with Laurentia (Figure 10; Poole et al., 2005).

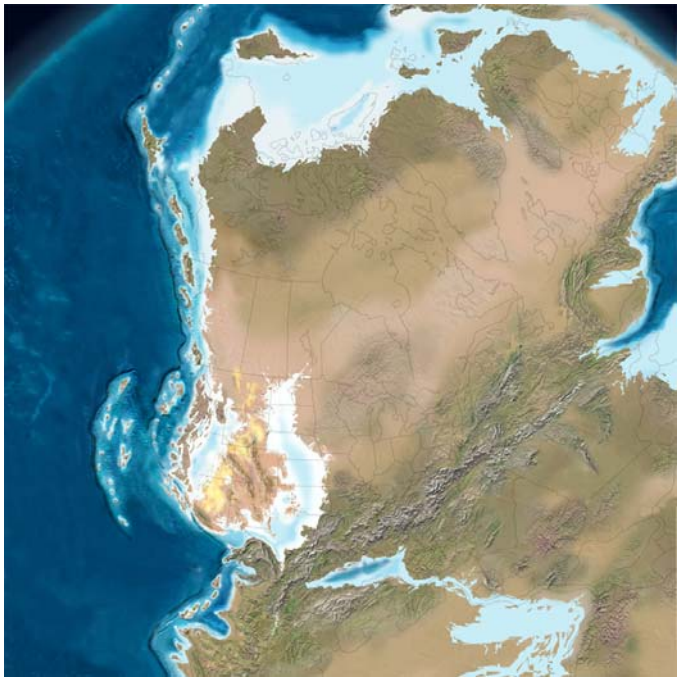

Figure 10: North America in the Early Permian (~290 m.a.) and the supercontinent of Pangaea. From Blakey, 2006.

A variety of major basins and uplifts characterize the foreland adjacent to the Ouachita-Marathon-Sonora thrust belt. The nappes and evolving thrust belts to the south supplied much of the Upper Mississippian to Permian flysch deposits that accumulated in asymmetrical foredeeps that developed subparallel and adjacent to the orogenic front (i.e., Black Warrior, Arkoma, Fort Worth, Kerr, Val Verde, Marfa, and Mina Mexico foredeeps; Poole et al., 2005). The asymmetric geometry of the foredeeps is consistent with a downward flexure under an isostatic load of thrust sheets (Beaumont, 1981). The thickest and deepest portions of the foredeeps occur closest to the thrust front. The frontal margins of these foreland basins consist of imbricately stacked thrust sheets where deep troughs formed and subsided as they filled with turbiditic sediment (Poole et al., 2005).

The Fort Worth Basin

The Fort Worth basin located in north-central Texas, is a linear foreland basin of the Ouachita Orogeny. The northern and northeastern boundaries of the basin are the buried structural highs of the Red River and Muenster Arches; the western and southwestern boundaries of this basin are the Bend Arch, the Lampasas Arch, and the Llano Uplift, respectively. Its eastern boundary is the Ouachita fold-thrust belt (Figure 11).

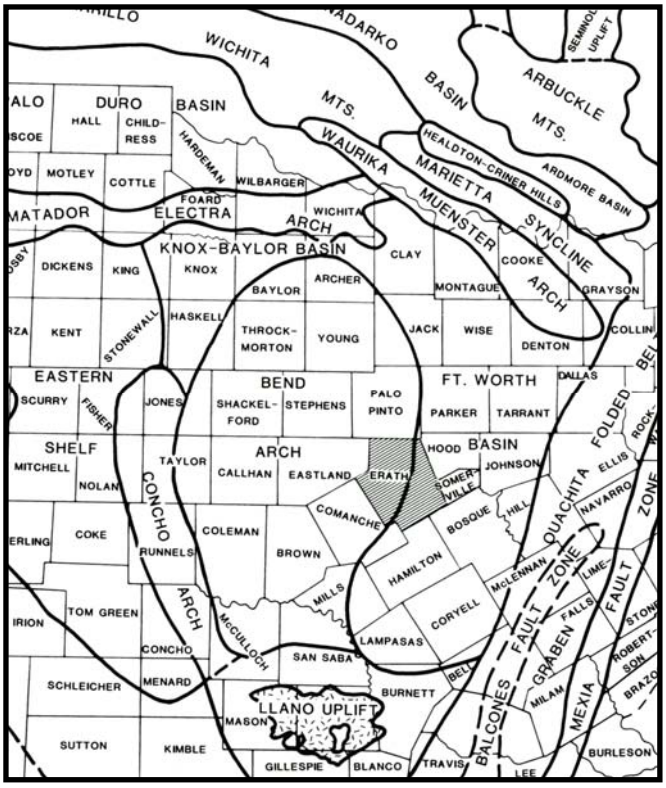

Figure 11: Structural features of central and North-Central Texas. From Flippin (1982)

In the Late Cambrian, the Wichita and the Reelfoot aulacogens served as the source for major deltaic sequences as seas transgressed across the craton (Walper,

1982) (Figure 12). These deltaic sediments, deposited on the shelf are known as the Ouachita facies. As the trailing plate margin of North America cooled, it slowly subsided, which allowed seas to rise across the craton and deposit Ordovician carbonates, such as the Ellenberger Limestone (Figure 13; Walper, 1982).

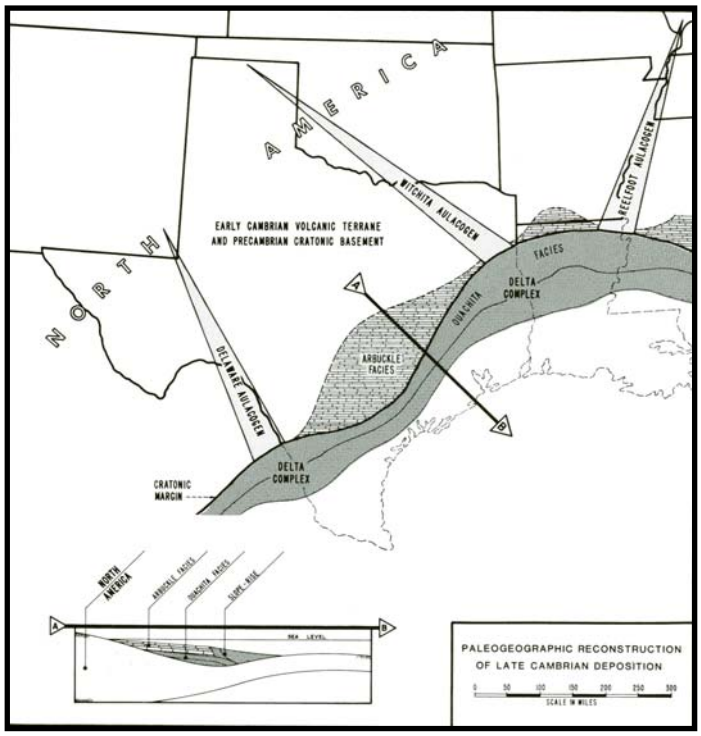

Figure 12: Aulacogens of the late Pre-Cambrian and Early Cambrian served as the source for major deltaic sequences as seas transgressed across the craton in the Late Cambrian. Image taken from Walper (1982).

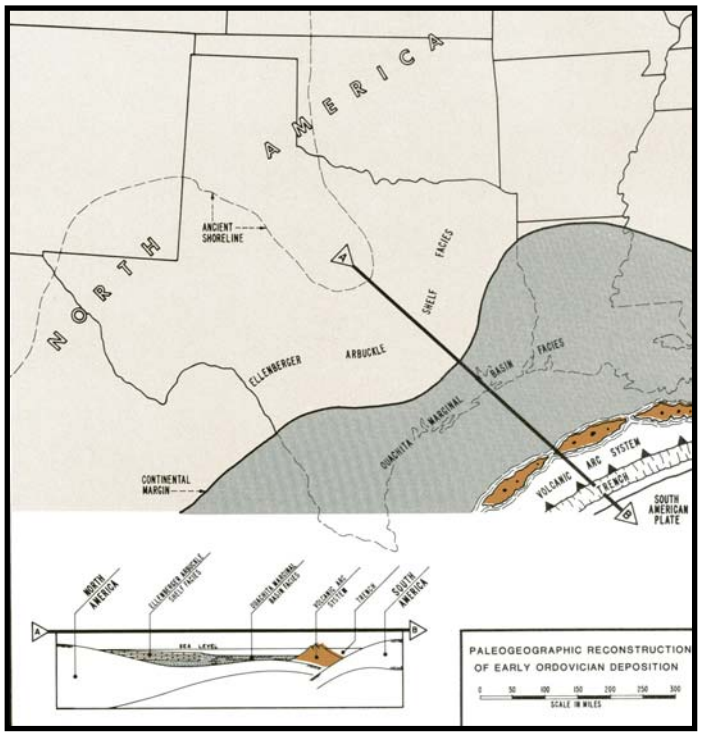

Figure 13: Early Ordovician reconstruction of the Texas Gulf Coast. The north-dipping subduction complex is consistent with the opening of an ocean basin. This image was taken from Walper, 1982.

The Ordovician Taconic Orogeny of the Appalachian region may have had some effect on sediment deposition in the Fort Worth basin. A large unconformity exists within the basin, and across most of central and north-central Texas. In some parts of the basin, the late Mississippian Barnett Shale overlies Ordovician Ellenberger Limestone. By the Silurian-Devonian, the Iapetus Ocean began to close (Figure 14) as the Ouachita portion of the orogeny, which affected Texas and Oklahoma, began.

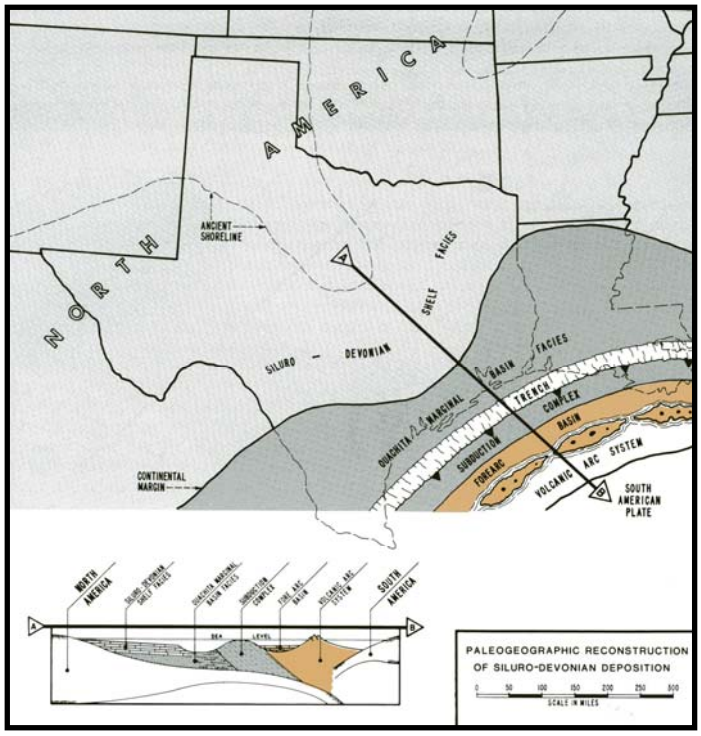

Figure 14: Paleogeographic reconstruction of the Gulf Coast in the Silurian-Devonian period. The south-dipping subduction complex indicates closing of the Iapetus Ocean, taken from Walper (1982)

From the late Mississippian to the Early Pennsylvanian, the Iapetus Ocean continued to close, and the Ouachita Orogeny began as South America collided with North America. A south-dipping subduction complex, which consumed the North American craton, and an overlying volcanic arc formed south of the craton. This volcanic arc complex was later thrust onto the craton in the closing stages of the orogenic event. With continued convergence, foreland basins immediately adjacent to the thrust belt began to subside.

By Mississippian time the subduction zone was nearing the continental margin (Figure 15). The subduction complex grew and was thrust over the continental margin, thus becoming the major source not only for synorogenic flysch deposits of

Mississippian-Pennsylvanian age, but also the later molasse sequence represented by the Atoka and Strawn sequences (Walper, 1982).

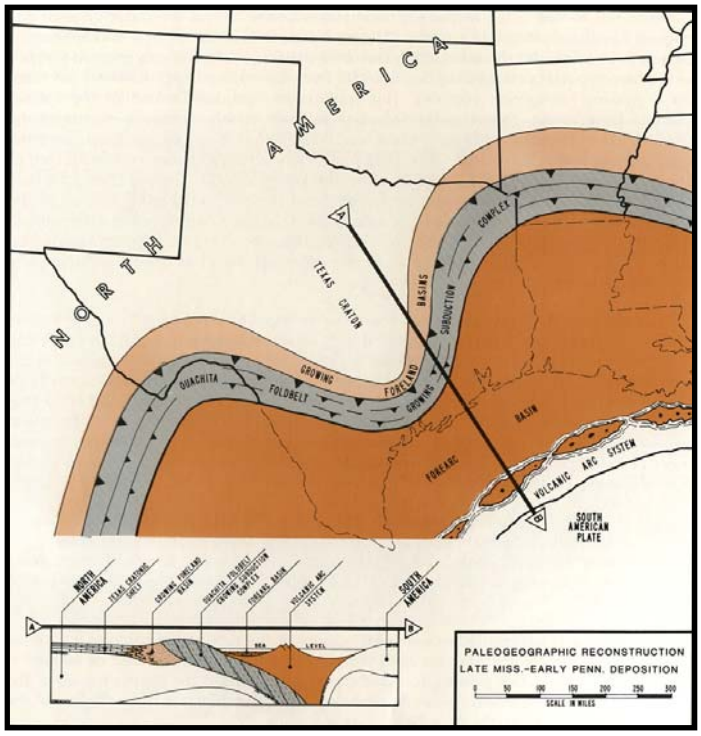

Figure 15: Paleogeographic reconstruction of the Late Mississippian - Early Pennsylvanian Gulf Coast, from Walper, 1982.

By the middle to late Pennsylvanian, the northward migration of the subduction complex stopped, and collision ceased. The aulacogens, which were re-activated and uplifted due to the compression, serve as natural barriers separating the Fort Worth, Arkoma, and Black Warrior Basins. The overall shape of the thrust belt reflects the interaction of thrusting with low-lying coastal re-entrants such as the South Oklahoma and Reelfoot aulacogens and stable buttresses, such as the Llano Uplift (Figure 16). For example, Walper (1977) stated:

> *"The Ouachita-Marathon core area is a subduction complex, formed of sediment scraped from the crust of a marginal sea between North*

America and a volcanic island arc, and thrust onto the cratonic margin of North America. Where it encountered coastal reentrants (such as the mouths of the Wichita and Delaware aulacogens with their deltaic ramps) it was thrust far into the continent in great dilation arcs to form the Ouachita and Marathon recesses. On the other hand, where it encountered a high-standing cratonic margin (such as the Texas craton or central Mississippi uplift) which acted as a stable buttress, it was crushed into a narrow, more highly metamorphosed belt." (Figure 16)

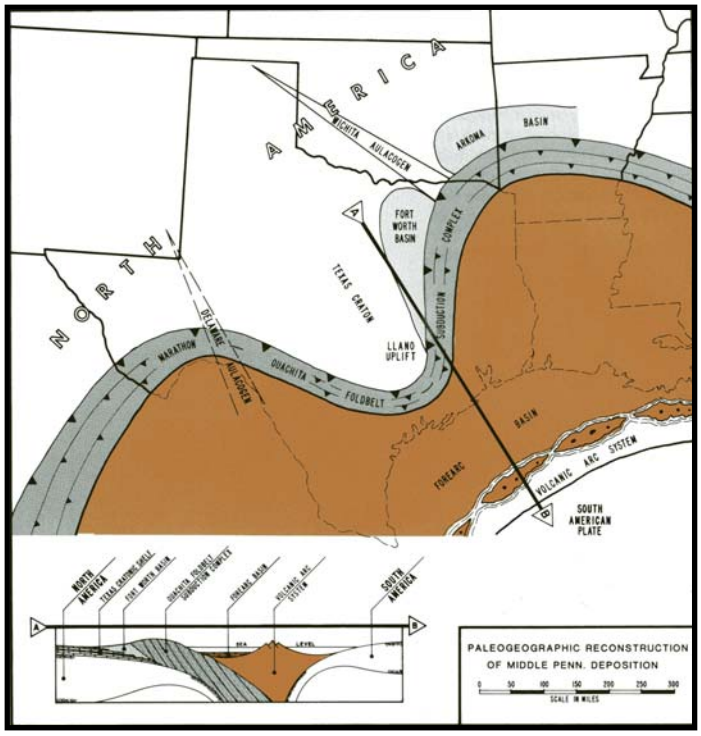

Figure 16: By the mid-Pennsylvanian, the northward migration of the subduction complex had stopped. Note that recesses occur where the thrust belt encounters the ancient aulacogens, while the Llano Uplift forms a prominent salient. From Walper (1982).

The proximity to either the Southern Oklahoma aulacogen or the Llano Uplift would presumably create different stress fields resulting in different fracture patterns. The foreland basins associated with the Ouachita Orogeny remained buried at great depths until the Late Cretaceous Laramide Orogeny, which provided the mechanism for uplift to their current depths.

Formation of the Gulf of Mexico

The Gulf of Mexico formed during the breakup of Pangaea in the Triassic and Early Jurassic time (Walper & Miller, 1985). Van der Voo et al. (1976) contend that the break up occurred as the result of counter-clockwise rotation of Gondwanaland relative to North America about a pole of spreading in the southern Sahara. The Bahama Platform is thought to have been the site of a plume-generated triple junction, which would have been the primary driving force behind initial rifting of the Gulf of Mexico (Dietz and Holden, 1973; Glockhoff, 1973; Sheridan, 1971). The presence of Mesozoic aulacogens within the Gulf, such as the Mississippi and Rio Grande embayments further support the hypothesis of a plume-generated break up of Pangaea (Burke and Dewey, 1973; Walper, 1976, 1980).

The rifting of Pangaea left the northern Gulf rimmed by the Ouachita fold-thrust belt (Walper, 1980). As a result of the extension, block faulting and grabens began to form. The Triassic-aged Eagle Mills Formation and terrigenous clastic equivalents are the lowermost stratigraphic units filling these grabens. The volcanic arc that formed in conjunction with the Ouachita Orogeny remained on the South American plate, suggesting that rifting was concentrated in the forearc basin (Figure 17; Walper, 1980).

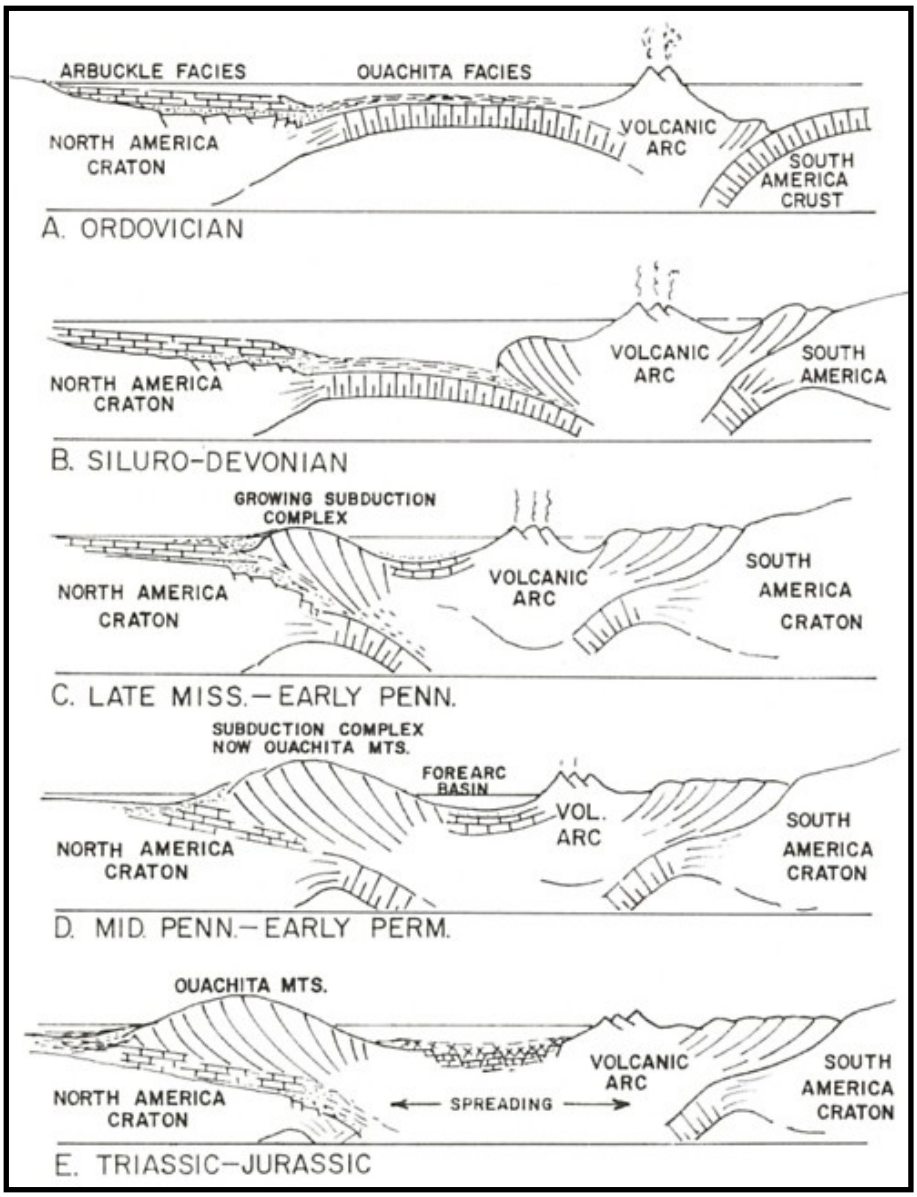

Figure 17: A schematic of cross sections illustrating the stages of closing of the Iapetus Ocean and formation of the Ouachita Mountains and the supercontinent Pangaea. The Triassic rifting of Pangaea to form the Gulf of Mexico began in the forearc basin. From Walper (1980).

The final shaping of the Gulf of Mexico occurred during the Laramide Orogeny, which not only rejuvenated hinterland sediment source areas, but transported peninsular Mexico eastward along the Torreon-Monterrey megashear,

forming the Sierra Madres and further closing the Gulf. The Ouachita Mountains marked the persistent strandline during the Early Cretaceous, and along with pre-existing cratonic uplifts (such as the Llano Uplift of Central Texas) was the source of clastic sediment for the Gulf Coastal plain (Woodruff and Foley, 1985). Subsidence continued throughout the Mesozoic, concomitant with the marine transgression that controlled deposition during the Cretaceous Period throughout the region (Caran et al., 1981).

By the Cretaceous and through the Miocene, en echelon normal faulting composing the Balcones, Luling, Mexia, and Talco fault zones displaced a two to three thousand feet of the Mesozoic to lower Tertiary rock units above the Ouachita outcrops (Caran et al., 1981), as the faulting continued to step back from the coast.

CHAPTER IV

GEOLOGIC ANALYSIS OF SELECTED AREAS

Possum Kingdom State Park

Four locations within the park (Table 1) were chosen for measurement of fractures in the Winchell Limestone (Upper Pennsylvanian). The data from these locations was combined into one main rose diagram. This locality was analyzed to determine fracture orientations resulting from regional tectonic stresses along the western edge of the Fort Worth basin.

Name	Coordinates
PK1	32° 53' 28.92" N; 98° 26' 17.46" W
PK2	32° 53' 21.78" N; 98° 26' 10.56" W
PK3	32° 52' 36.72" N; 98° 26' 44.52" W
PK4	32° 52' 36.36" N; 98° 24' 54.84" W

Table 1: The four localities in Possum Kingdom State Park and their respective coordinates

Previous Studies

The area around Possum Kingdom State Park was studied by two authors, Hoskins (1982) and Wermund (1966). Wermund's work focused on the stratigraphy surrounding Possum Kingdom Lake, while Hoskins studied fracture sets/groups in Pennsylvanian carbonates of the Graford Group in parts of Jack, Palo Pinto, and Wise counties. Hoskins (1982) noted that rocks exposed on the surface were systematically jointed, and hypothesized that the joints were likely related to local structures, such as the Bend Arch. The Bend Arch is a broad subsurface, north plunging, positive structure that acts as a fulcrum between the subsiding eastern flank, which dips into the Fort Worth basin and the western flank, which was activated in the later Paleozoic and formed the Midland basin (Flippin, 1982).

Hoskins (1982) noted three dominant jointing patterns, which were all caused by tensile stresses either present during burial, or introduced during erosion of overburden. The three sets were oriented: (1) N60^{o}E, (2) N60^{o}W, and (3) N25^{o}W (Figure 18). He concluded that set 1 was related to the Balcones fault system and the Ouachita trend, and resulted from regional tilting to the southeast. Scattered fracture sets, including set 2 were not related to any known structural features and likely resulted from variations in rock fabric and geometry. Set 3 trends parallel to known structural features in the subsurface of this region; Hoskins (1982) concluded that they must therefore be related.

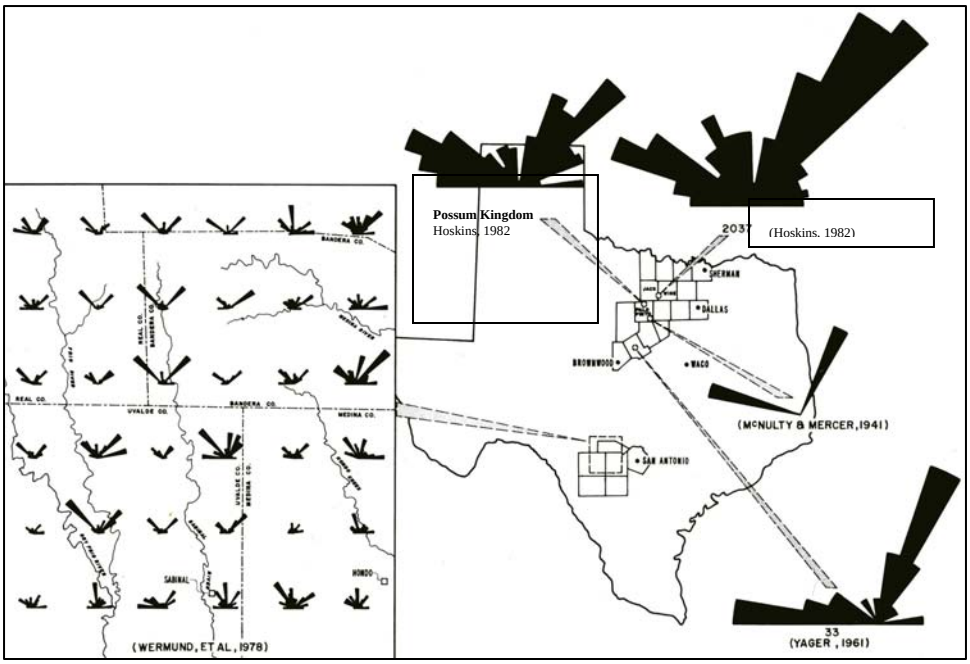

Figure 18: Regional fracture patterns across Texas, modified from Hoskins (1982).

Outcrop Description

The Graford Group (Figure 19) consists of the Upper Brownwood Shale, the Adams Branch Limestone, the Cedarton Shale, and the Winchell Limestone. Fractures were measured in the Winchell Limestone. The Graford formation has been described by Hoskins (1982) as being a part of a deltaic system that existed near the end of the Ouachita Orogeny. Wermund (1966) described the Winchell Limestone as:

> *"Two limestone units separated by a shale unit. The upper limestone is fine grained; thick bedded in south to thin bedded northward; gray color; contains brown algal structures; thickness 4-10 ft, getting thicker to the northeast. The middle shale unit is calcareous northeastward, and contains thin limestone lentils, gray color; thickness 3-15 ft, thinning southwestward. The lower limestone is fine grained to coarsely bioclastic, calcareous shale with individual beds that are a few inches thick. Black chert nodules with white fossil fragments exist in the lower part of the shale. Bedding is irregular and thin to med medium bedded, nodular upward, with marine megafossils. In thickened portion, the limestone is bioclastic, containing algal structures It is about 65% fine grained; thinly*

bedded; locally nodular, 30% coarse grained; thick bedded, and the remainder of the lower limestone contains thin interbeds of shale, which are gray forming broad dip slopes and prominent scarps. Overall thickness of Winchell Limestone 15-50 feet, and thickens northeastward. The Winchell abruptly thickens to about 190 feet near Possum Kingdom Lake, and interfingers with overlying Placid Shale and underlying Wolf Mountain Shale."

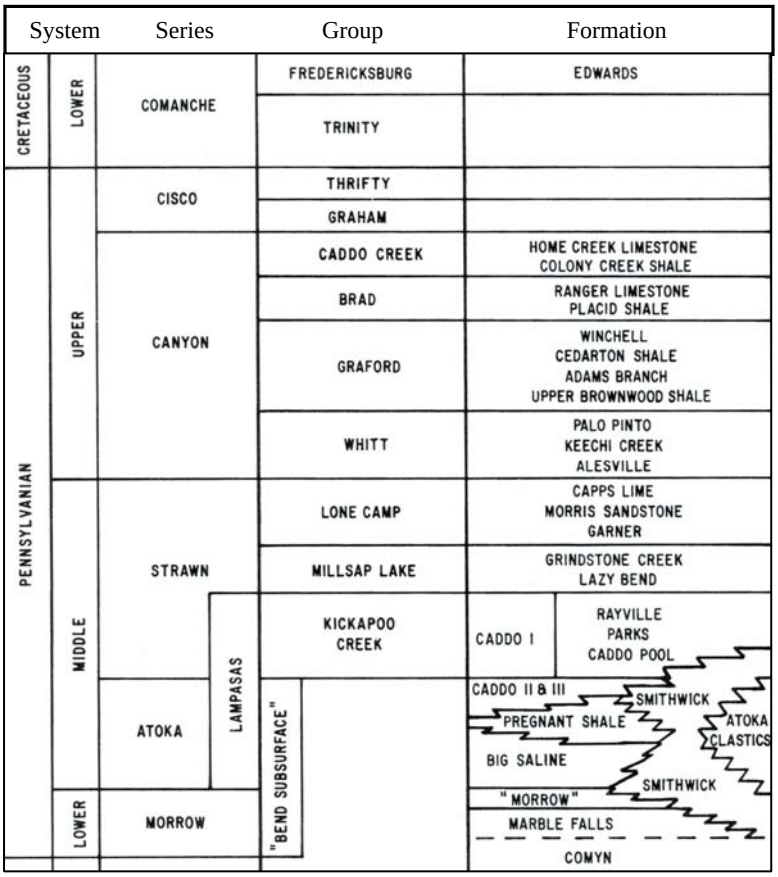

Figure 19: Generalized stratigraphic nomenclature of north-central Texas. Modified from Flippin (1982)

The Winchell Limestone crops out along the southern perimeter of Possum Kingdom Lake, and formed resistive cliffs that were adequate for measurement of fractures (Figure 20).

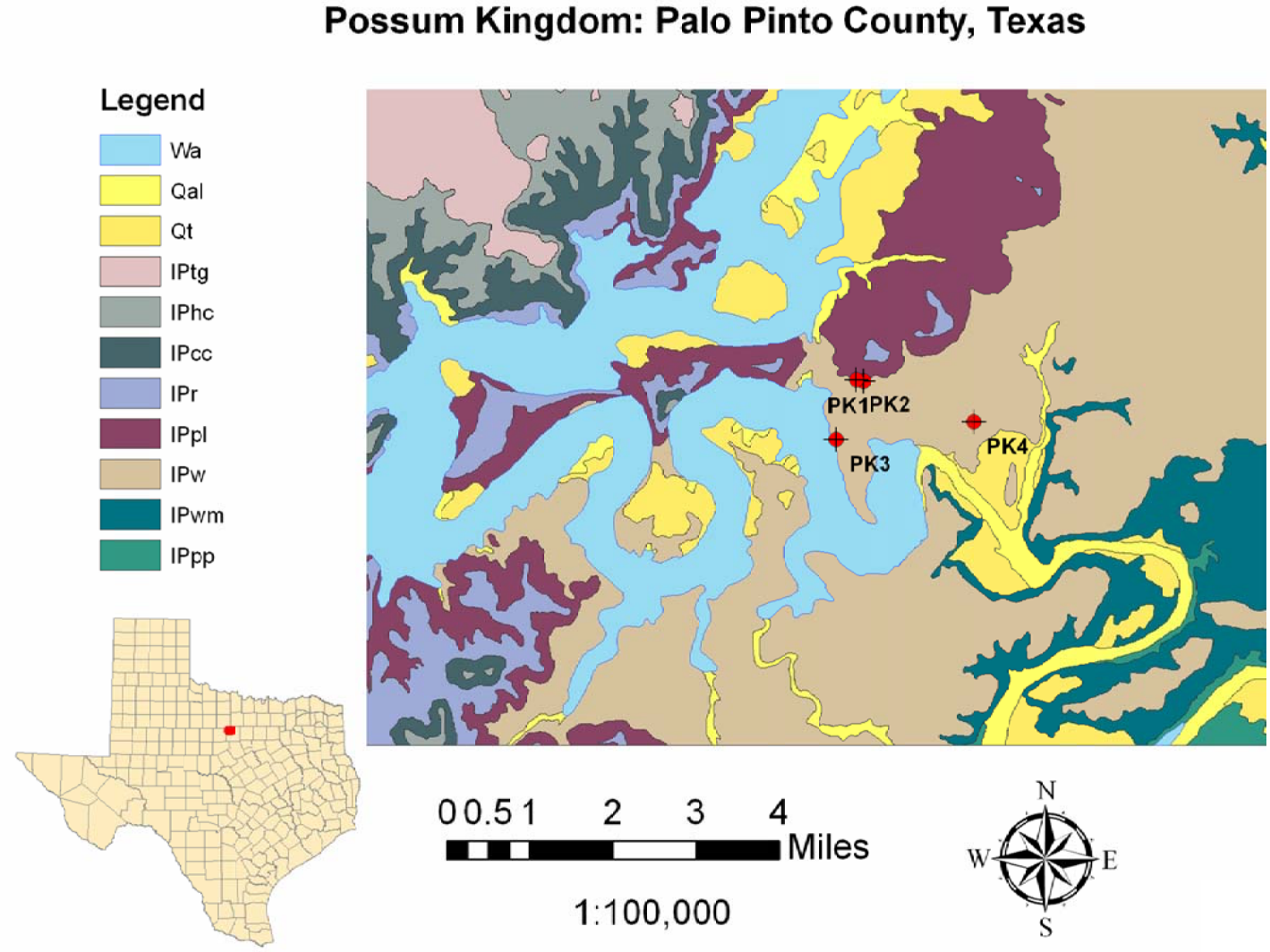

Figure 20: Geologic map of the Possum Kingdom area. Map digitized from Wermund (1966).

Fracture Measurement

A total of 238 fractures were measured and described from all four locations. Fractures at the Possum Kingdom locality were poorly exposed, and mostly found along cliff forming ledges and thick vegetation (Figure 21). Because of this, it was not possible to describe aperture, intensity, or fracture morphology. An exception was the PK4 locality (Figure 22), where the exposure is not covered by vegetation. The fractures occur in two dominant orientations: (1) N50-60^{o}W, and (2) N30-40^{o}E (Figure 23). All measured fractures were nearly vertical, indicating that they are tensile mode-I fractures. There was no evidence of shearing or offsetting along fracture planes. Eleven fractures contained calcite fill.

Cross-cutting relationships indicate that the northwest-southeast fracture set was oldest. The northwest set trends roughly perpendicular to the thrust front, and therefore likely formed as a result of Ouachita tectonics. The younger northeast-southwest set is likely related to movement along the Balcones fault system and overall extension due to opening of the Gulf of Mexico.

Figure 21: Typical fractures in the Possum Kingdom area. Blocks breaking along fracture planes form low cliffs or steps along hill tops.

Figure 22: Fractures at PK4, with vegetation growing in fracture planes.

X-Ray Diffraction

Three samples of rock were obtained from PK1, PK2, and PK4, and analyzed using powder diffraction techniques to examine the role of mineral composition on the brittle or ductile nature of rock deformation. A detailed description of bulk mineralogy of each sample can be found in Appendix A.

The samples had similar compositions, and consisted primarily of quartz, calcite, illite, and kaolinite. PK1 and PK2 had qualitatively more illite and kaolinite compared to PK4. Thus, lower fracture intensities in PK1 and PK2 are likely the result of increased clay contents and generally more ductile behavior.

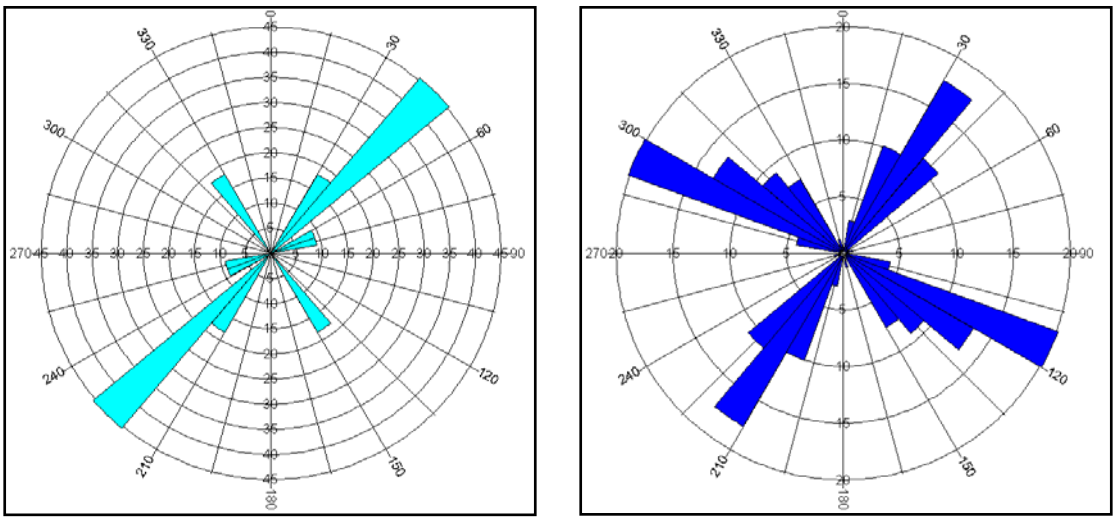

Figure 23: Rose diagrams showing the orientations of fractures measured at PK1, PK2, PK3, and PK4. The diagram on the left shows the orientations of all fractures that contained mineral fill; the diagram on the right shows fracture orientations containing no mineral fill.

Brownwood Spillway

Location

The Lake Brownwood Spillway, located 7.5 miles north of the town of Brownwood, Texas, contains outcrops of the Winchell Limestone (Table 2). This locality was chosen because it was thought to be representative of deformation resulting from tectonism outside of the foreland basin, but away from features which may alter the transfer of stress in the foreland, such as the Llano uplift.

Name	Coordinates
Brownwood Spillway	31° 50' 31.48" N; 98° 59' 57.67" W

Table 2: The location of the Brownwood Spillway

Previous Studies

The Lake Brownwood Spillway has been the topic of many studies in the literature; however, no studies have been published on fracture systems in the Winchell of in the vicinity of the Brownwood Spillway. A Study by Warme and Olsen (1971) was cited for the outcrop descriptions at this locality.

The spillway was measured and described in a field guidebook by Warme and Olsen (1971). The guidebook described the entire geologic section, focusing on the presence of trace fossil assemblages within the spillway (Figure 24). The basal portions of the spillway contain rocks of the Cedarton Shale Member, while the upper portion of the spillway contains the Winchell Limestone.

The late Pennsylvanian shelf sediments of north-central Texas were deposited in a shallow sea, where offshore limestone banks and marginal prograding deltas shed a

variety of sediments, resulting in strata that are laterally as well as vertically complex (Warme and Olsen, 1971). The upper 100 feet of section at the Lake Brownwood Spillway are classified by Eargle (1960) as being Winchell Limestone. Carbonates, mudstones, and minor sandstones of the Winchell beds display features characteristic of Pennsylvanian cyclothems of the mid-continent region (Warme and Olsen, 1971).A geologic map of the area can be seen in Figure 25.

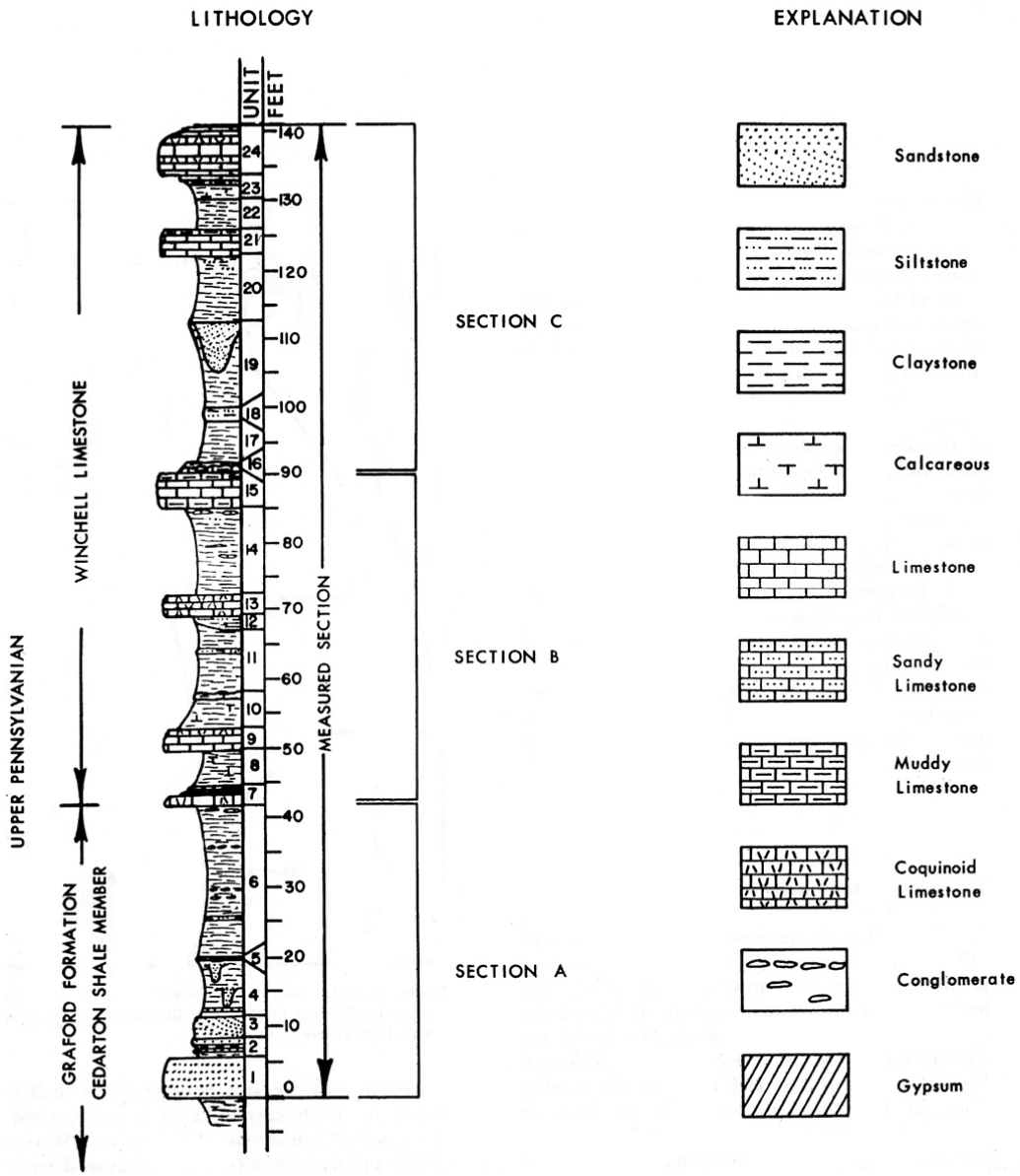

Figure 24: The stratigraphic section at Lake Brownwood Spillway, described by Warme and Olsen (1971)

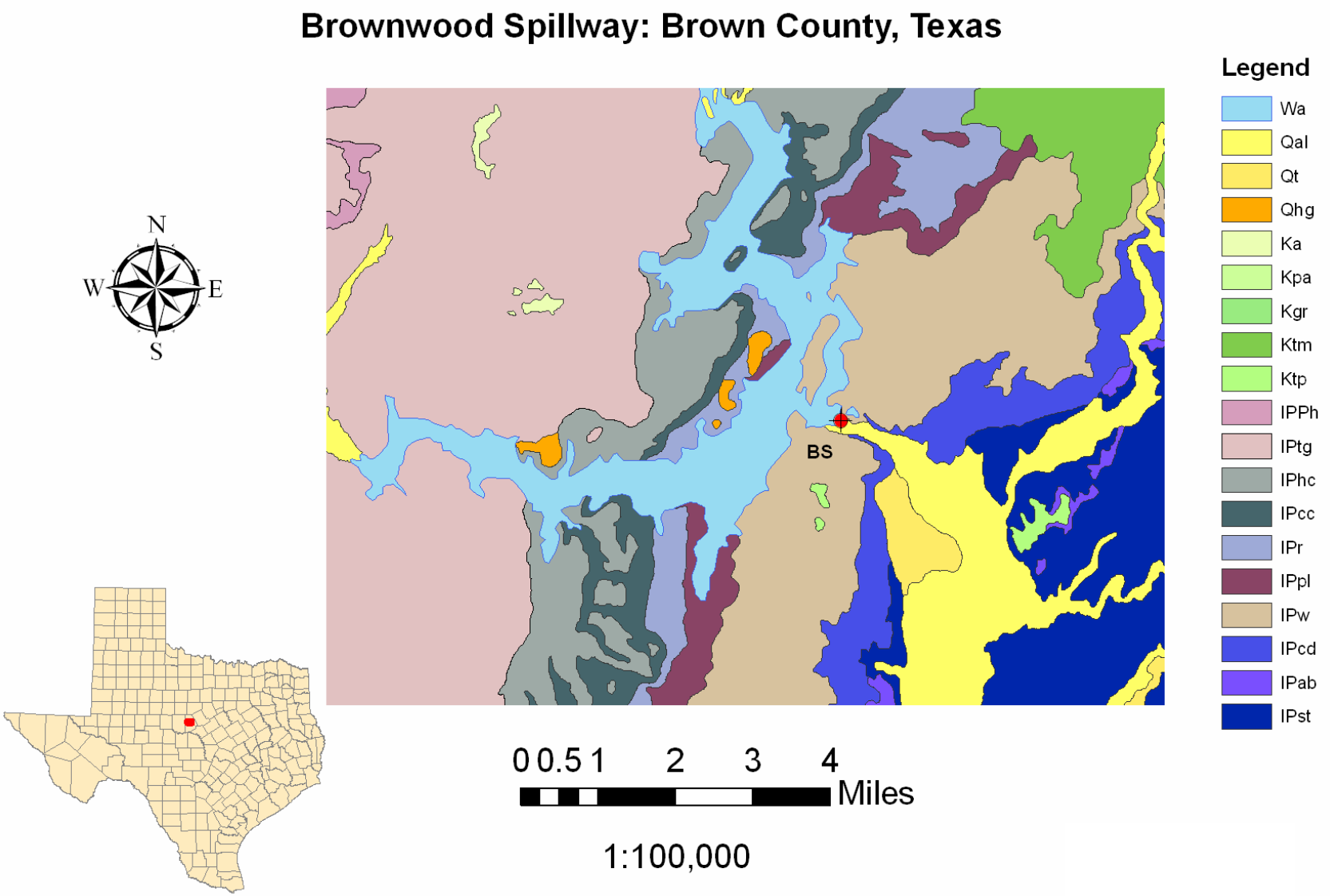

Figure 25: Geologic map of the Brownwood Spillway. Map digitized from Stitt (1964).

Outcrop Description

Unit 13 of Warme and Olsen (1971; Figure 26) is one of four limestone units within the Winchell Limestone, and the only one that contained enough fractures to warrant measurement. Unit 13 was well cemented and highly resistive to weathering, a characteristic ideal for the preservation of fractures (Figure 27). Unit 13 was described by Warme and Olsen (1971) as:

> *"A light to medium gray; massive coarse to very fine; recrystallized shell hash; some sandy horizons; gritty, especially near the bottom. Fossils present are brachiopods, bryozoa, echinoid spines and plates, as well as foraminifers. Trace fossils present are U-shaped burrows at the top; anastomosing feeding probes at the base."*

The spillway is highly eroded, which exposes the resistive units and allows easy access to the rocks (Figure 28). The amount of erosion and removal of overburden may have generated secondary fracture sets completely unrelated to tectonics.

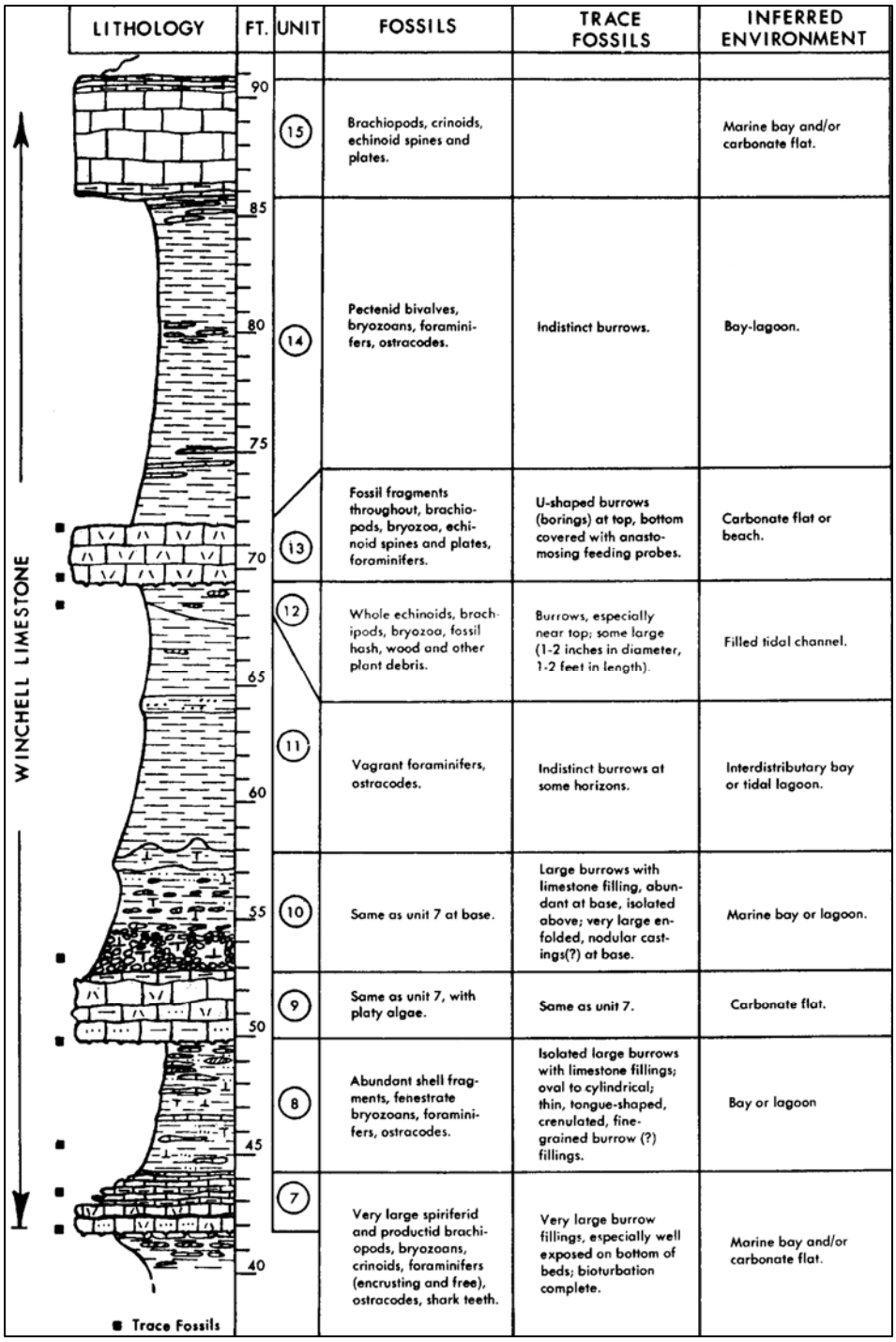

Figure 26: Detailed description of rock units at Brownwood Spillway. From Warme and Olsen (1971)

Figure 27: An image of Unit 13 and the fracture sets that form the ledge at the Brownwood Spillway

Figure 28: A panoramic image of the Brownwood Spillway. The four most resistive units from the top down are 15, 13, 9, and 7 as published by Warme and Olson (1971).

Fractures

A total of 129 fractures were measured and described in Unit 13 at the Brownwood Spillway. All fractures measured had vertical dips, suggesting that they were formed due to tensile mode-I loading. Sixty fractures contained calcite mineral fill; these were frequently cross cut by younger fracture sets (Figure 29).

Figure 29: An image showing a fracture (N75^{o}E) filled with calcite being cross-cut by a younger fracture (N15^{o}W) at the Brownwood Spillway

Four distinct sets of fracture orientations were observed at the spillway: (1) N75^{o}-80^{o}E, (2) N15^{o} -20^{o}E, (3) N15^{o}-20^{o}W, and (4) N75^{o}-80^{o}W (Figure 30). Age relationships were easy to determine because fractures were well preserved and easily accessible in the outcrop. Fracture Sets 2 and 3 were frequently seen terminating at Sets 1 and 4 (Figure 31) indicating that sets 2 and 3 are younger then 1 and 4. There was no example of cross cutting relationships between fracture set 1 and 4, or 2 and 3, and therefore, no age relationship could be determined.

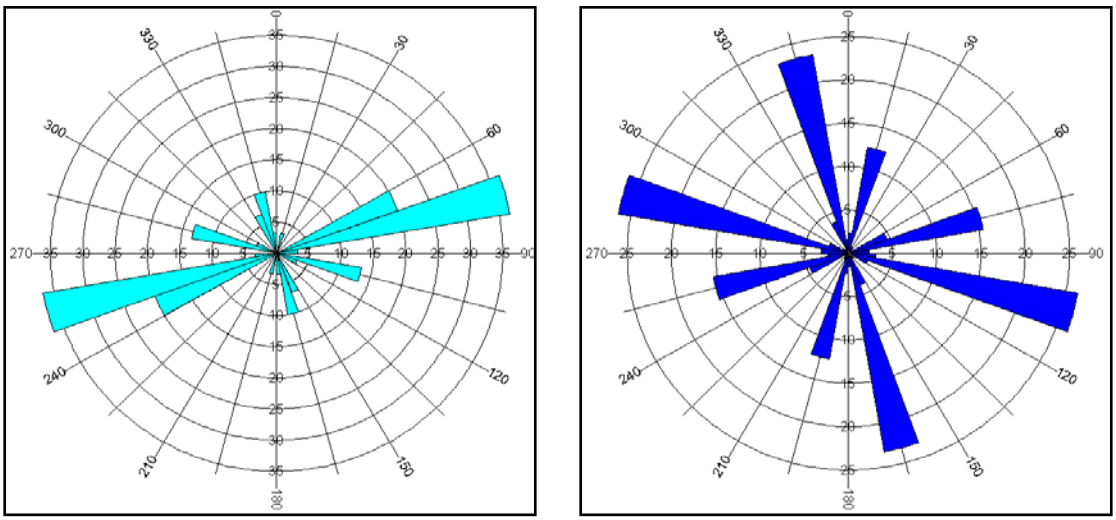

Figure 30: Rose diagrams showing orientations of fractures measured at the Brownwood Spillway. Fractures containing mineral fill are illustrated in the diagram on the left, while those containing no mineral fill are represented in the diagram on the right.

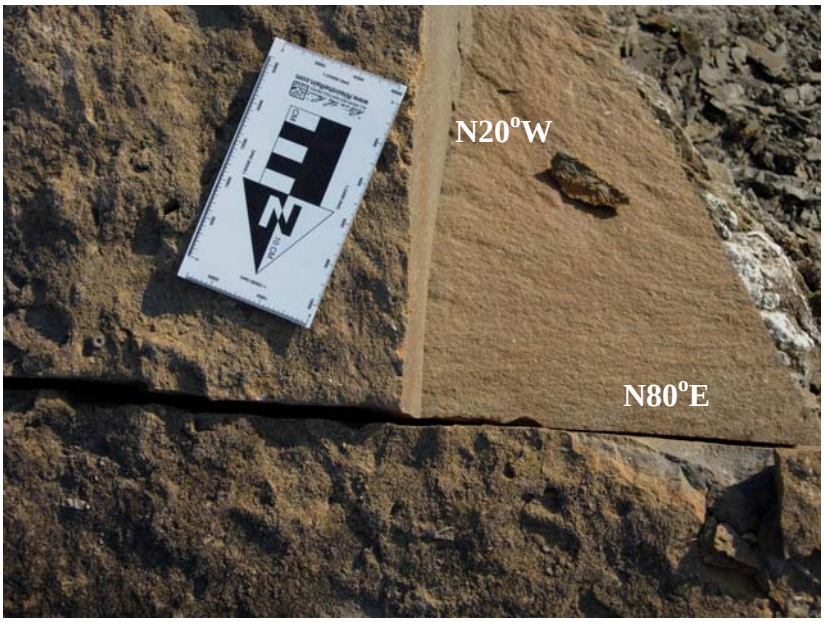

Figure 31: An image showing a fracture trending N20°W (Set 3) terminating at an older fracture trending N80°E (Set 1).

Fractures measured at the spillway exhibited plumose markings (Figure 32) on the inside of their fracture planes. The plumose markings were well preserved along the cliff faces of the exposure (Figure 32). These markings originate at a point or flaw in the rock, and represent the inhomogeneous transfer of stress throughout the rock body. Plumose structures are unequivocal indicators of the mode and direction of fracture propagation.

Figure 32: Plumose markings along a cliff face at Brownwood Spillway

The origin of the fracture sets at the Brownwood Spillway is difficult to determine because of the great number of modern stresses exerted on the outcrop. Because fluid movement is conventionally believed to occur syntectonically with compression, mineral-filled fracture sets 1, 3, and 4 are likely related to compressional orogenic events. Fracture sets 1 and 4 are likely related to the Ouachita orogeny because they are the oldest fractures at the outcrop, and they strike perpendicular to the trend of the orogen. Fracture set 3 may be related to the Bend Arch, which strikes north-south through Brown County.

Fracture set 2, contained no mineral fill, and cross-cuts fracture sets 1 and 4. It is possible that this fracture set is related to extensional movement along the Balcones fault system. Alternatively, this fracture set may also be the result of fracturing related to removal of overburden, which would make this a localized fracture set, not related to tectonics.

X-Ray Diffraction

Two samples were analyzed via x-ray diffraction: (1) BWS1 and (2) BWS2 (Appendix A). BWS2 was collected in a portion of Unit 13 that contained significant bioturbation and a low fracture intensity, while BWS1 was collected from a non-bioturbated region. BSW1 contained a very dominant quartz peak, and few, if any, clay peaks. BWS2 had a qualitatively higher counts associated with clay minerals (Appendix A). The bioturbation in BWS2 yielded a clay mineral content which, in turn, generated a lower fracture intensity measurement.

Bend River Locality

Location

The Bend River locality is located on the south bank of the Colorado River approximately 0.7 miles southwest of the town of Bend, Texas (Table 3). This locality was chosen because it is thought to be representative of forces felt at the edge of the Llano Uplift, which are assumed to be different from those felt in the foreland away from such structures as this.

Name	Coordinates
Bend River Locality	31° 5' 26.04" N; 98° 31' 12.66" W

Table 3: The location of the Bend River locality

Previous Studies

Merrill (1980) described the rocks of the Llano region, specifically mentioning the fossil assemblages seen in the units at this locality. A geologic map of the Bend River locality is provided in Figure 33. Plummer (1943) published a book about the Carboniferous rocks of the Llano region of central Texas. In this book, he offered detailed descriptions of the every rock unit found in the Llano region. I utilized the book for the descriptions of the Marble Falls and Smithwick formations. I also relied heavily on personal communication with Bo Henk, Chief Geologist for Matador Resources, for interpretations and descriptions of the rock units present at this locality.

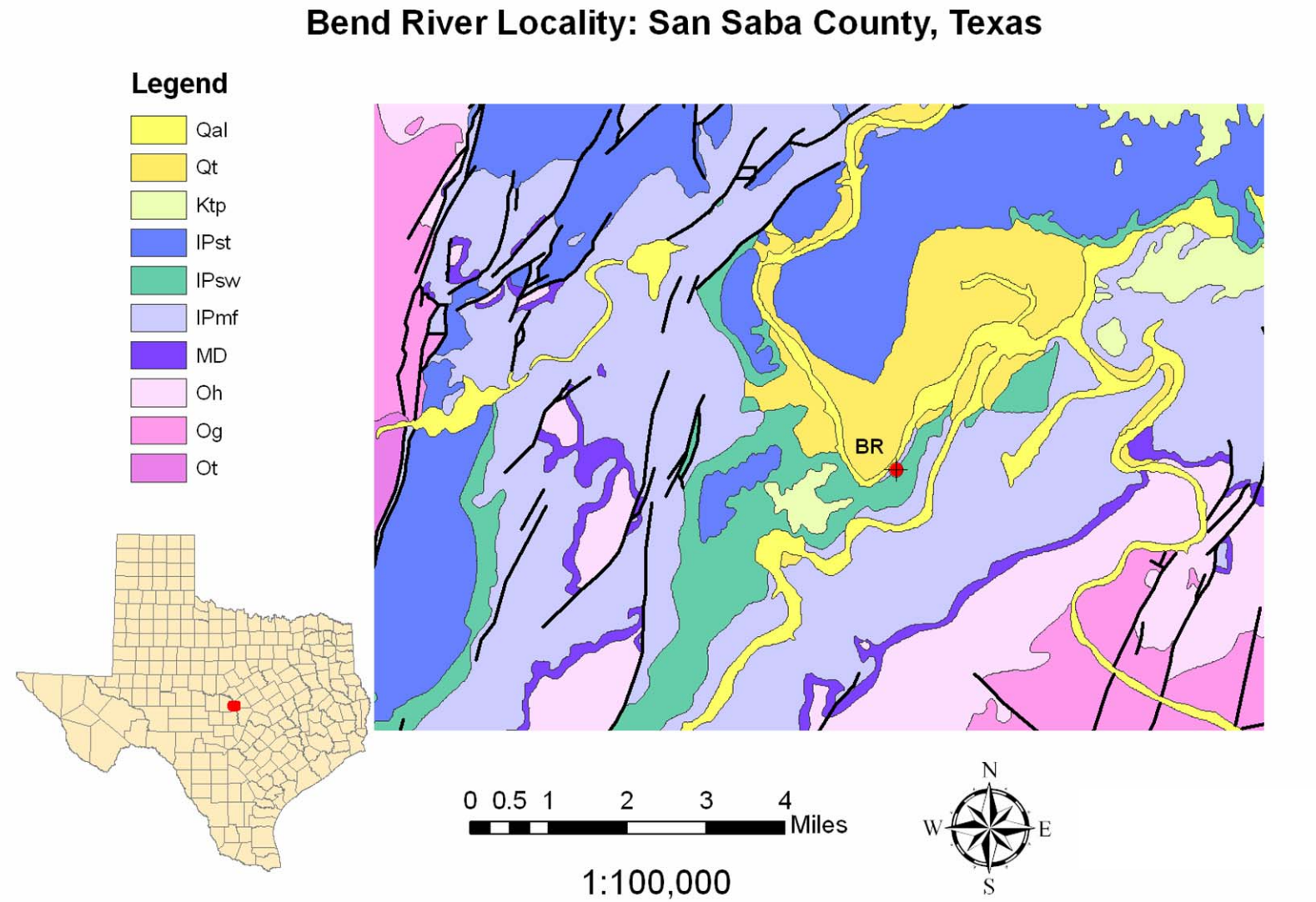

Figure 33: Geologic map of the Bend River locality. Map digitized from Stitt (1964)

Outcrop Description

The Bend River locality contains the upper portion of the Marble Falls Limestone and the contact between the Marble Falls and the overlying Smithwick Shale. The Smithwick lies unconformably on top of the Marble Falls Limestone (Plummer, 1943) (Figure 34).

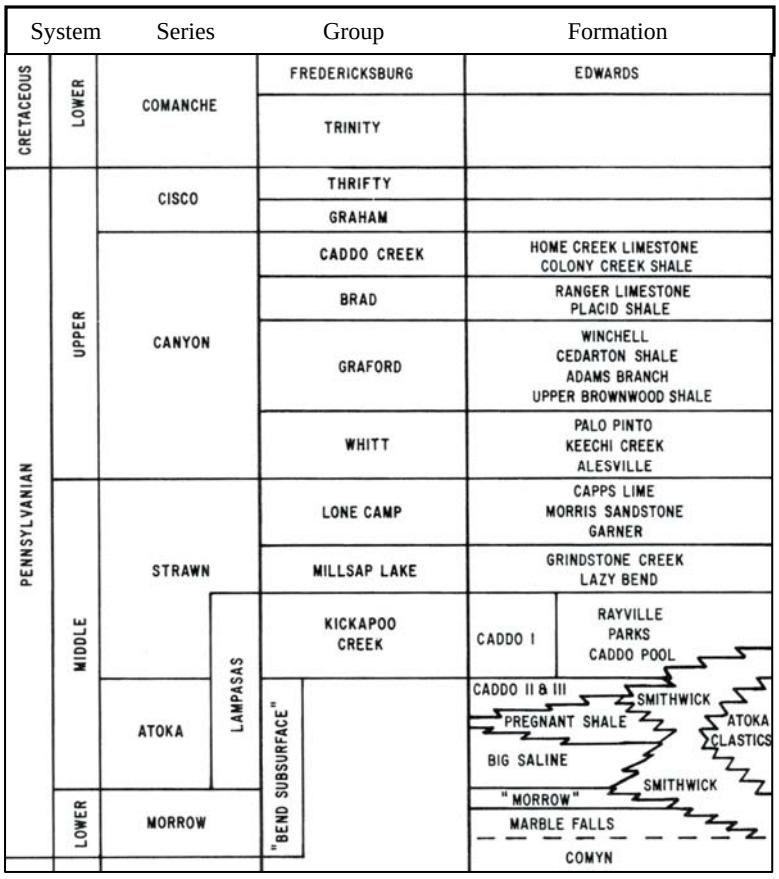

Figure 34: General stratigraphic nomenclature of central Texas. Taken from Flippin (1982).

The Marble Falls Limestone is described as having two main members: a lower unit called ‘the spiculitic portion’ and the upper unit described as a crinoidal member (McCrary, 2003). The thickness of the Marble Falls in Central Texas is highly variable,

and has been described as a gray to black, siliceous, fossiliferous limestone, which is generally thinly bedded and contains layers of black shale (Plummer, 1943). Plummer (1943) described the thickness of the Marble Falls near Bend, Texas as being 149 ft, 6 in thick. The overlying Smithwick Shale is described by Merrill (1980) as being soft, black and poorly fossiliferous throughout with a few thin siltstone interbeds. At the Bend River locality, the uppermost portion of the Marble falls contains an abundance of *Cephalopods*, *Zoophycus* (feeding traces), *Ophiomorpha* (shrimp burrow networks), and massive heads of *Chaetetes sp.* coral. (Figures 35, 36, 37)

Figure 35: *Zoophycus* in the same stratigraphic unit with *Ophiomorpha* (shrimp burrows)

Figure 36: *Chaetetes* coral in the same stratigraphic unit as Ophiomorpha (shrimp burrows).

Figure 37: *Cephalopods* in the upper portion of the Marble Falls at the Bend River Locality

Depositionally, this set of fossils poses an interesting question concerning water depth at the uppermost portion of the Marble Falls. Typically, *Ophiomorpha*, and *Chaetetes* coral are thought to exist in shallow water depths. *Zoophycus* and *Cephalopods* suggest a deeper water depth. The presence of all four fossils in the same unit suggests a deepening and re-working of this surface (Bo Henk, 2007, personal communication).

The *Ophiomorpha* and *Chaetetes* coral existed while this unit was a shallow marine carbonate shelf. As the water level rose, the *Chaetetes* and the *Ophiomorpha* were drowned out, allowing intermediate to deep-water fossils such as the *Zoophycus* and the *Cephalopods* to move in. Basinal deposits that comprise the Smickwick formation represent a flooding surface. This all must have taken place prior to lithification due to the presence of these fossils within the same unit.

It is not clear what caused the rise in water depth. The rise could be eustatic, occurring globally, or it could have been the result of tectonic forces. In either event, the deepening at this locality caused a change in the depositional pattern, bringing in more clay size particles. Increasing clay content caused a change in the mineralogic make up of the limestone. This in turn had a profound affect on fracture intensity of this unit.

This boundary cannot be a sequence boundary however because sequence boundaries are unconformities that bound conformable packages of genetically related strata. Very little has been published on the sequence stratigraphy of the Carboniferous rocks of Central Texas.

I informally divided the Bend River locality into three units (I, II and III). Unit I, the highest in the section, is the lower carbonate member of the Smithwick Shale. The top of the Marble Falls was defined as Unit II. It lies directly beneath Unit I and contains two

members: (1) the re-worked surface consisting of the diverse fossil assemblage, and a very brittle unit which contained no fossils beneath it. Finally, Unit III is the upper Marble Falls, which crops out along the riverbed. It lies directly beneath Unit II, and is separated from the brittle member of Unit II by an interbedded ductile layer. It is the lowest in the section unit of measure at this locality. Each of the three units brittle units used for fracture measurement was separated by interbedded ductile units which contained no fractures. Like the Brownwood Spillway, fractures were contained within specific lithologic units, which appeared to be a function of mineralogic make up.

UNIT I

271 fractures were measured in Unit I. All fractures were vertical, and none were cemented. Fractures in this unit exhibited J-hooking (Figure 6). This phenomenon was observed several times in this unit. Initially, it appeared that the curved joint sets formed first, and were displaced by the second set. However, this explanation did not explain why the joints were curving as they approached a free surface. Furthermore, fracture displacements along the same joint were not the same, and thus were not formed first and then displaced (Figure 38). The curving phenomenon likely indicates that these fractures formed under more complex local forces, which were not seen in other localities.

Figure 38: An example of fractures curving in the presence of a free surface. Displacements along the same fracture were never the same. Colored dots indicate sets of related fractures.

Two fracture sets were present in Unit I: (1) East-West and (2) N60^{o}-75^{o}E (Figure 39). Determining the relative ages of sets 1 and 2 was difficult, since both sets were observed cross cutting each other. I believe these fracture sets formed at the same time. Their slight difference in orientation, coupled with their unique interaction with one another made this unit a particularly difficult unit to describe. The collective results of Unit I are shown in Figure 40. Fracture set 1 was only seen in Unit I, whereas fracture set 2 was seen in all three units.

Figure 39: Image showing the two fracture sets in Unit I

Fracture set 1, which doesn't occur in any underlying rock units at this locality, cannot be the result of a separate geologic event. If it were, east-west fractures would be seen in all units at this locality. I believe this fracture set is an example of strain

partitioning, which occurred as a direct result of interbedded ductile units that are lithologically different from the brittle units.

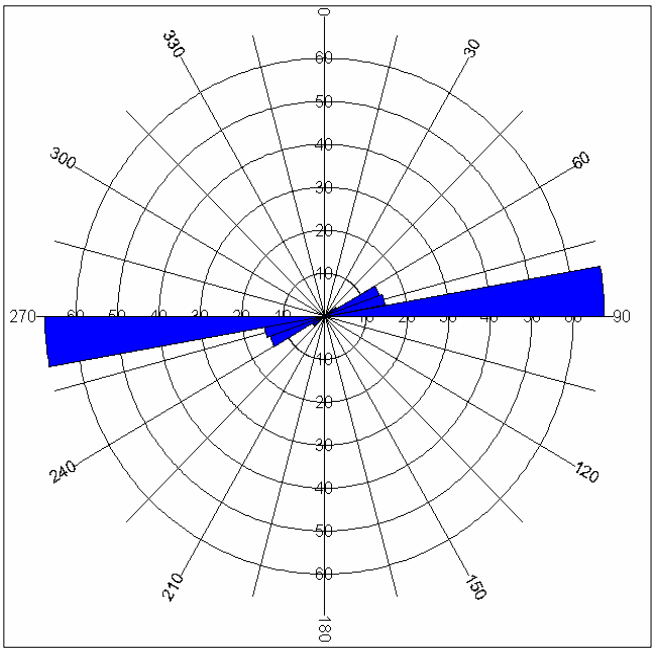

Figure 40: Rose diagram illustrating the orientations of fractures measured in Unit I

Strain partitioning is the manner in which strain (in the form of fractures) manifests itself when stress is transferred inhomogeneously throughout the rock body. In a perfectly homogeneous case, stress would be homogeneously transferred from one unit into another; overlying units would fracture in the same manner as underlying units.

Alternatively, inhomogeneous stress transfer can occur when ductile units separate brittle units from one another, which can also add an element of anisotropy. Inhomogeneous stress transfer that significantly affects the perfect transfer of stress throughout the rock body can result in slightly variable fracture patterns from one unit into another. Other factors that can affect the transfer of strain, and cause partitioning in a

rock body include local variations in fluid pressure, confining pressure, temperature, and strain rate (Hatcher, 1995).

This imperfect transfer of stress likely manifests itself as a slight ($\leq 10^{o}$) change in orientation of fractures from one unit into another. Different strains result from the bulk properties of the rocks being deformed (Hatcher, 1995). Relatively weak rocks (shale, salt, and schist) commonly exhibit styles of deformation that contrast with those of stronger rocks (sandstone, limestone, etc.) (Hatcher, 1995).

UNIT II

117 fractures were measured in the brittle member of Unit II (Figure 41), which lies immediately beneath the ductile member. Only one orientation ($N75^{o}$-$80^{o}E$) was measured for fractures in this unit (Figure 42). All fractures were vertical in dip, and none contained any cement. Fracture orientations seen in Unit II were seen in all three units measured at this locality.

Figure 41: Picture illustrating fractures in Unit II with only one orientation.

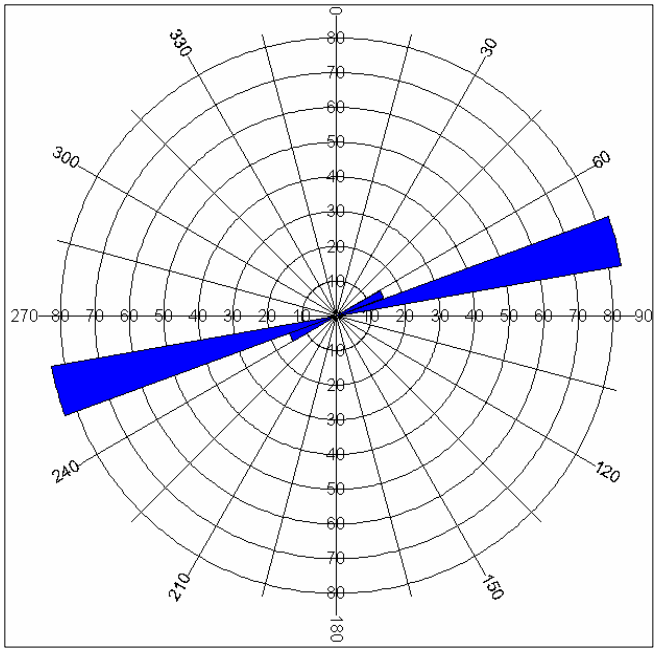

Figure 42: Rose diagram illustrating the orientations of fractures measured in Unit II

Unit II also demonstrated how fracture orientations could change dramatically in the presence of a local deviation in the stress field (Figure 43). In this area, the deviations were commonly topographically low features. Orientations of these fracture sets were not recorded since they continuously changed while in the presence of the structure, making an accurate measurement impossible.

Figure 43: An example of how fracture orientations can be affected by a topographically low feature, which causes a change in the local stress field.

UNIT III

114 fractures were measured in Unit III (Figure 44). All fractures measured were vertical, and none contained any cement. Three orientations (Figure 45) were present in this unit: (1) N75^{o}-80^{o}E, (2) N15^{o}-30^{o}E, and (3) N0^{o}-15^{o}W. Set 3 was the oldest set based on cross cutting relationships, and because it was not seen in any overlying units. Set 2, which was older then set 1, was never observed interacting with set 3, and thus no relative age dating could be applied. Set 1 is the youngest set since it was present in all overlying units. The geologic events that caused fracture sets 2 and 3 must have been isolated to this unit, since it was never found in overlying units. It is not clear exactly what caused these fractures to form. Fracture set 1 was probably related to Ouachita tectonism partly because it strikes perpendicular to the thrust front, but it also affects all units at this locality.

Figure 44: Picture illustrating the three fracture sets in Unit III at the Bend River locality

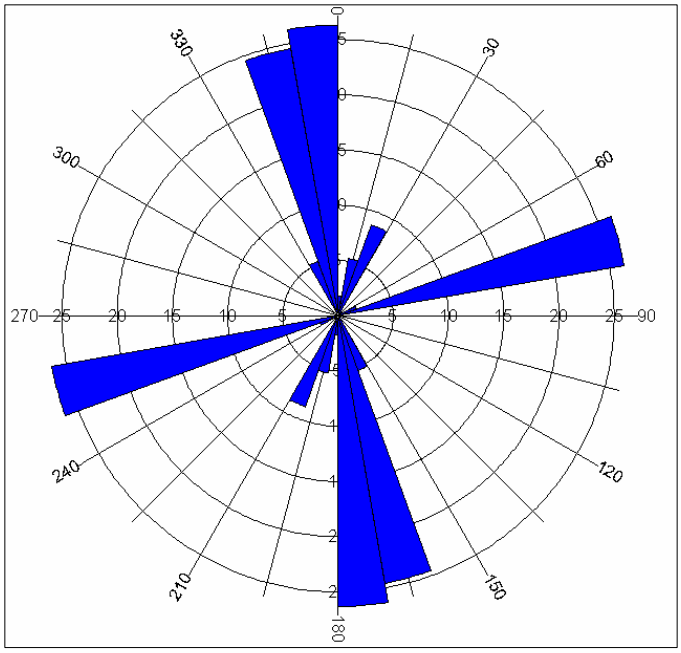

Figure 45 Rose diagram illustrating the orientations of fractures measured in Unit III

When data is combined (Figure 46), one dominant trend stands out from the Bend River locality. The Llano uplift did have an effect on the fracture orientations at this locality. I observed fractures related to the Ouachita orogeny, but unlike any other locality in this thesis, the Bend River locality did not display a fracture set indicative of extension along the Balcones fault zone. The Llano Uplift probably shielded the rocks at this locality from extensional forces.

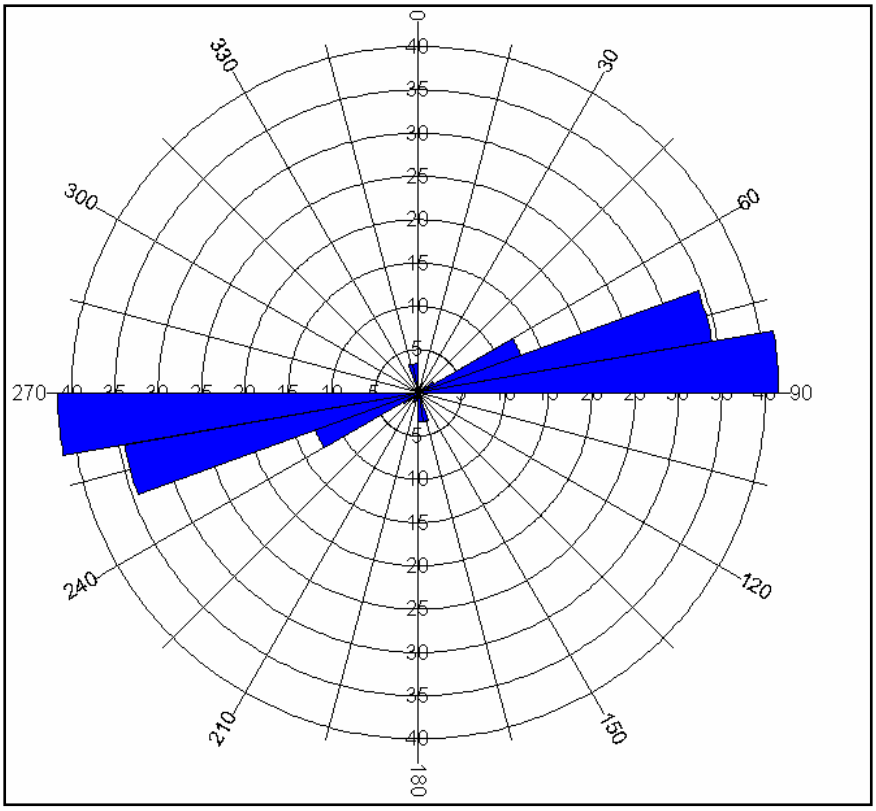

Figure 46: Rose diagram that combines data from all three units

Changes in orientation from one unit to another are likely the result of strain partitioning. A steep cliff, possibly part of an anticlinal feature or fault, exists immediately across the road to the south from this locality. The beds along the river dip towards the hill, indicating that the hill may be part of a local fold or fault. Also, on the property immediately across the road the heavily bioturbated member of Unit II was seen along the cliff above my head (Figure 47).

Figure 47: An image showing the same ductile member of Unit II from the river bed containing Ophiomorpha above my head. This image taken on Laura White's property across the street from the Bend River locality.

The presence of ductile units, such as the one described in Unit II, appeared to have an effect on fracture orientation as well as fracture intensity. An enigmatic feature of this outcrop was the change in fracture orientations as a result of strain partitioning. Fractures were observed to be isolated within specific layers, a phenomenon which likely occurred as a result of mineralogic differences as well as bedding thickness (Figures 48 & 49).

Figure 48: An example of the Marble Falls Limestone from Laura White's property illustrating the layering of fractures, which is a function of bed thickness, and lithology.

Figure 49: Another example of the Marble Falls Limestone from Laura White's property illustrating the layering of fractures, which is a function of bed thickness, and lithology.

X-Ray Diffraction

Six samples from the Bend River were taken and analyzed with powder diffraction: BR1, BR2, BR3, BR4, BR5, and BR6 (Appendix A). Samples BR1 and BR2 came from the Smithwick Shale in Unit I. BR2 contained slightly less fractures then BR1, both were tested for differences in mineralogic components. BR2 contained more clay minerals then BR1; these clay minerals may have had an effect on fracture intensity.

BR3 and BR5 came from the ductile member of Unit II. BR 4 and BR6 came from the brittle member of Unit II. The members of Unit II clearly showed that differences in mineralogic make up had an effect on fracture intensity. The results were inconclusive because the amount of the calcite present in the samples masked any chance of determining what clay minerals were present.

Clay extraction techniques were used to determine which of the two units contained more clay minerals. BR 4 and BR 5 were chosen for this experiment. The clay extraction showed clearly that sample BR5 from the ductile unit, and contained more Illite then sample BR4 (Appendix B).

Sample	**Illite Peaks (Counts)**	**Rock Characteristics**
BR4	2,465	Brittle Behavior
BR5	10,521	Ductile Behavior

Table 4: A table illustrating the correlation between clay content and mechanical behavior observed in the samples taken from the Bend River locality.

.

Archer Ranch

Location

The Archer Ranch Locality is located 4.3 miles east of Johnson City, is located between the Llano Uplift and the Ouachita thrust belt.

Name	Coordinates
The Archer Ranch Locality	30° 16' 39.64" N; 98° 19' 28.28" W

Table 5: The location of the Archer Ranch locality

Previous Studies

In 1956, this locality was first described in a guidebook published by the San Angelo Geological Society (Barnes et al, 1956). Barnes et al. (1956) conducted extensive studies on the rocks units exposed at the Archer Ranch locality. A geologic map of the Archer Ranch Locality is provided in Figure 50. McCrary (2003) discussed the sequence stratigraphy of the Pedernales Falls State Park, a locality approximately four miles east of the Archer Ranch.

Outcrop Description

Rock units (oldest to youngest) exposed at the Archer Ranch are: (1) Honeycut Formation (Ordovician.), (2) Stribling Formation (Devonian), (3) Ives Breccia (Mississippian), (4) Marble Falls Limestone (Pennsylvanian), and (5) Travis Peak Formation (Cretaceous) (Figure 51).

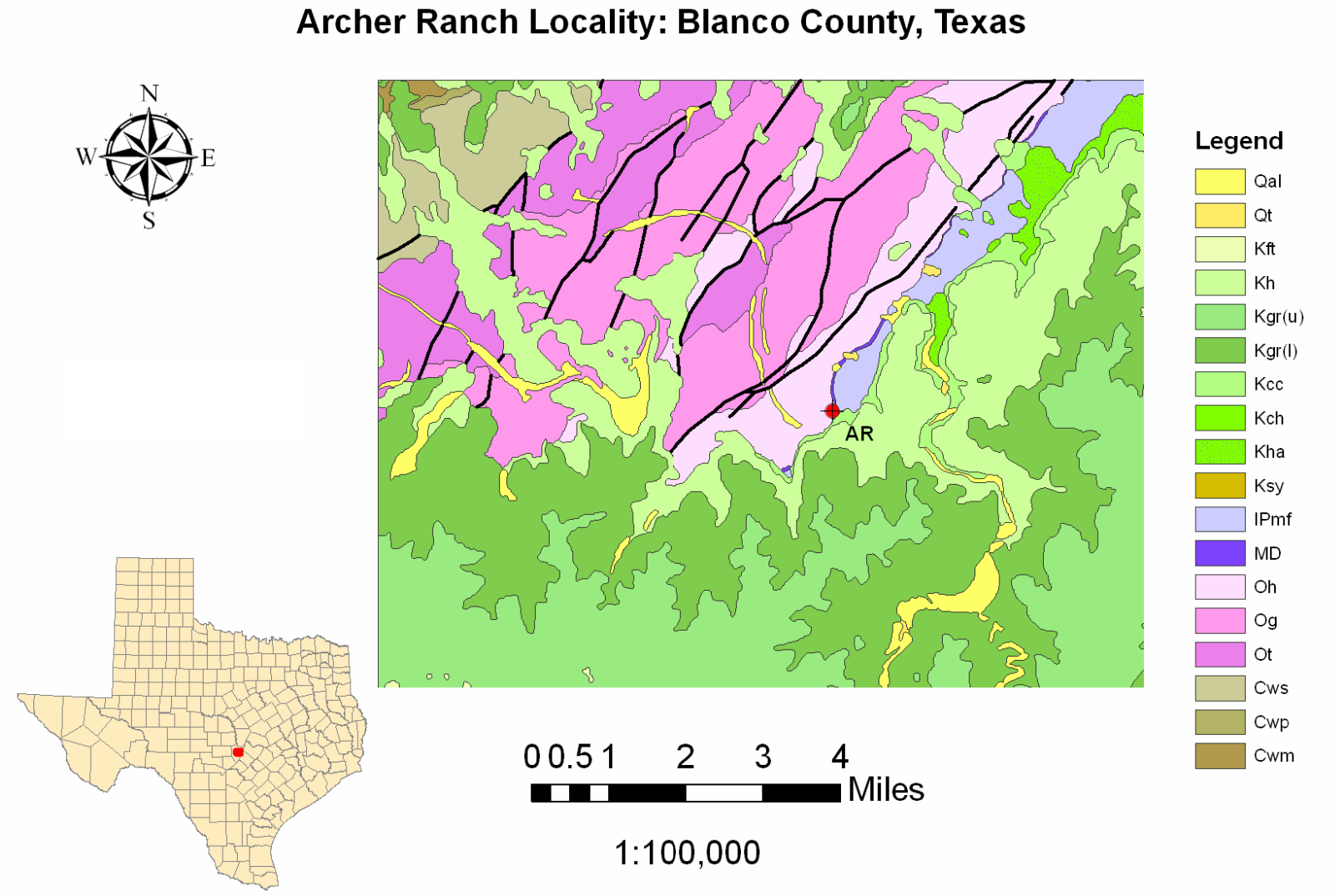

Figure 50: Geologic map of the Archer Ranch locality. Map digitized from Barnes (1981).

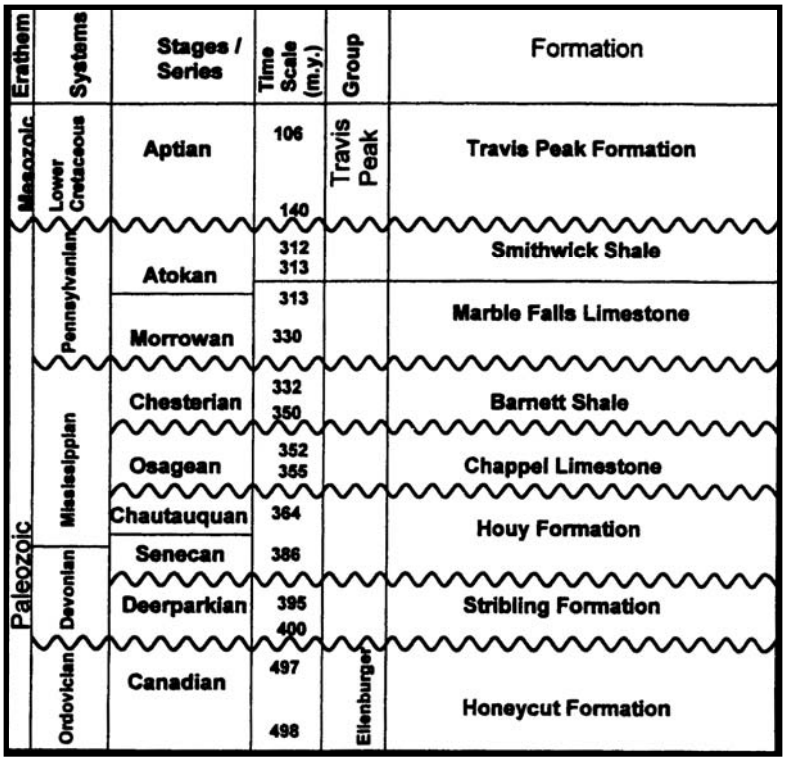

Figure 51: Generalized stratigraphic nomenclature of the Archer Ranch area. From McCrary (2003).

The thickest section (679 feet) of Honeycut rocks in the Llano uplift is exposed along the Pedernales River (Barnes et al., 1956). The Honeycut is divisible into three units in this section: (1) a lower alternating limestone-dolomite unit, (2) a middle dolomite unit, and (3) an upper limestone unit (Barnes et al., 1956). The upper unit is exposed along the riverbed at this locality. The Honeycut is interpreted as having been deposited in an open marine shelf environment in relatively deep water. It occurs as a microcrystalline, light gray limestone occurring in beds ranging in thickness from 6” to 2’. Angular fragments of chert, which are somewhat translucent to gray with an olive-green cast, are sparsely distributed throughout the Honeycut (Barnes et al., 1956).

Disconformably overlying the Honeycut is the Devonian age Stribling Formation. The Stribling formation is approximately 10 feet thick. It is described as being a microgranular limestone, medium light gray in color to reddish gray with a yellowish gray to olive-gray cast (Barnes et al., 1956). The Stribling occurs in wavy, thin-bedded, cherty beds (McCrary, 2003). Except for the lower 2 feet, the Stribling consists mostly of chert, which is translucent to subtranslucent in the upper portion, and ranges downward to an opaque brownish to grayish color occurring in irregular lenses and false joint fillings (Barnes et al., 1956). The Stribling is interpreted as having been deposited in relatively shallow water with medium energy due to the wavy nature of the bedding and the crinoidal wackestone facies (McCrary, 2003).

Disconformably overlying the Stribling is the Mississippian – Devonian age Ives Breccia. Approximately 18" thick at this locality, the Ives Breccia is composed of mostly angular chert fragments and a small amount of phosphatic limestone matrix (Barnes et al., 1956). According to Barnes et al. (1956), the Ives Breccia at this point seems to be the accumulation, essentially in place, of the insoluble constituents of the underlying Stribling formation.

McCrary (2003) claimed that a small exposure of Barnett Shale exists at this locality, and lies on top of the Ives Breccia (Figure 52). As early as 1946, Dr. G.A. Cooper determined that the biohermal unit is Morrowan in age, based on fossil assemblages (Barnes et al., 1956). Because of the lack of elaboration concerning this fossil assemblage, samples from were taken from the black shale for analysis of Conodonts. Within this unit, two types of Conodonts were found: (1) *Idiognathodus* and (2) *Idiognathoides* (D. Boardman, 2007, personal communication). The presence of these

two types of Conodonts conclusively shows that this unit is Atokan in age, and therefore cannot be Barnett Shale.

Figure 52: The lower biohermal member of the Marble Falls Limestone

The Marble Falls Limestone lies unconformably above the Ives Breccia, and measures approximately 19 feet in thickness (McCrary, 2003). Because of the Conodont work, the Marble Falls at this locality must represent the portion of the Marble Falls that is time-transgressive occurring across the Morrowan-Atokan boundary. The spiculite unit is dark gray and calcareous containing a mat of spicules in a calcareous groundmass (Barnes et al., 1956). Some of the Marble Falls section contains traces of iron, which

turns the rock various shades of yellow and orange depending on the amount of iron present in the rock mass.

The Lower Cretaceous Cow Creek Limestone of the Travis Peak group lies disconformably on top of the Marble Falls, and represents a period of non-deposition spanning 170 million years (McCrary, 2003). Deposition did not occur in the foreland of the Ouachita mountain belt until the mountains had eroded enough to allow for deposition. By the lower Cretaceous, the mountains were lowered enough to allow deposition of Cretaceous sediments directly atop older Paleozoic sediments. Two pictures (Figures 53 and 54) illustrate the Archer Ranch locality and the rock units present.

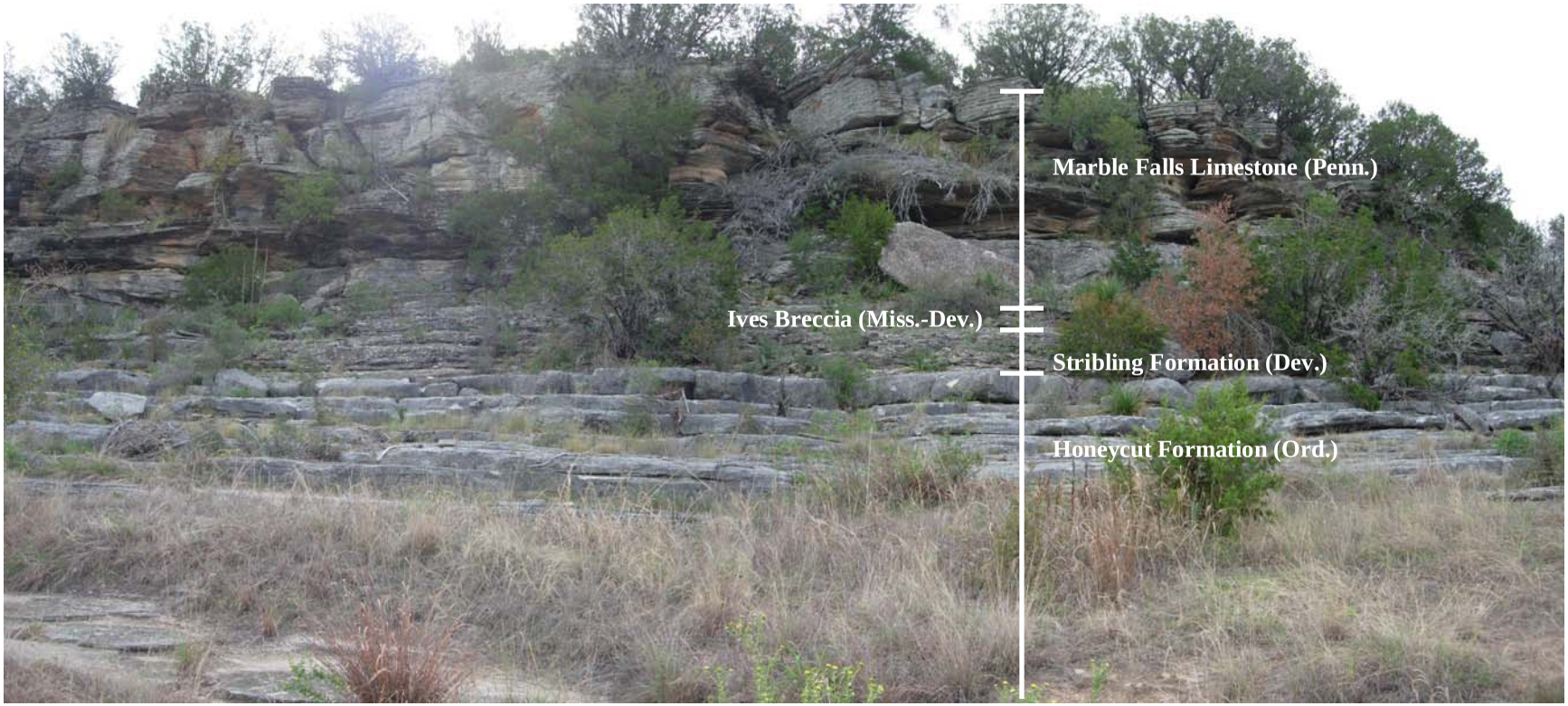

Figure 53: A picture of the Archer Ranch locality, and the positions of the rock formations present.

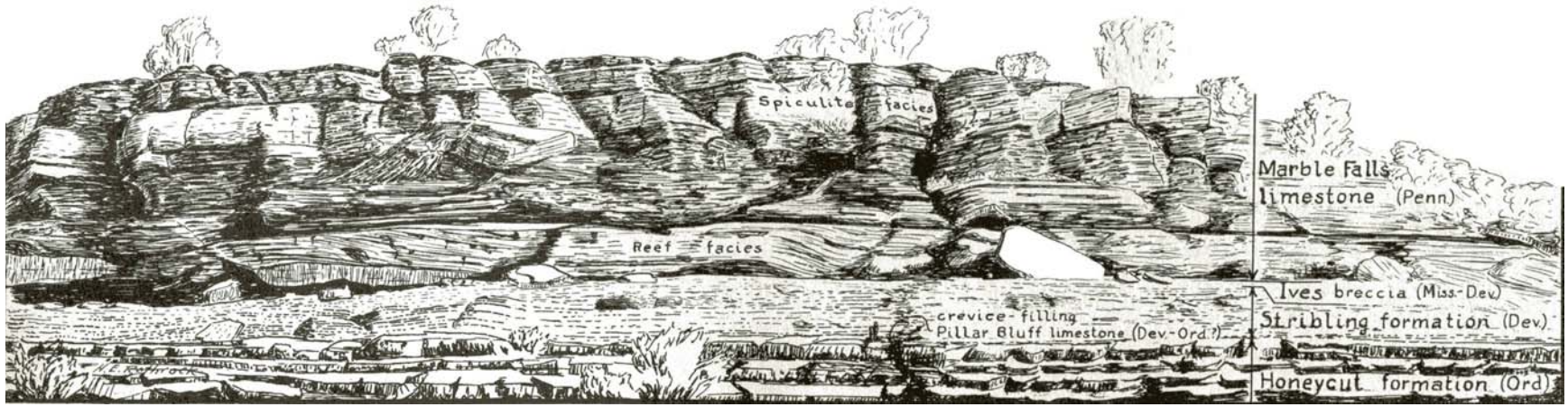

Figure 54: The original description of the Archer Ranch locality from Barnes et al. (1956)

Fractures

The Honeycut Formation

317 fractures were measured in the Honeycut formation, of these 115 contained calcite cement (Figure 55). The healed fractures often had aperture measurements ranging in width from ranging from 1/16" to 1/4". All fractures measured were vertical, indicating Mode I displacement.

Figure 55: Healed fractures in the Honeycut at Archer Ranch

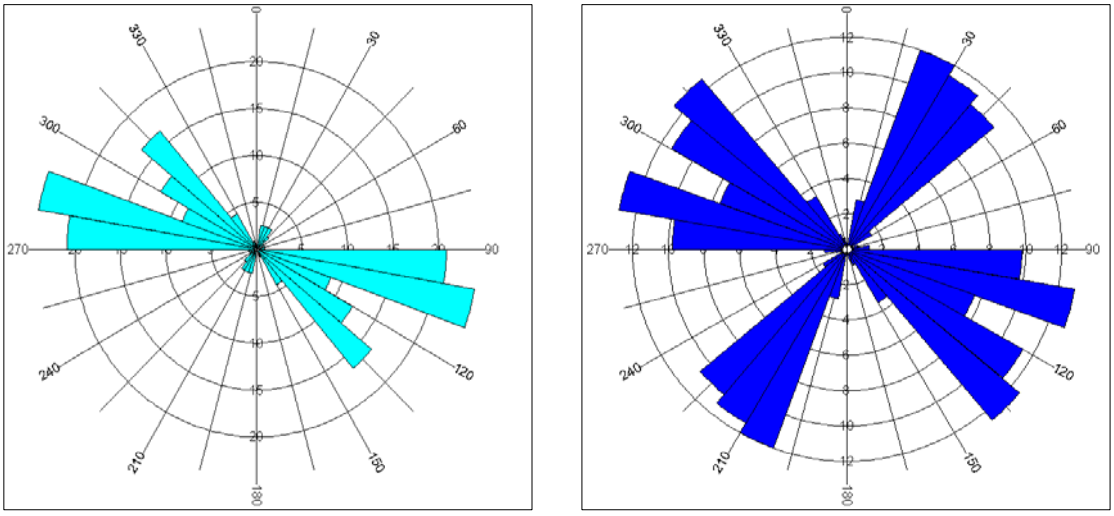

Figure 56: Rose diagrams showing orientations of fractures measured in the Honeycut Formation. Fractures containing mineral fill are illustrated in the diagram on the left, while those containing no mineral fill are represented in the diagram on the right.

Three distinct sets (Figure 56) of fractures were measured in the Honeycut: (1) N75^{o}-89^{o}W, (2) N45^{o}-60^{o}W, and (3) N18^{o}-55^{o}E. Fracture sets 1 and 2 were both observed to cross-cut each other. Thus, these sets likely formed at the same time. Fracture set 3 was the youngest and was observed on multiple instances crosscutting or terminating at the older fracture sets. Fracture set 3 was also the hardest to see because the outcrop strikes parallel to this set at N35^{o}E, dipping 5^{o}SE.

The thickness of individual beds within the Honeycut seemed to have an effect on fracture intensity. Thinner beds (Figure 57) contained fractures adequate for measurement, while the thicker beds (Figure 58) contained noticeably less fractures.

Figure 57: Thinner beds within the Honeycut contained significantly higher fracture intensities

Figure 58: Thicker beds within the Honeycut contained significantly lower fracture intensities

The Marble Falls Formation

194 fractures were measured in the Marble Falls formation. All fractures measured were vertical and none contained any mineral fill. The same three trends seen in the Honeycut were also seen in the Marble Falls: (1) N75^{o}-89^{o}W, (2) N45^{o}-60^{o}W, and (3) N18^{o}-55^{o}E (Figure 59). The Marble Falls differed from the Honeycut because there were no cemented fractures. Also, fracture set 3 was much less pronounced.

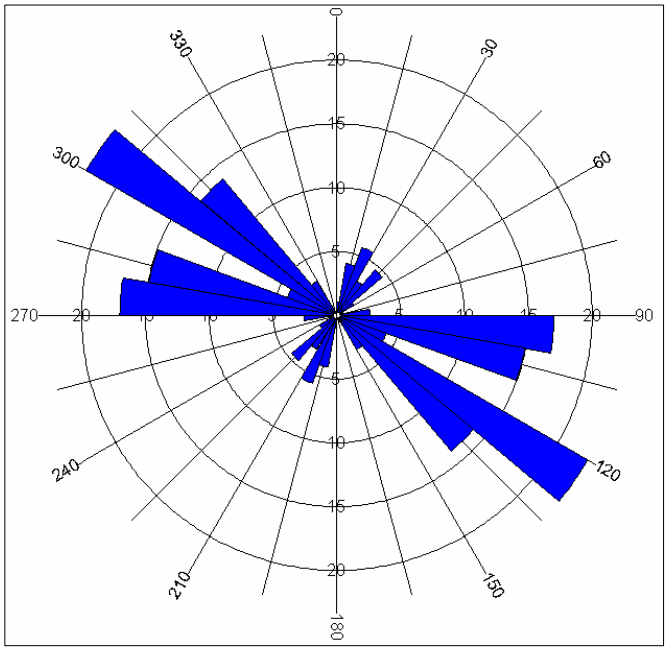

Figure 59: Rose diagram illustrating fracture measurements in the Marble Falls at Archer Ranch

The Archer Ranch locality, unlike the Bend River locality did not exhibit changing fracture orientations from one lithologic unit to another. Here, the same three trends were seen in every unit measured. The two sets of Ouachita related fractures (sets 1 and 2) illustrate the effects seen as a result of the fold-thrust belt

wrapping around the Llano Uplift. This locality serves as an extreme example of how fracture orientations can change in the presence of a local anomaly in the stress field (a massive granitic pluton in this case).

Three main trends of fractures exist in the entire Archer Ranch locality (Figure 60), one related to the east-west component of the Ouachita Orogeny (fracture set 1), one related to the bend or 'kink' in the thrust belt that occurs when the orogen interacts with the Llano Uplift (fracture set 2), and one related to the opening of the Gulf of Mexico (fracture set 3).

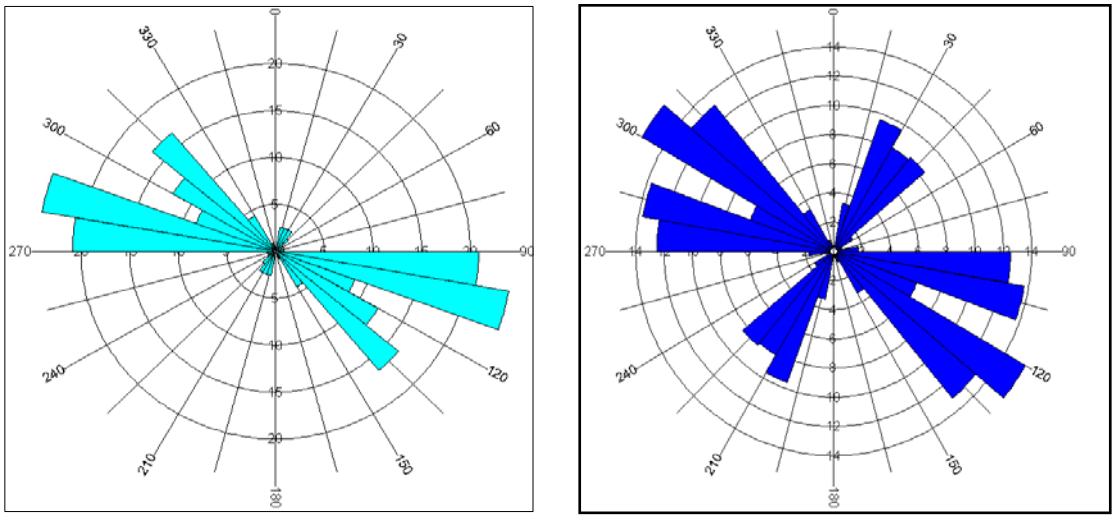

Figure 60: Rose diagrams showing the orientations of all fractures measured at the Archer Ranch Locality. The diagram on the left contains the orientations of fractures containing mineral fill found only in the Honeycut. The diagram on the right is the summation of all fractures containing no mineral fill from both the Honeycut and the Marble Falls.

X-Ray Diffraction

Six samples from Archer Ranch were taken and analyzed with powder diffraction: AR1, AR2, AR3, AR4, AR5, and AR6 (Appendix A). AR1 and AR2 came from the Honeycut Formation, and were analyzed to determine if mineralogy or

bed thickness controlled fracture intensity. AR1 came from the thicker unit with a lower fracture intensity; AR2 came from a thinner bed with a higher fracture intensity. XRD results were inconclusive because the amounts of quartz and calcite masked any clay minerals that might be present (Appendix A). Clay mineral extraction demonstrated that AR1 had higher illite concentrations as compared to AR2 (Appendix B). Thus, it appears as if mineralogy (i.e., clay content) as well as bed thickness controlled the degree of fracture intensity in the Honeycut Formation.

Sample	**Illite Peaks (Counts)**	**Rock Characteristics**
AR1	194	Brittle Behavior
AR2	9,263	Ductile Behavior

Table 6: A table illustrating the correlation between clay content and mechanical behavior observed in the samples taken from the Archer Ranch locality.

Subsurface Correlation

FMI logs are used to quantify properties such as fracture count, fracture spacing, the presence or absence of mineral fill, orientation strike, and dip. However, the inability to study crucial elements such as cross cutting relationships, and the interaction of the fractures beyond the image of the borehole wall severely limits the understanding of the intricacies contained within these fracture sets.

Two wells with horizontal FMI's in the Barnett Shale were donated for this project from EOG Resources: one in Palo Pinto County, the other in Erath County. The well from Palo Pinto County serves as a subsurface comparison for the Possum Kingdom outcrop and illustrates the deformation resulting from stresses observed on the western edge foreland basin. The well in Erath County, which serves as a subsurface comparison for the Brownwood and Bend River localities, represents the deformation resulting from tectonic forces observed on the southwestern edge of the foreland basin.

Four types of fractures are described from FMI logs: open, healed, partially healed, and drilling induced. Open fractures, also called 'conductive fractures' have no mineral fill in the fracture plane. Healed, or 'resistive fractures' are sealed with mineral fill. Partially healed fractures are those where the fracture plane is only partially sealed with mineral fill. Typically fracture fill consists of calcite. However, fractures can also contain subsidiary amounts of quartz, albite, pyrite, barite, and dolomite (Gale et al., 2007). In this study, healed and partially healed subsurface fractures were combined into one group, since healed and partially healed fractures could not be discriminated in the outcrop. Finally, drilling induced fractures are those

fractures that develop as a result of the drilling process, and are thought to represent modern horizontal stresses existing in the basin. The drilling induced fracture set was not considered in this study since the focus is on fractures related to the Ouachita Orogeny and the formation of the Gulf of Mexico. Similarly, only those outcrop fractures that demonstrated repeatable, systematic trends, due to ancient tectonic events, were included in the correlation.

Well A: Palo Pinto County

The well from Palo Pinto County contained 231 fractures in the length of the borehole (Figure 61). Of these, 90 contained no mineral fill, 70 were partially healed, and 71 were completely healed. Of the 231 fractures measured, the average dip angle was 87.35^{o}, indicating mode I opening nearly perpendicular to bedding. Four orientations were observed in the fractures in this well: (1) Northwest-southeast; (2) north-south; (3) N20^{o}-30^{o} E; (4) N45^{o} -60^{o} E.

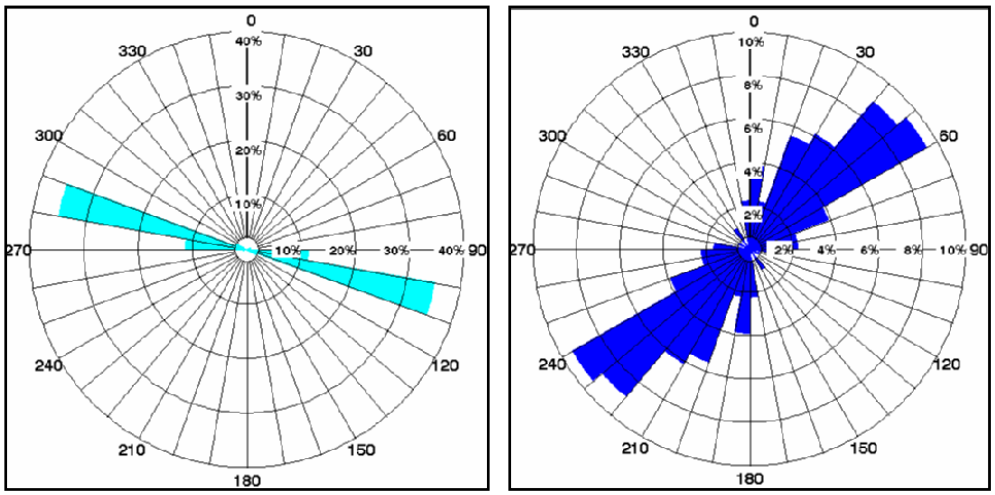

Figure 61: Rose Diagrams from Well A. The diagram on the right is a plot of fractures containing no mineral fill, while the plot on the left shows all fractures that contained mineral fill.

Ouachita related fractures are thought to be represented by fracture set 1, because it contains mineral fill. It is conventionally believed that fluid migration occurs syntectonically with compression. Set 2 is possibly related to the proximity to the Bend Arch, or local structures in the area. Sets (3) and (4) are likely related to modern forces, possibly extension

Well B: Erath County

This well from Erath County contained 1467 natural fractures in the length of the borehole (Figure 62). 127 fractures contained no mineral fill, 566 were partially healed, and 774 were completely healed. The average dip angle for all of the fractures was 87.83^{o}, again indicating mode I opening. Three dominant orientations were observed in this well: (1) East-West; (2) N10^{o} -30^{o} E; (3) N50^{o} -60^{o} E. Set 1, which contains mineral fill is interpreted to be related to compression. Set 2 is likely related to modern forces acting in the subsurface – possibly related to extension. Set 3, which sometimes contains mineral fill is interpreted as being related to known subsurface structures in the vicinity of the wellbore.

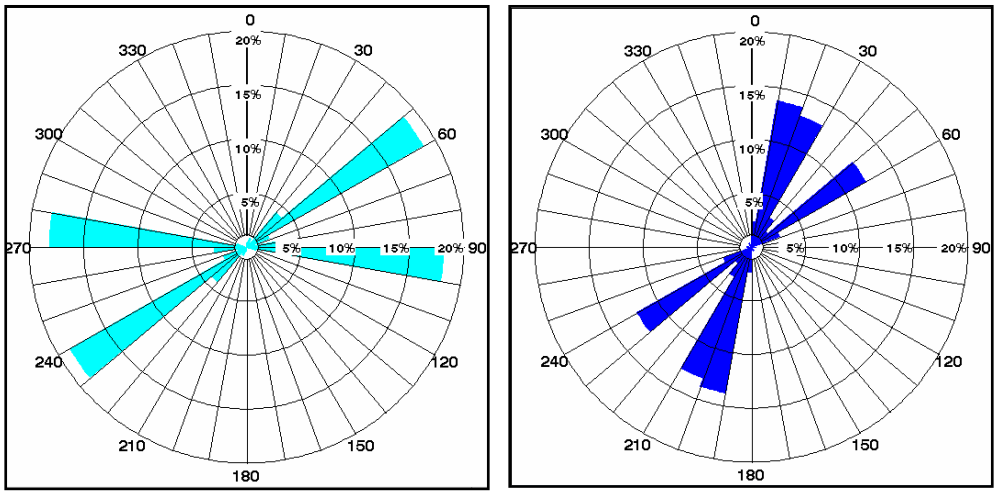

Figure 62: Rose Diagrams from Well B. The diagram on the right is a plot of fractures containing no mineral fill, while the plot on the left shows all fractures that contained mineral fill.

Ouachita related fractures are thought to be east-west due to the fact that this orientation does not appear in the open fracture sets. The healed northeast-southwest fracture set may be related to local folds or faults in the vicinity of the borehole, due

to the presence of mineral fill. However, the high-angle northeast-southwest set that is not healed may be related to the opening of the Gulf of Mexico.

CHAPTER V

CONCLUSIONS

This thesis was successful in demonstrating the following:

- Tectonically related natural fracture sets are correlative within 10^{o}-15^{o} from one locality to another in the orogenic foreland of the Ouachita fold-thrust belt.
- Fractures related to compression typically contained mineral fill, which is commonly thought to occur syntectonically with compressive events.
- Local structures such as folds, faults, salients (Llano Uplift), and recesses (South Oklahoma Aulacogen) caused fracture orientations to deviate from the regional trend. Thus, proximity to any of these features would have an effect on fracture orientation.
- Fracture sets observed in the surface are similar, and therefore correlative to fracture sets observed in the Fort Worth Basin in regards to their origin and crosscutting relationships
- Correlation of surface and subsurface fracture sets allowed the relative dating of fractures observed in FMI logs. Such a correlation has not yet been published.

- Extensional tectonics, related to the opening of the Gulf of Mexico was a major element in all subsurface fractures. It was also a major element in three of the four surface locations, the only exception being the Bend River locality. Here, the Llano Uplift acted as a shield, not allowing extensional tectonics to affect orientations within the uplift itself.
- A much better understanding of the intricacies within fracture sets was observed by the J-hooking and strain-partitioning phenomenon observed at the Bend River and Archer Ranch localities.
- Clay mineralogy, as determined by x-ray diffraction was a major control on the overall brittle or ductile nature of rocks measured in the thesis area. The amounts of clay minerals present were shown to have an effect on fracture intensity.

This study also raised questions, which could be addressed in future research:

- More localities within the Paleozoic rocks need to be studied in order to provide a more extensive dataset. A higher sampling resolution would better test the hypothesis that these fracture sets are not just coincidental, but rather are clear trends depicting two stress regimes: (1) compressional and (2) extensional.
- Fractures in Cretaceous rocks should be measured. These localities should be chosen in relatively close proximity to the localities measured in the Paleozoic rocks. A comparison of fracture patterns from Cretaceous and Paleozoic rocks would delineate fracture sets related to tectonic forces from the Ouachita Orogeny versus fracture sets related to forces occurring throughout the Mesozoic and Cenozoic.

- Deviations in fracture orientations relative to regional stress directions result from proximity to local structures. Higher resolution studies that map the extent of these local structures would help quantify the effects of these local structures on regional fracture patterns.

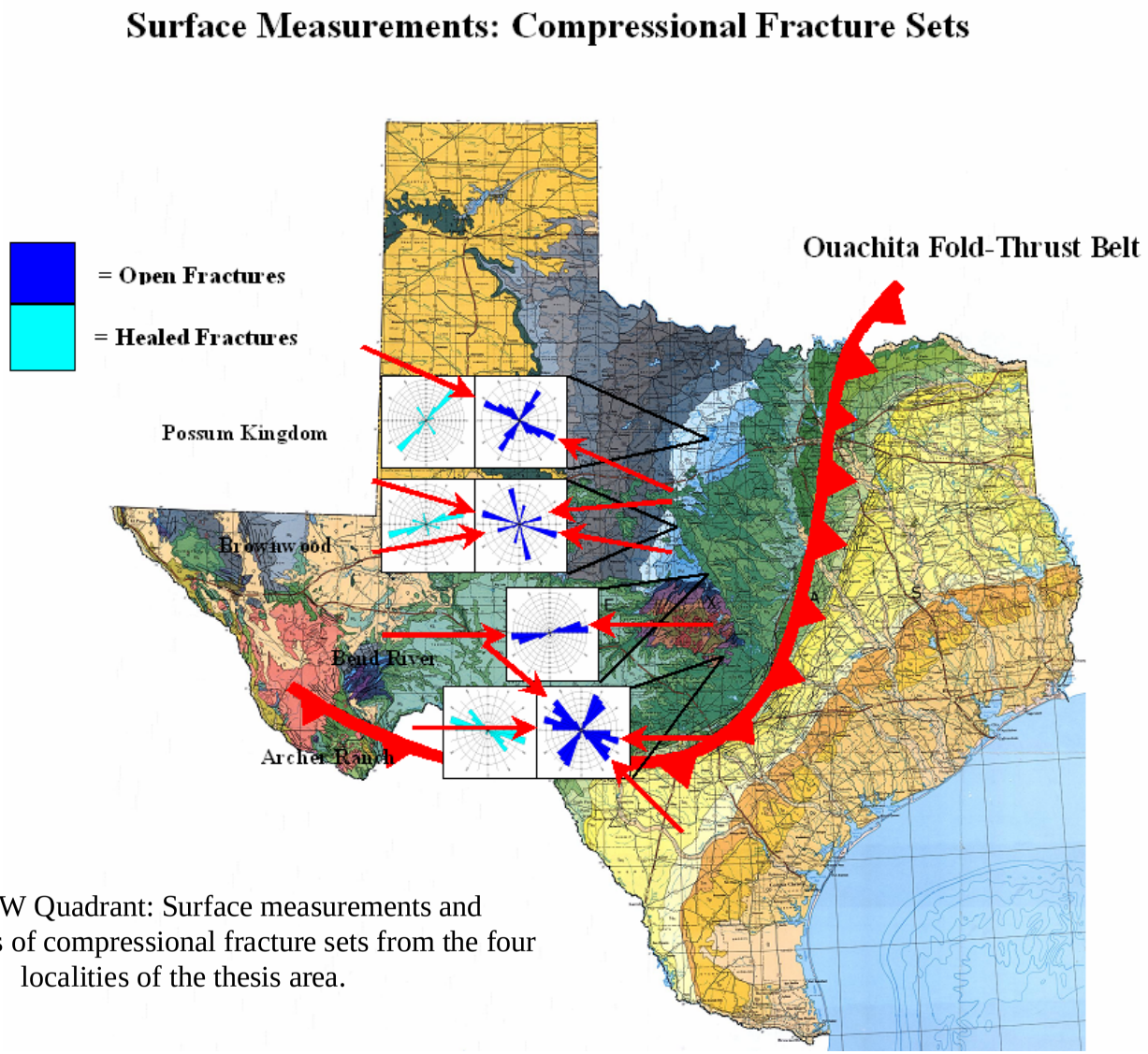

Plate I NW Quadrant: Surface measurements and interpretations of compressional fracture sets from the four localities of the thesis area.

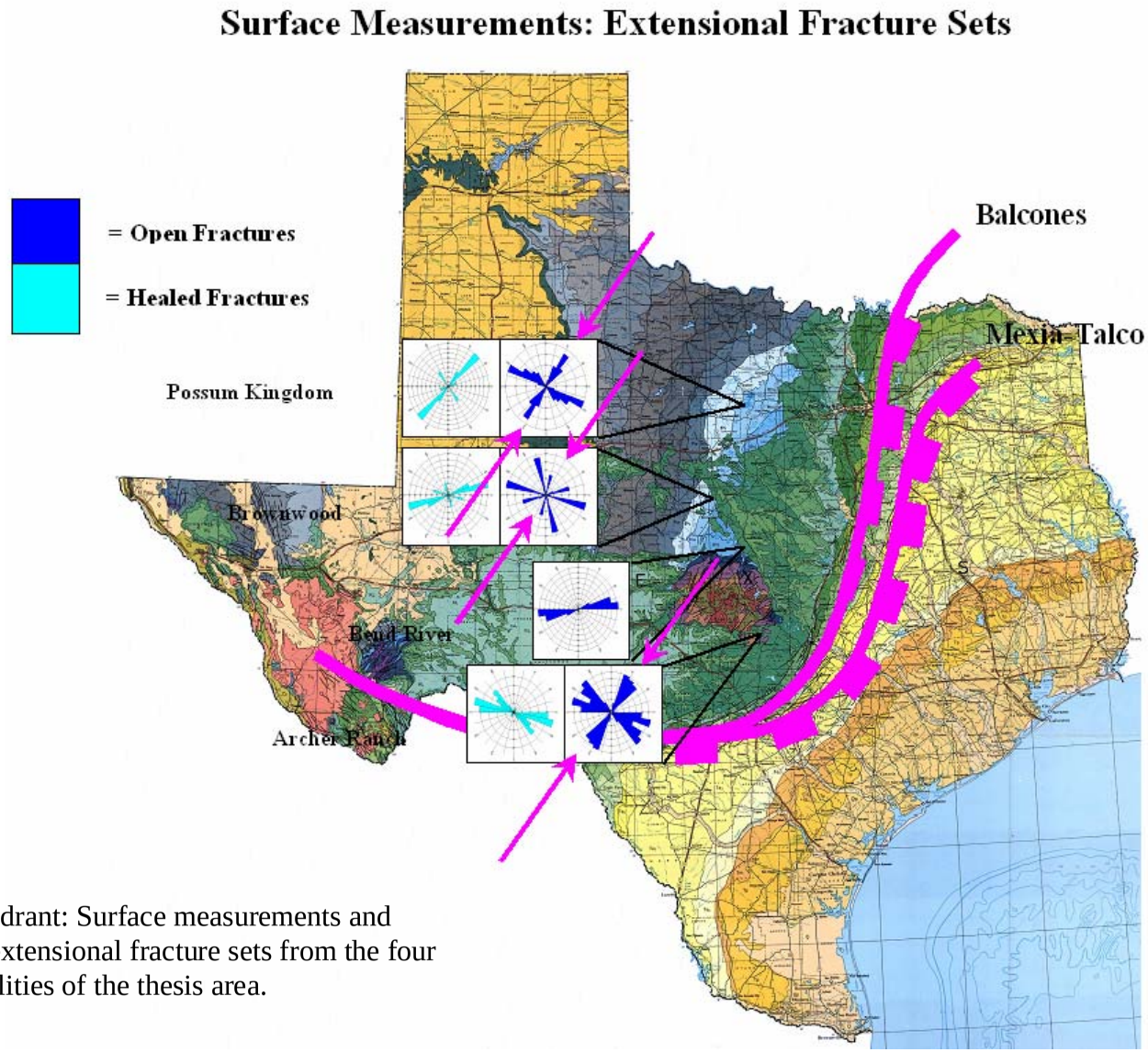

PlateI SW Quadrant: Surface measurements and interpretations of extensional fracture sets from the four localities of the thesis area.

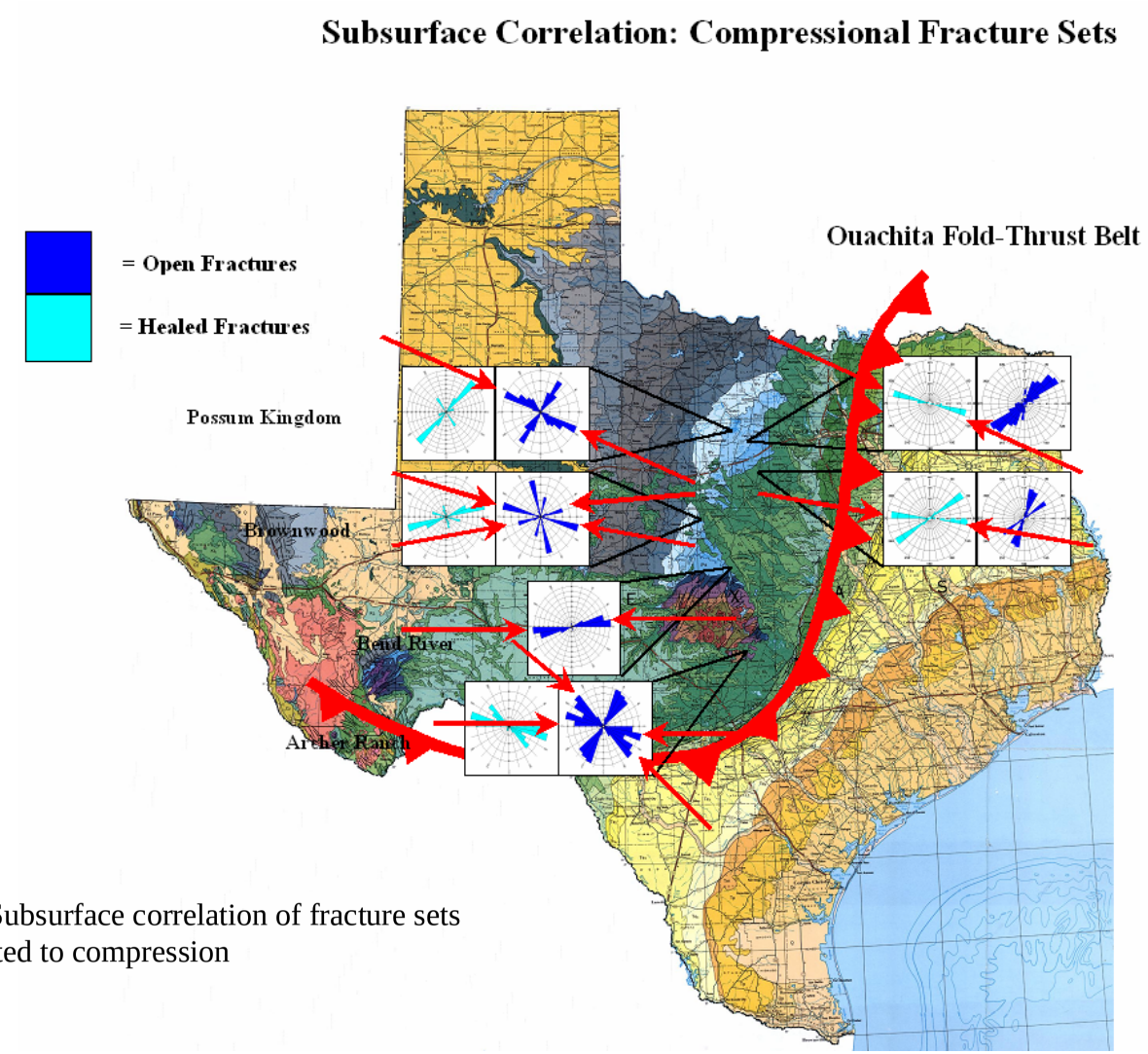

Plate I NE Quadrant: Subsurface correlation of fracture sets related to compression

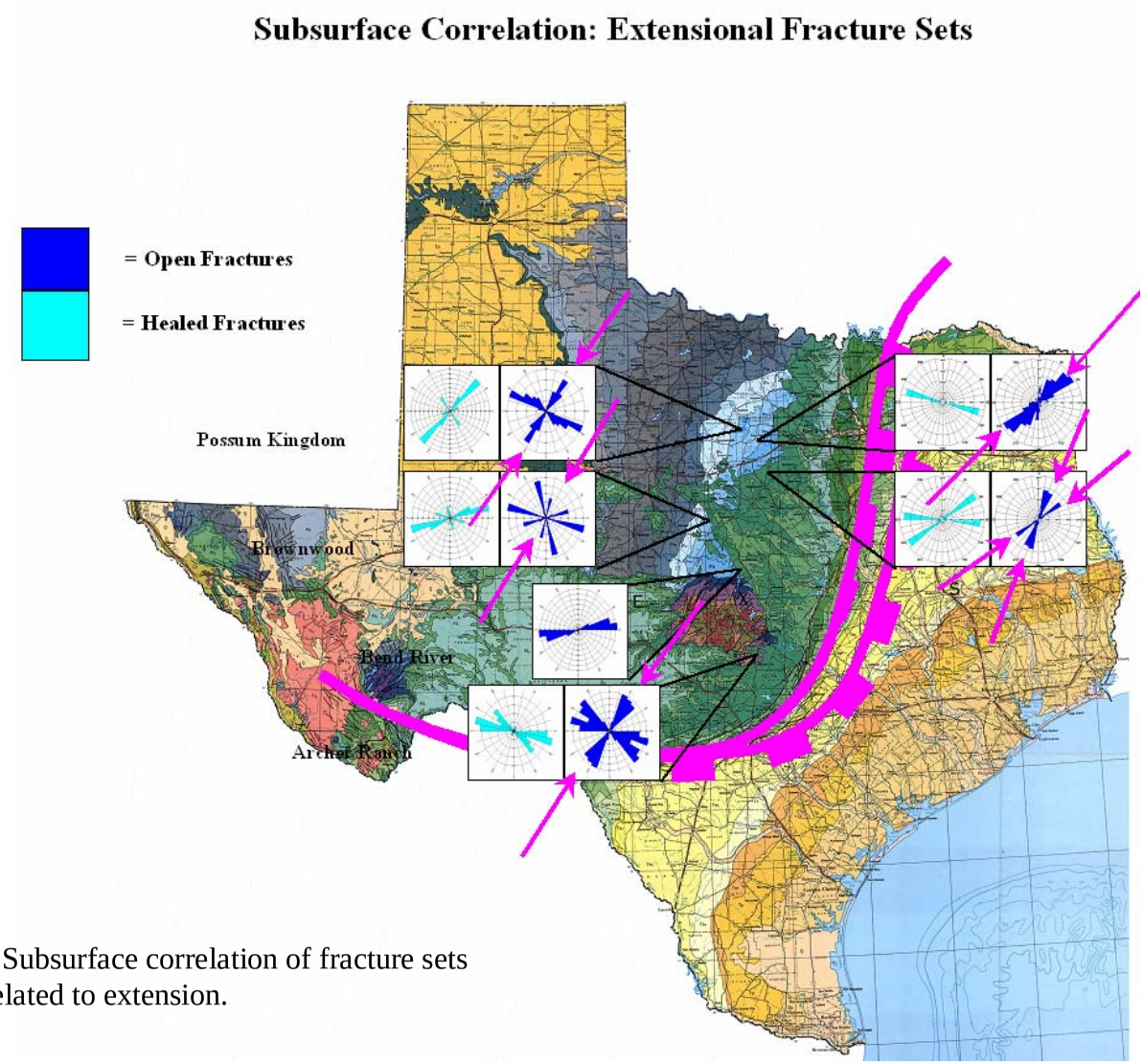

Plate I SE Quadrant: Subsurface correlation of fracture sets related to extension.

REFERENCES

Barnes, Virgil E., Pavlovic, Robert, Hazzard, Roy T., 1956, Four Provinces Field Trip: Central Mineral Region, Balcones Fault Zone, Kerr Basin, Rio Grande Embayment: in San Angelo Geological Society, March 16-17, 1956, Guidebook, (leaders) Virgil E. Barnes, Robert Pavlovic, and Roy T. Hazzard, p. 23-30.

Barnes, Virgil E., 1981, Geology of the Pedernales Falls quadrangle, Blanco County, Texas, University of Texas, Austin, Bur. Econ. Geology Geol. Quad. Map 49, *in* V.E. Barnes (director): The Geologic Atlas of Texas, Llano Sheet, Virgil E. Barnes Memorial Edition. The Bureau of Economic Geology, Austin, TX, 1986.

Beaumont, C., 1981, Foreland basins: Geophysical Journal of Royal Astronomical Societs, y. 65, no. 2, p. 291-329.

Blakey, R.C.. "Paleogeography and Geologic Evolution of North America." 4 December 2006. Northern Arizona University. 17 March 2007. <http://www4.nau.edu/geology/master.html?http://www4.nau.edu/geology/blakey.html>

Brace, W.F., 1961, Dependence of fracture strength of rocks on grain size, Proceedings of the 4th symposium on Rock Mechanics, pp. 99-103.

Burke, K., and Dewey, J.F., 1973. Plume-generated triple junctions: key indicators in applying plate tectonics to old rocks. Journal of Geology, 81, p. 406-433.

Caran, C.S.; Woodruff, C.M.; Thompson, E.J., 1981, Lineament analysis and inference of geologic structure; examples from the Balcones/Ouachita trend of Texas: Gulf Coast Assoc. Geol. Socs. Trans., v. 31, p. 59-69.

Dietz, R.S., and Holden, J.C., 1970. Reconstruction of Pagaea: breakup and dispersion of continents, Permian to Present. Journal of Geophysical Research, 75, p. 4939-4956.

Eargle, H.E., 1960, Stratigraphy of Pennsylvanian and lower Permian rocks in Brown and Coleman counties, Texas: U.S.G.S. Prof. Paper 315-D, p. 55-77, plates 25-30, figs. 11-12.

Flawn, P.T.; King, P.B.; Weaver, C.E., 1961, The Ouachita System. The University of Texas at Austin, Bureau of Economic Geology: Austin, TX. 401 p.

Flippin, J.W., 1982, The stratigraphy, structure, and economic aspects of the paleozoic strata in Erath county, north-central Texas, *in*, Martin, C.A. (ed.): Petroleum Geology of the Fort Worth Basin and Bend Arch Area, Dallas Geological Society, pp. 129-155.

Freund, R., 1974, Kinematics of Transform and Transcurrent Faults, Tectonophysics, vol. 21, pp. 93-134.

Friedman, M., 1969, "Structural Analysis of Fractures in Cores from the Saticoy Field, Ventura County, California," *American Association of Petroleum Geology Bulletin*, vol. 53, no. 2, pp. 367-389.

Friedman, M., 1975, "Fracture in Rock," *Reviews of Geophysics and Space Physics*, vol., 13, no. 3, U.S. National Report 1971-1974, 16th General Assembly International Union of Geodesy and Geophysics, Grenoble, France, August 24-September 6, Peter M. Bell, Ed., pp. 352-358.

Gale, J.F., Reed, R.M., Holder, J., 2007, Natural Fractures in the Barnett Shale and their importance for hydraulic fracture treatments, AAPG Bulletin, v. 91, no. 4, pp. 603-622.

Gallagher, J.J. Jr., 1976, Fracturing of quartz sand grains, Proceedings of the 17th US symposium on Rock Mechanics, pp. 2A4.1-2A4.8

Glockhoff, C., 1973. Geotectonic evolution and subsidence of Bahama platform: discussion. Geological Society of America Bulletin, 84, p. 3473-3476.

Hatcher, Robert D., 1995, Mechanical Behavior of Rock Materials, *in* McConnin, Robert A. (ed.), Structural Geology Principles, Concepts and Problems, Prentice-Hall, Inc., p. 96-110.

Hoskins, Wayne B., 1982, Fracture analysis of Pennsylvanian Carbonate Bank systems, *in* Martin, C.A., ed., Petroleum Geology of the Fort Worth Basin and Bend Arch area: Dallas Geological Society, p. 179-192.

Jamison, W.R., Stearns, D.W., 1982, Tectonic deformation of the Wingate Sandstone, Colorado National Monument, AAPG Bulletin, v. 66, issue 12, pp. 2584-2608.

Klein, C., Hurlbut, C.S., 2002. Analytical Methods in Mineral Science, *in* Mills, C., Tavares, K. (eds.), The 22nd Edition of the Manual of Mineral Science: John Wiley & Sons, Inc., New York, NY, pp. 290-332.

Lacazette, A. "Natural Fracture Types." Al Lacazette's Natural Fractures.com. 17 March 2007. <www.naturalfractures.com>.

Laubach, S.E., Lander, R.H., Bonnell, L.M., Olson, J.E., Reed, R.M., 2004, Opening histories of fractures in sandstone, *in* Cosgrove, J.W., and Engelder, T. (eds.), The Initiation, Propagation, and Arrest of Joints and Other Fractures: Geological Society, London, Special Publications, 231, p. 1-9.

McCrary, Joseph M., 2003, Sequence Stratigraphy of the Marble Falls Limestone, Pedernales Falls State Park, Blanco County, Central Texas: Master's Thesis, Stephen F. Austin State University, Nacogdoches, TX, 130 p.

McNulty, C.L., and Mercer, M.M., 1941, Description of the Rock Cities at Palo Pinto, Texas with an Estimate on the Rate of Rock Creep: Field and Lab, v.9, p. 1-7.

Merrill, G.K., 1980, Road log-Day two, in Geology of the Llano region, central Texas: Guidebook to the Annual Field Trip of the West Texas Geological Society, October 19-21, 1980, p. 60-199.

Moore, D.M., Reynolds, R.C., 1997. Sample Preparation Techniques for Clay Minerals, *in* Moore, D.M., and Reynolds, R.C. (eds.), X-Ray Diffraction and the Identification and Analysis of Clay Minerals: Oxford University Press, New York, NY, pp. 204-226.

Nelson, R., 2001. Geologic Analysis of Naturally Fractured Reservoirs: Gulf Professional Publishing Company; 2 ed., 320 p.

Nicholls, I.N., 1985, A regional subsurface study of the Kerr Basin, south central Texas: Bachelor's Thesis, Baylor University, Waco, TX. 35 p.

Norris, D.K., 1966, "Structural Analysis of the Queensway Folds, Ottawa, Canada," 47th Annual Amer. Geop. Union Meeting, Paper T-85.

Olson, J.E., Pollard, D.D., 1989. Inferring paleostresses from natural fracture patterns: A new method. Geology, 17, 345-348.

Olson, J.E.; Pollard, D.D., 1991. The Initiation and growth of en echelon veins. Journal of Structural Geology, v. 13, Issue 5, pp. 595-608.

Olson, J.E., 2004, Predicting fracture swarms – the influence of subcritical crack growth and the crack-tip process zone on joint spacing in rock, *in* Cosgrove, J.W., and Engelder, T. (eds.), The Initiation, Propagation, and Arrest of Joints and Other Fractures: Geological Society, London, Special Publications, 231, p. 73-87.

Ostrum, M.E., 1961, Separation of clay minerals from carbonate rocks by using acid: *J. Sed. Petrol.* 31, 123-129.

Plummer, F.B., 1943, The Carboniferous Rocks of the Llano Region of Central Texas: The University of Texas Publication No. 4329, issued Feb 1950, 170 p.

Pollard, D.D., Segall, P., 1987. Theoretical displacements and stresses near fractures in rock: with applications to faults, joints, veins, dikes and solution surfaces, *in* Atkinson, B.K. (ed.), Fracture Mechanics of Rock. Academic Press, London, 277-350.

Pollard, D.D., Segall, P., Delaney, P.T., 1982. Formation and interpretation of dilatant echelon cracks. Geological Society of America Bulletin, 93, 1291-1303.

Poole, F.G.; Perry, W.J.; Madrid, R.J.; Amaya-Martinez, R., 2005, Tectonic synthesis of the Ouachita-Marathon-Sonora orogenic margin of southern Laurentia: Stratigraphic and structural implications for timing of deformational events and plate-tectonic model, *in* Anderson, T.H., Nourse, J.A., McKee, J.W., and Steiner, M.B. (eds.), The Mojave-Sonora megashear hypothesis: Development, assessment, and alternatives: Geological Society of America Special Paper 393, p. 543-596.

Ramez, M.R.H; Mosalmy, F.H., 1969, The deformed nature of various size fractions in some clastic sands, Journal of Sedimentary Petrology, v. 39, issue 3, pp. 1182-1187.

Renfro, H.B.; Feray, D.E.; King, P.B., 1979, The Geological Highway Map of Texas, H.B. Renfro Memorial Edition, The American Association of Petroleum Geologists, Tulsa, OK.

Roberts, D.G., and L. Montadert, 1979, Evolution of passive rifted margins – perspective and retrospective of DSDP Leg 48, *in* Montadert, L., D.G. Roberts, et al., Init. Repts., Deep Sea Drilling Proj., Washington, D.C., U.S. Govt. Printing Office, v. 48, p. 1143-1153.

Roepke, H.H., 1970, Petrology of carbonate units in the Canyon Group (Missourian Series), Central Texas: Univ. Texas, Austin, Ph.D. dissertation, *in* V.E. Barnes (director): The Geologic Atlas of Texas, Brownwood Sheet, Monroe George Cheney Memorial Edition. The Bureau of Economic Geology, Austin, TX, 1986.

Shepard, T.M., and J.L. Walper, 1982, Tectonic evolution of the Trans-Pecos, Texas: Gulf Coast Assoc. Geol. Soc. Trans., v. 32, p. 165-172.

Sheridan, R.E., 1971. Geotectonic evolution and subsidence of Bahama platform: discussion. Geological Society of America Bulletin, 82, p. 807-810.

Skehan, J.W., 1968, "Recognition of Faults of Regional Importance by Mapping Joints," 3rd Annual Geological Society of America, Northeastern Sect. Meeting, 2/15-17/68, Program, pp. 56-57.

Stearns, D.W., 1964, "Microfracture Patterns on Teton Anticline, Northwest Montana," *Amer. Geophys. Union Trans.* vol. 45, pp. 79-95.

Stearns, D.W., 1968a, "Fracture as a Mechanism of Flow in Naturally Deformed Layered Rock," *in* A.J. Baer and D.K. Norris (eds.), Kink Bands and Brittle Deformation: Geol. Surv. Can., Paper 86-52, pp. 79-95.

Stearns, D.W., 1968b, "Certain Aspects of Fracture in Naturally Deformed Rocks," *in* R.E. Rieker (ed.), NSF Advanced Science Seminar in Rock Mechanics: Special Report, Air Force Cambridge Research Laboratories, Bedford, Massachusetts, AD 6693751, pp. 97-118.

Stearns, D.W., 1972, "Structural Interpretation of the Fractures Associated with the Bonita Fault," Guidebook 23rd Annual Field Conf., New Mexico Geol. Soc., East Central New Mexico, pp.. 161-164.

Stearns, D.W., and M. Friedman, 1972, Reservoirs in Fractured Rock, American Association of Petroleum Geology, Memoir 16, pp. 82-100.

Stitt, J.H., 1964, Carboniferous stratigraphy of the Bend area, San Saba County, Texas: Univ. Texas, Austin, Master's Thesis, *in* V.E. Barnes (director): The Geologic Atlas of Texas, Brownwood Sheet, Monroe George Cheney Memorial Edition. The Bureau of Economic Geology, Austin, TX, 1986.

Tchalenko, J.S., and N.N. Ambraseys, 1970, Structural Analysis of Dashte Bayaz (Iran) Earthquake Fractures, Geolgical Society of America Bulletin, vol. 81, pp. 41-60.

Van Der Pluijm, B.A.; Marshak, S., 2004, Brittle Deformation, *in* Wiegman, L.A.W. (ed.): Earth Structure, 2nd Edition. W.W. Norton & Company, p. 114-138.

Van der Voo, R., Mauk., F.J., and Franch, R.B., 1976. Permian-Triassic continental configurations and the origin of the Gulf of Mexico. Geology, 4, p. 177-180.

Viele, G.W., 1989, The Ouachita orogenic belt in Arkansas and Oklahoma, *in* Hanshaw, P.M. (ed.), Metamorphism and Tectonics of eastern and central North America: volume 1, contrasts in style of American thrust belts: American Geophysical Union, Washington, D.C., pp. 37-63.

Walper, J.L., 1976. State-of-the-art for assessing earthquake hazards in the United States; plate tectonics and earthquake assessment. Miscellaneous Paper S-73-1, Report 5, March 1976, U.S. Army Engineer Waterways Experiment Station, CE, Vicksburg, Miss., 104 p.

Walper, J.L., 1977, Paleozoic tectonics of the southern margin of North America: Gulf Coast Assoc. Geol. Socs. Trans., v. 27, p. 230-241.

Walper, J.L., Henk, F.H., Loudon, E.J., Raschilla, S.N., 1979, Sedimentation of a Trailing Plate Margin: The Northern Gulf of Mexico: Gulf Coast Assoc. Geol. Socs. Trans., v. 29, p. 188-201.

Walper, J.L., 1980, Geological Evolution of the Gulf of Mexico-Caribbean Region: Canadian Society of Petroleum Geologists, 7, p. 503-525.

Walper, J.L., 1982, Plate Tectonic Evolution of the Fort Worth Basin, *in*, Martin, C.A. (ed.): Petroleum Geology of the Fort Worth Basin and Bend Arch Area, Dallas Geological Society, pp. 237-251.

Walper, J.L; Miller, R.E., 1985, Tectonic evolution of Gulf Coast Basins, *in* Perkins, B.F.; Martin, G.B. (eds.): Habitat of oil and gas in the Gulf Coast. Earth Enterprises Publishing: Austin, TX. pp. 25-42.

Warme, J.E.; Olsen, R.W., 1971, Trace Fossils: A Field Guide to Selected Localities in Pennsylvanian, Permian, Cretaceous, and Tertiary rocks of Texas and Related Papers: The Society of Economic Paleontologists and Mineralogists Field Trip: April 1-3, 1971, p 27-43.

Wermund, E.G., Copeda, J.C., and Luttrell, P.E., 1978, Regional Distribution of Fractures in the Southern Edwards Plateau, and their relationship to tectonics and caves: University of Texas Bureau of Economic Geology, Geological Circular, 78-2, 14-p.

Wermund, E.G., 1966, Geologic Map of Possum Kindgom Vicinity: Graduate Research Center Journal, vol. 35, no. 2, Pl. I, *in* V.E. Barnes (director): The Geologic Atlas of Texas, Abilene Sheet, Frederick Byron Plummer Memorial Edition. The Bureau of Economic Geology, Austin, TX, 1972.

Woodruff, C.M. Jr.; Foley, D., 1985, Thermal Regimes of the Balcones/Ouachita Trend, central Texas: Gulf Coast Assoc. Geol. Socs. Trans., v. 35, p. 287-292.

Yager, M.K., 1961, Pennsylvanian Geology of North-Central, Comanche County, Texas: Master's Thesis, University of Texas, Austin.

Yamaguchi, T., 1965, "Tectonic Study of Rock Fractures," *Journal Geol. Soc. Japan*, vol. 71, no. 837, p. 257-275.

APPENDICIES

APPENDIX A: RESULTS OF X-RAY DIFFRACTION

Possum Kingdom State Park

PK 1: Winchell Limestone, Possum Kingdom Locality

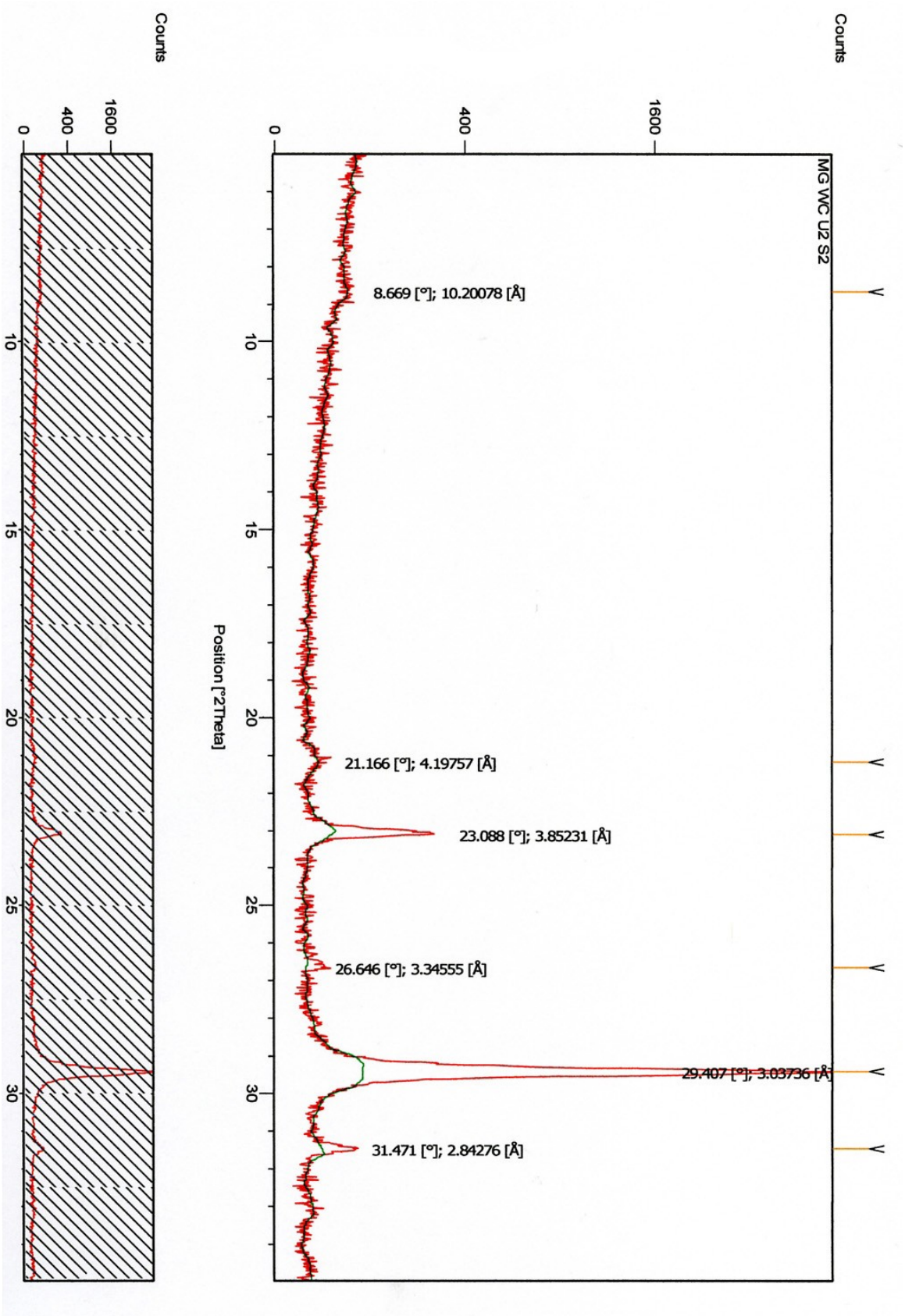

PK 1: Winchell Limestone, Possum Kingdom Locality

Location: 32° 53' 28.92" N; 98° 26' 17.46" W

2Θ	d-Spacing	Mineral
8.669	10.20078	Illite
21.166	4.19757	Unidentified Clay Mineral
23.088	3.85231	Kaolinite
26.646	3.34555	Quartz
29.407	3.03736	Calcite
31.471	2.84276	Kaolinite

Dominant Peaks from X-Ray diffraction and interpretations

Location of sample for XRD

PK 2: Winchell Limestone, Possum Kingdom Locality

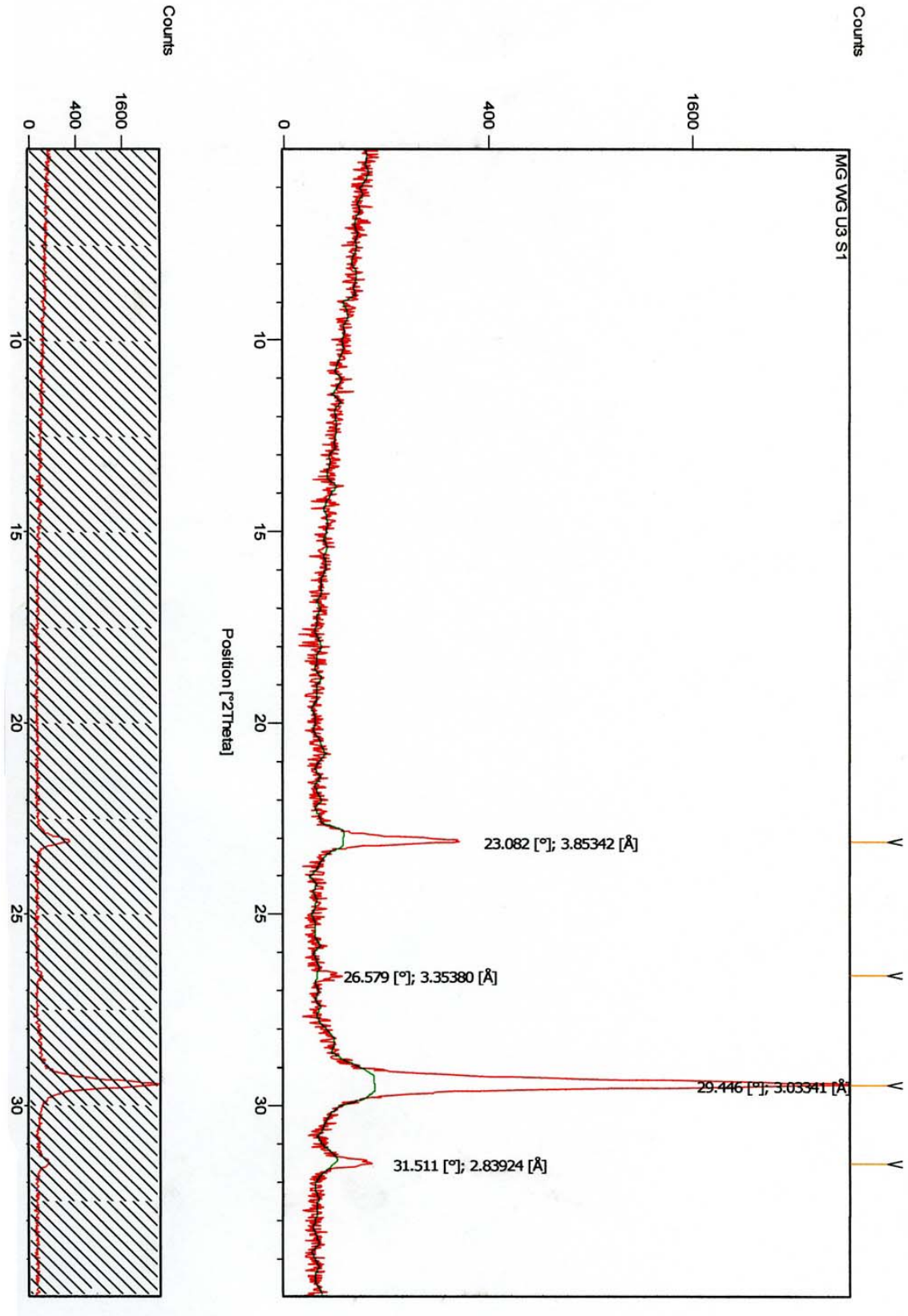

PK 2: Winchell Limestone, Possum Kingdom Locality

Location: 32° 53' 21.78" N; 98° 26' 10.56" W

2Θ	d-Spacing	Mineral
23.082	3.85342	Calcite
26.579	3.3538	Quartz
29.446	3.03341	Calcite
31.511	2.83924	Kaolinite

Dominant Peaks from X-Ray diffraction and interpretations

Location of sample for XRD

PK 4: Winchell Limestone, Possum Kingdom Locality

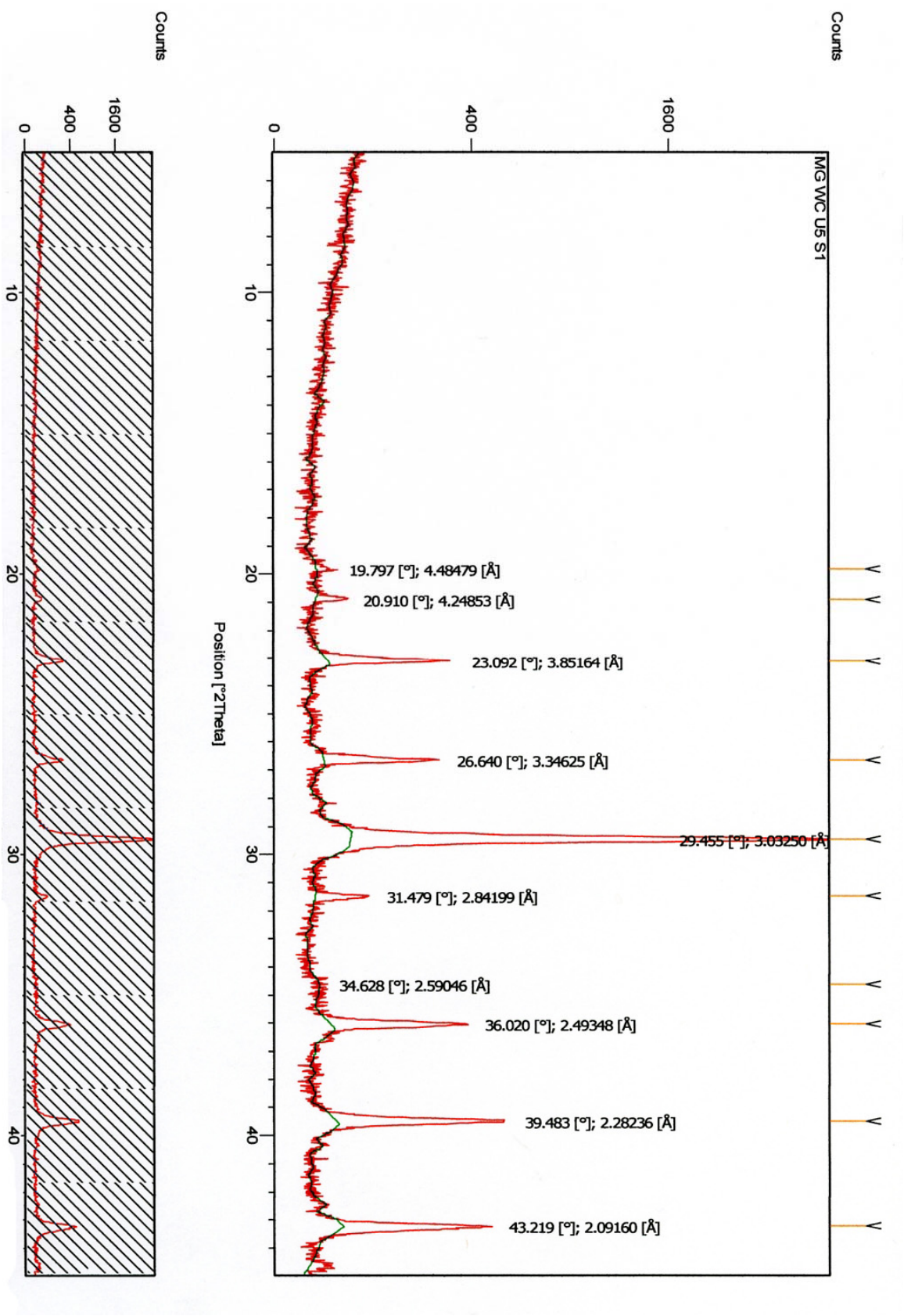

PK 4: Winchell Limestone, Possum Kingdom Locality

Location: 32° 52' 36.36" N; 98° 24' 54.84" W

2Θ	d-Spacing	Mineral
19.797	4.448479	Illite
20.910	4.24853	Quartz
23.092	3.85164	Calcite
26.640	3.34625	Quartz
29.455	3.03250	Calcite
31.479	2.84199	Kaolinite
34.628	2.59046	Unidentified Clay Mineral
36.020	2.49348	Calcite
39.483	2.28236	Quartz
43.219	2.0916	Calcite

Dominant Peaks from X-Ray diffraction and interpretations

Location of sample for XRD

The Brownwood Spillway

BWS1: Winchell Limestone, Brownwood Spillway

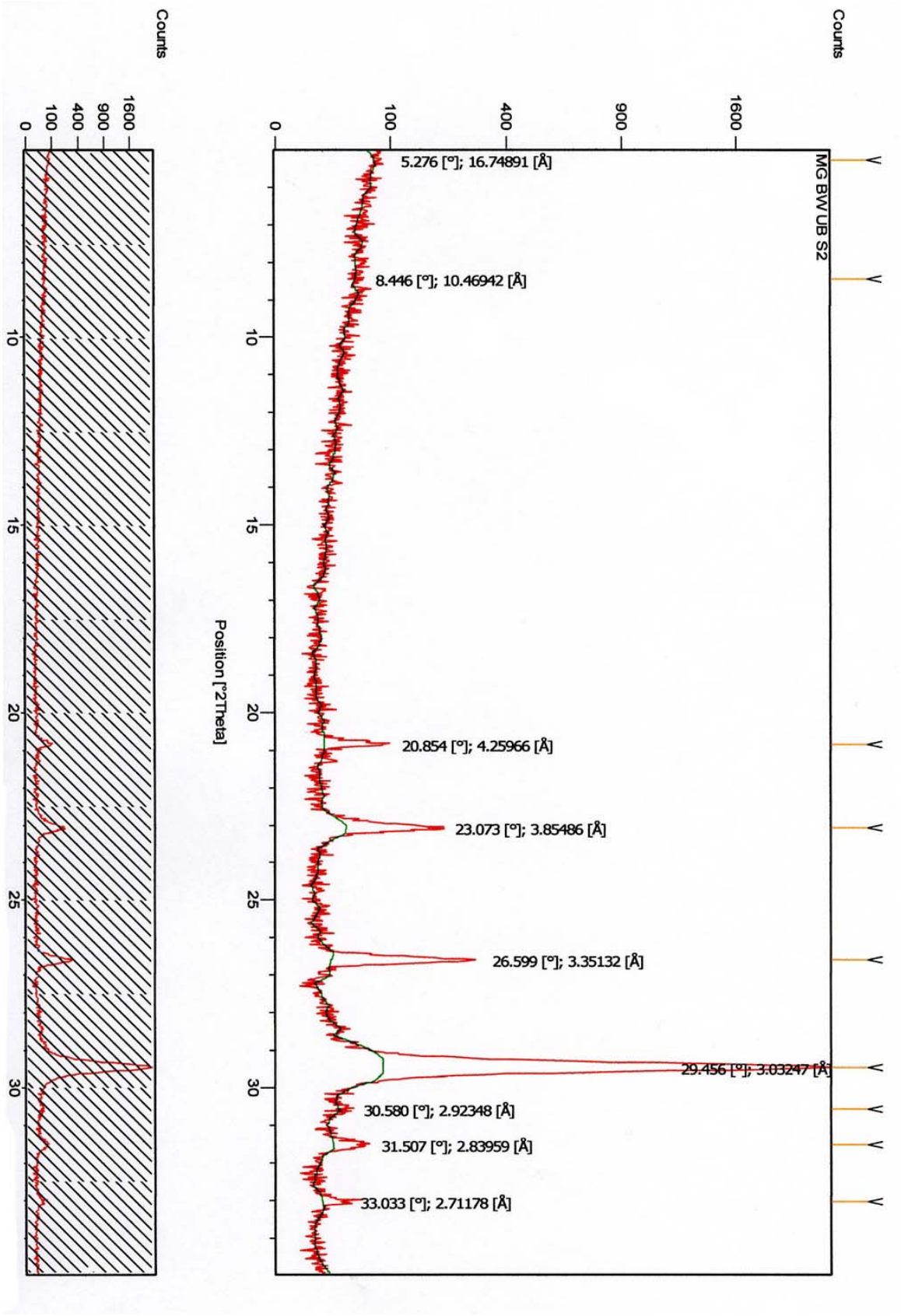

BWS1: Winchell Limestone, Brownwood Spillway

Location: 31° 50' 31.48" N; 98° 59' 57.67" W

2Θ	d-Spacing	Mineral
5.276	16.74891	Unidentified Clay Mineral
8.446	10.46942	Illite
20.854	4.25966	Quartz
23.073	3.85486	Calcite
26.599	3.35132	Quartz
29.456	3.03247	Calcite
30.580	2.92348	Kaolinite
31.507	2.83959	Kaolinite?
33.033	2.71178	Unidentified Clay Mineral

Dominant Peaks from X-Ray diffraction and interpretations

Location of sample for XRD

BWS2: Winchell Limestone, Brownwood Spillway

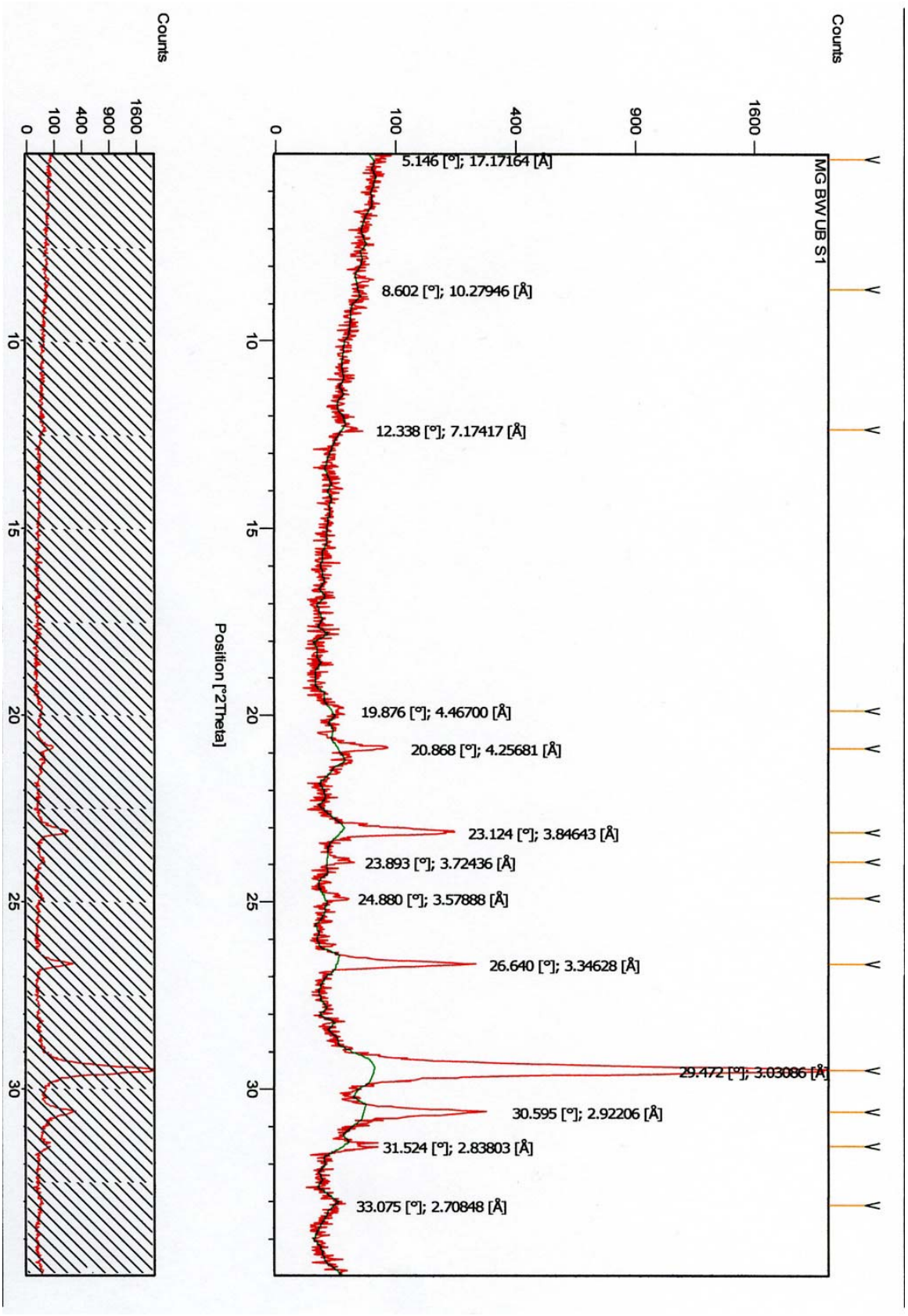

BWS2: Winchell Limestone, Brownwood Spillway

Location: 31° 50' 31.48" N; 98° 59' 57.67" W

2Θ	d-Spacing	Mineral
5.146	17.17164	Unidentified Clay Mineral
8.602	10.27946	Illite
12.338	7.17417	Unidentified Clay Mineral
19.976	4.46700	Kaolinite
20.868	4.25681	Quartz
23.124	3.84643	Calcite
23.893	3.72536	Unidentified Clay Mineral
24.880	3.57888	Unidentified Clay Mineral
26.640	3.34628	Quartz
29.472	3.03086	Calcite
30.595	2.92206	Kaolinite
31.524	2.83803	Kaolinite?
33.075	2.70848	Aragonite?

Dominant Peaks from X-Ray diffraction and interpretations

(No Picture Available)

The Bend River Locality

BR1: Smithwick Shale, Bend River Locality

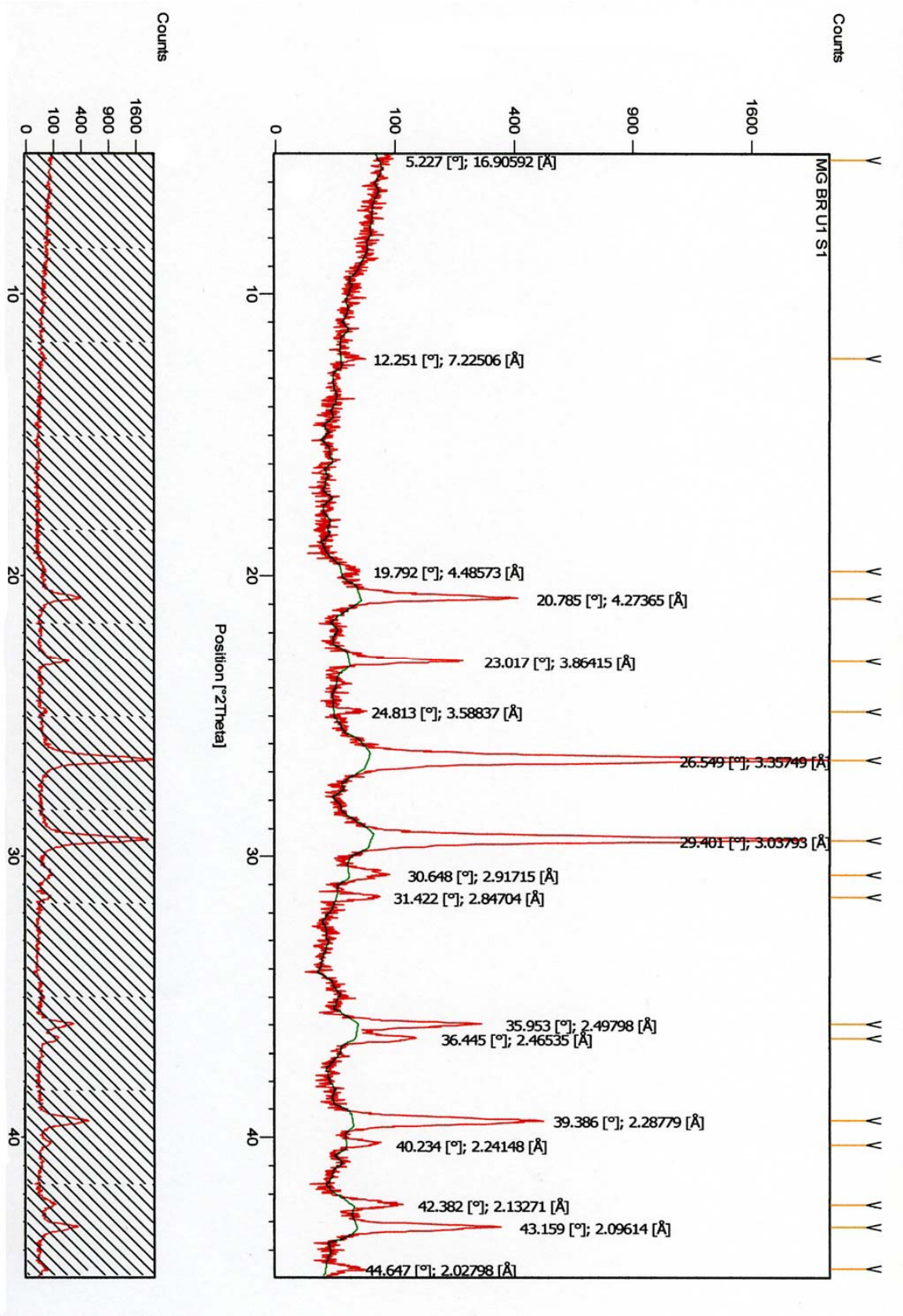

BR1: Smithwick Shale, Bend River Locality

Location: 31° 5' 26.04" N; 98° 31' 12.66" W

2Θ	d-Spacing	Mineral
5.227	16.90592	Unidentified Clay Mineral
12.251	7.22506	Kaolinite?
19.792	4.48573	Kaolinite
20.785	4.27365	Quartz
23.017	3.86415	Calcite
24.813	3.58837	Clay (Mica Polytype)
26.549	3.35749	Quartz
29.401	3.03793	Calcite
30.648	2.91715	Clay (Mica Polytype)
31.422	2.84704	Illite
35.953	2.49798	Calcite
36.445	2.46535	Quartz
39.386	2.28779	Calcite
40.234	2.24148	Quartz??
42.382	2.13271	Quartz
43.159	2.09614	Calcite
44.647	2.02798	Dolomite?

Dominant Peaks from X-Ray diffraction and interpretations

Location of sample for XRD

BR2: Smithwick Shale, Bend River Locality

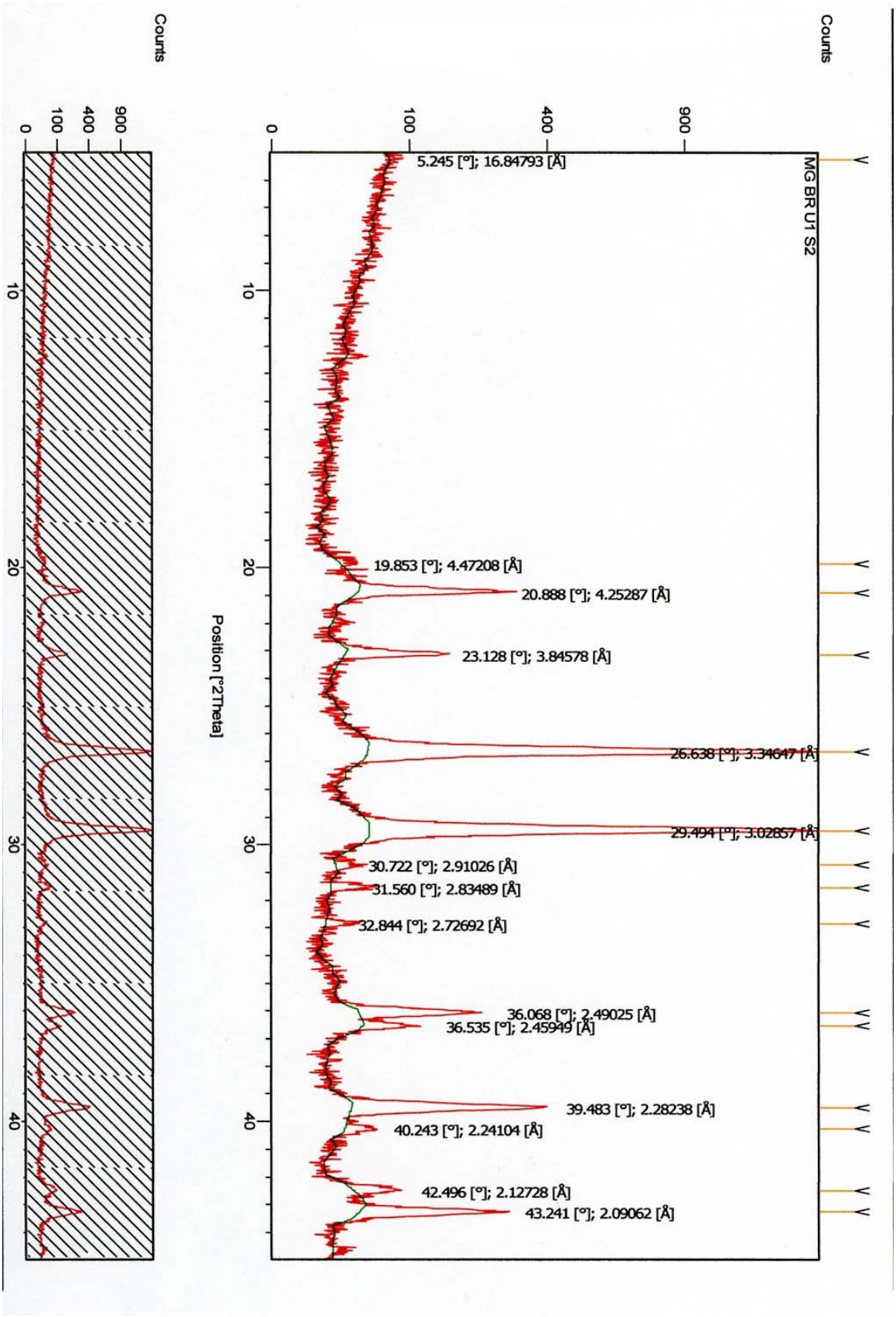

BR2: Smithwick Shale, Bend River Locality

Location: 31° 5' 26.04" N; 98° 31' 12.66" W

2Θ	d-Spacing	Mineral
5.245	16.84793	Unidentified Clay Mineral
19.853	4.47208	Kaolinite?
20.888	4.25287	Quartz
23.128	3.84578	Calcite
26.638	3.34647	Quartz
29.494	3.02857	Calcite
30.722	2.91026	Dolomite
31.560	2.83489	Illite
32.844	2.72692	Kaolinite
36.068	2.49025	Calcite
36.535	2.45949	Quartz
39.483	2.28238	Quartz
40.243	2.24104	Quartz
42.496	2.12728	Quartz
43.241	2.09062	Calcite

Dominant Peaks from X-Ray diffraction and interpretations

Location of sample for XRD

BR3: Marble Falls/Smithwick Contact, Bend River Locality

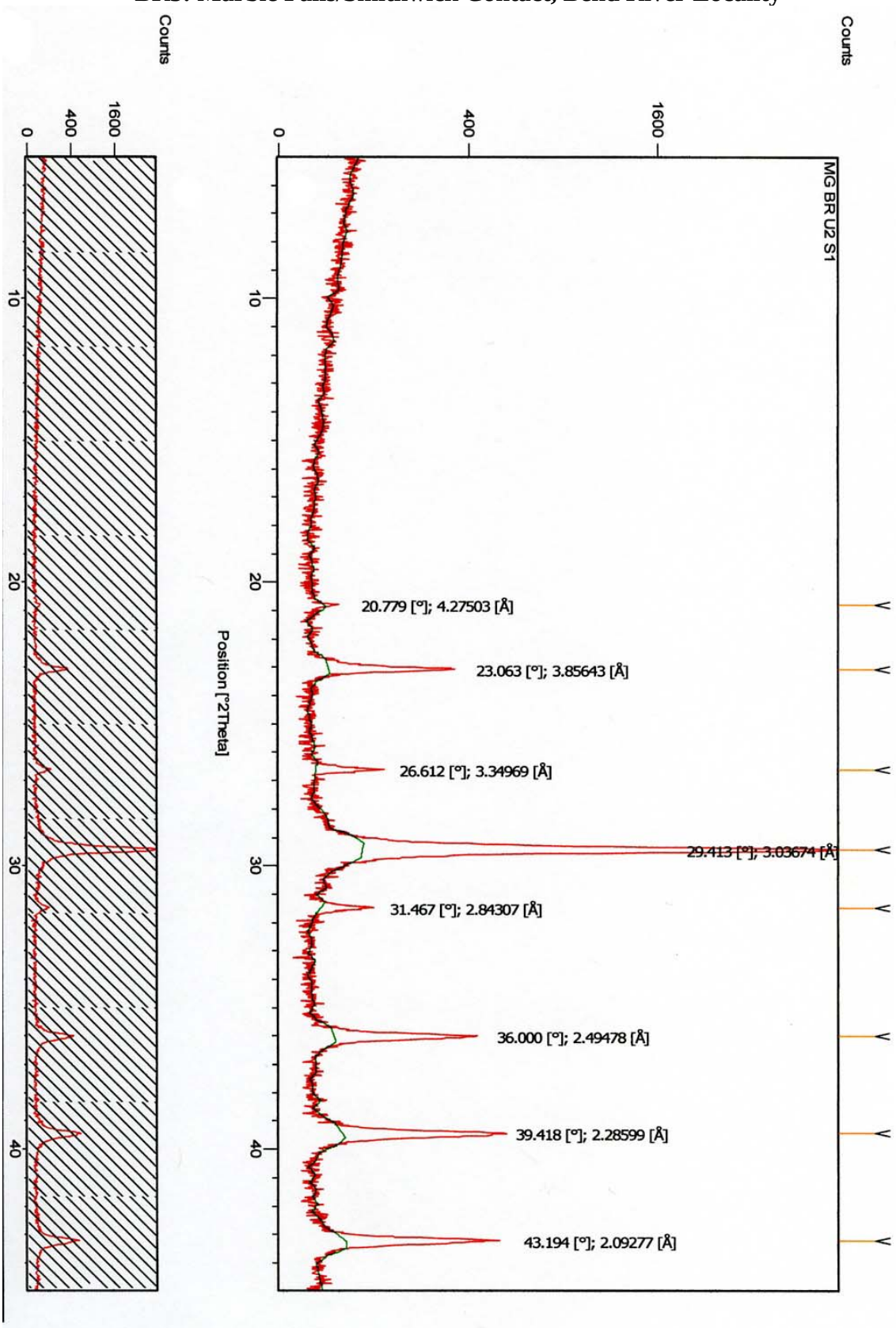

BR3: Marble Falls/Smithwick Contact, Bend River Locality

Location: 31° 5' 26.04" N; 98° 31' 12.66" W

2Θ	d-Spacing	Mineral
20.779	4.27503	Quartz
23.063	3.85643	Calcite
26.612	3.34969	Quartz
29.413	3.03674	Calcite
31.467	2.84307	Illite
36.000	2.49478	Calcite
39.418	2.28599	Calcite
43.194	2.09277	Calcite

Dominant Peaks from X-Ray diffraction and interpretations

Location of sample for XRD (Unfractured unit on right)

BR4: Marble Falls/Smithwick Contact, Bend River Locality

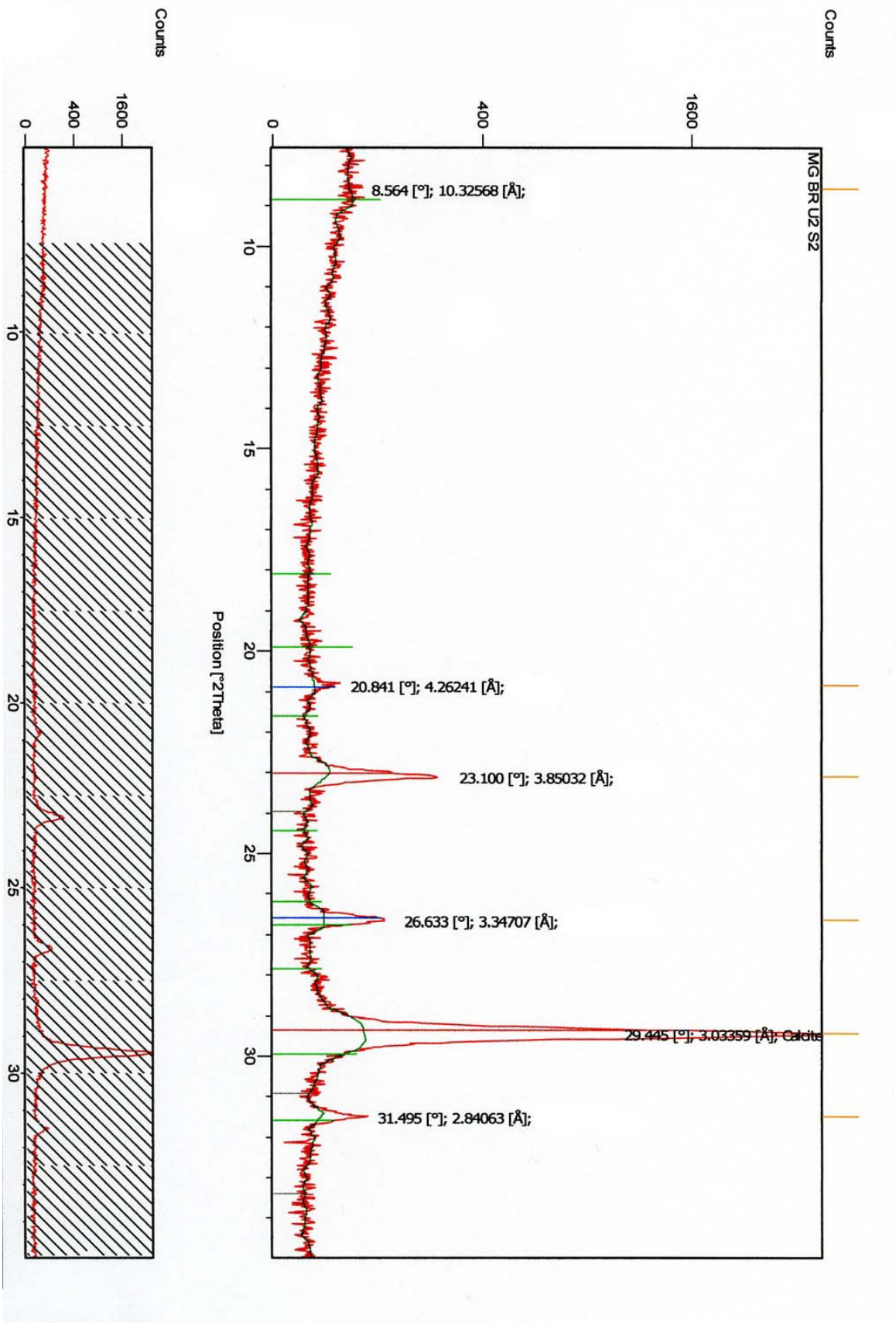

BR4: Marble Falls/Smithwick Contact, Bend River Locality

Location: 31° 5' 26.04" N; 98° 31' 12.66" W

2Θ	d-Spacing	Mineral
8.564	10.32568	Illite
20.841	4.26241	Quartz
23.100	3.85032	Calcite
26.633	3.34707	Quartz
29.445	3.03359	Calcite
31.495	2.84063	Illite

Dominant Peaks from X-Ray diffraction and interpretations

Location of sample for XRD (Highly fractured Unit on bottom)

BR5: Marble Falls/Smithwick Contact, Bend River Locality

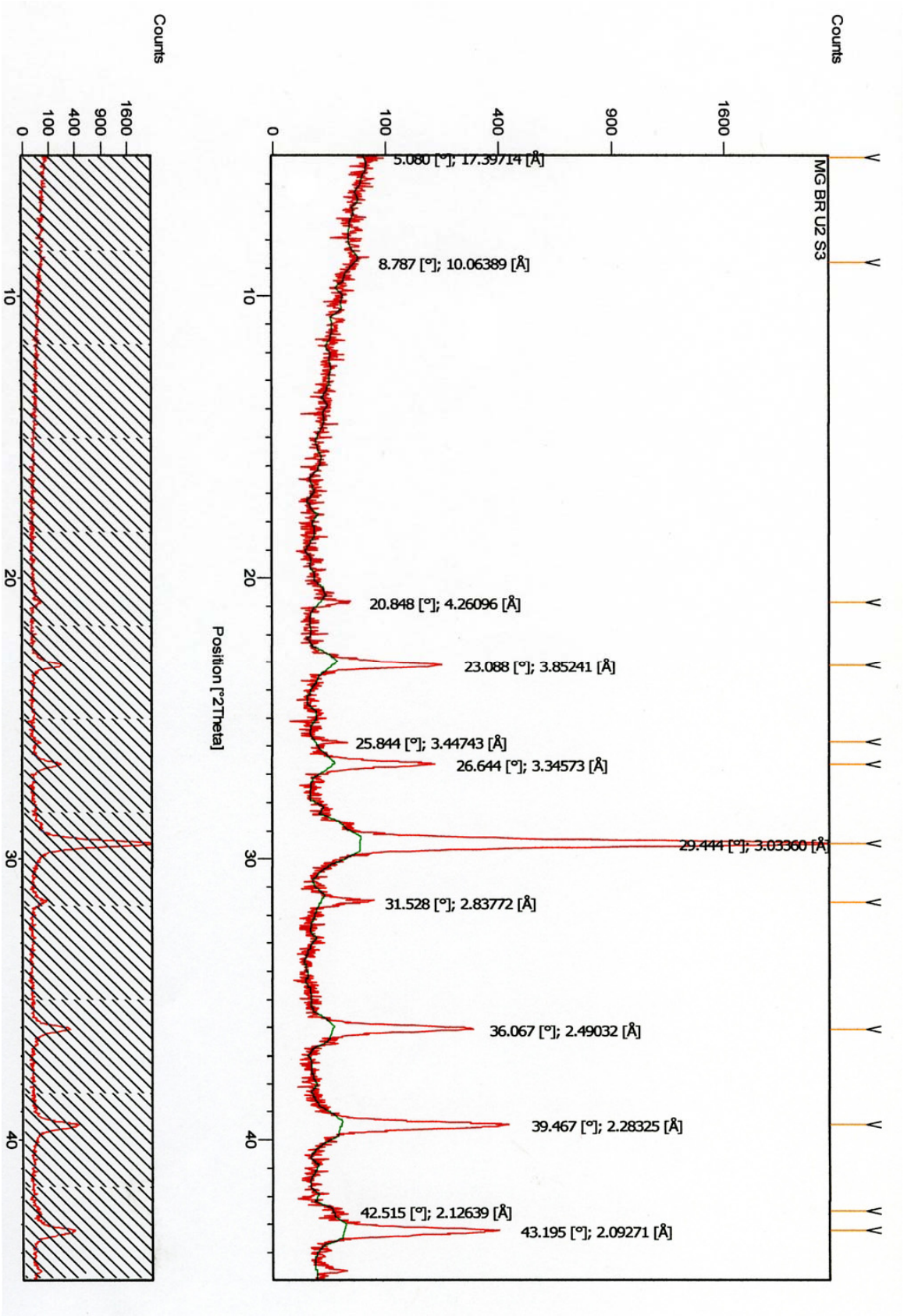

BR5: Marble Falls/Smithwick Contact, Bend River Locality

Location: 31° 5' 26.04" N; 98° 31' 12.66" W

2Θ	d-Spacing	Mineral
5.080	17.39714	Unidentified Clay Mineral
8.787	10.06389	Illite
20.848	4.26096	Quartz
23.088	3.85241	Calcite
25.844	3.44743	??
26.644	3.34573	Quartz
29.444	3.03360	Calcite
31.528	2.83772	Illite
36.067	2.49032	Calcite
39.467	2.28325	Calcite
42.515	2.12639	Quartz
43.195	2.09271	Calcite

Dominant Peaks from X-Ray diffraction and interpretations

Location of sample for XRD (Unfractured base of unit shown)

BR6: Marble Falls/Smithwick Contact, Bend River Locality

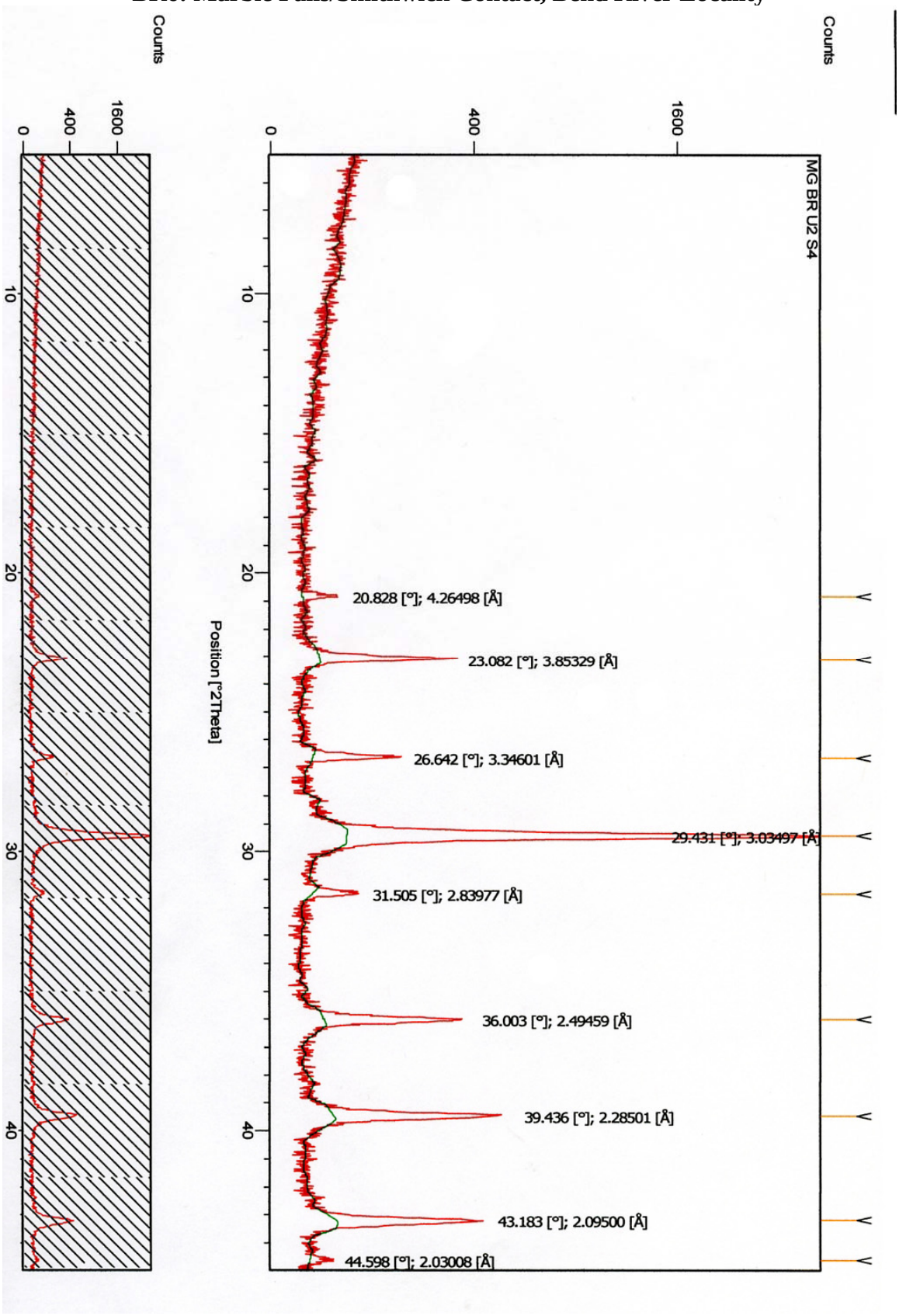

BR6: Marble Falls/Smithwick Contact, Bend River Locality

Location: 31° 5' 26.04" N; 98° 31' 12.66" W

2Θ	d-Spacing	Mineral
20.828	4.26498	Quartz
23.082	3.85329	Calcite
26.642	3.34601	Quartz
29.431	3.03497	Calcite
31.505	2.83977	Illite
36.003	2.49459	Calcite
39.436	2.28501	Calcite
43.183	2.09500	Calcite
44.598	2.03008	??

Dominant Peaks from X-Ray diffraction and interpretations

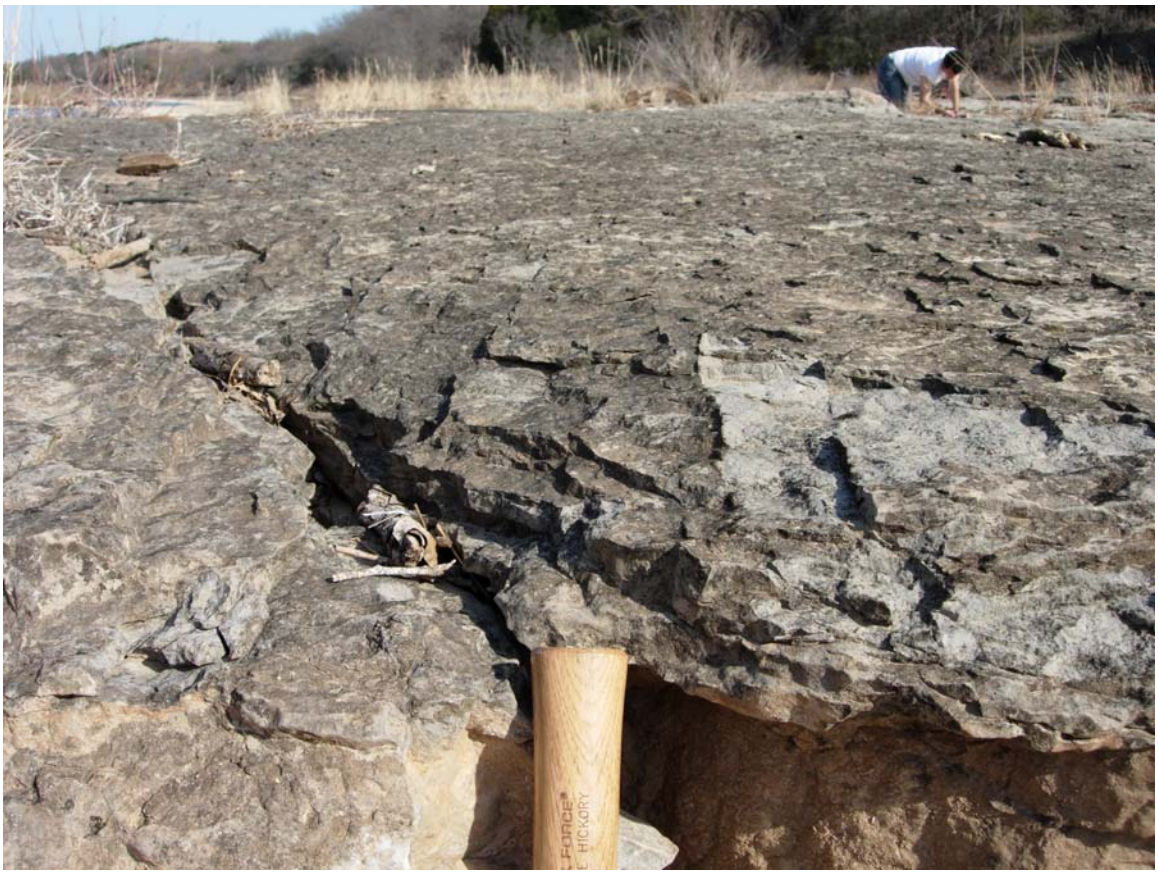

Location of sample for XRD (Highly Fractured top of BR5)

The Archer Ranch Locality

AR1: Honeycut Formation, Archer Ranch Locality

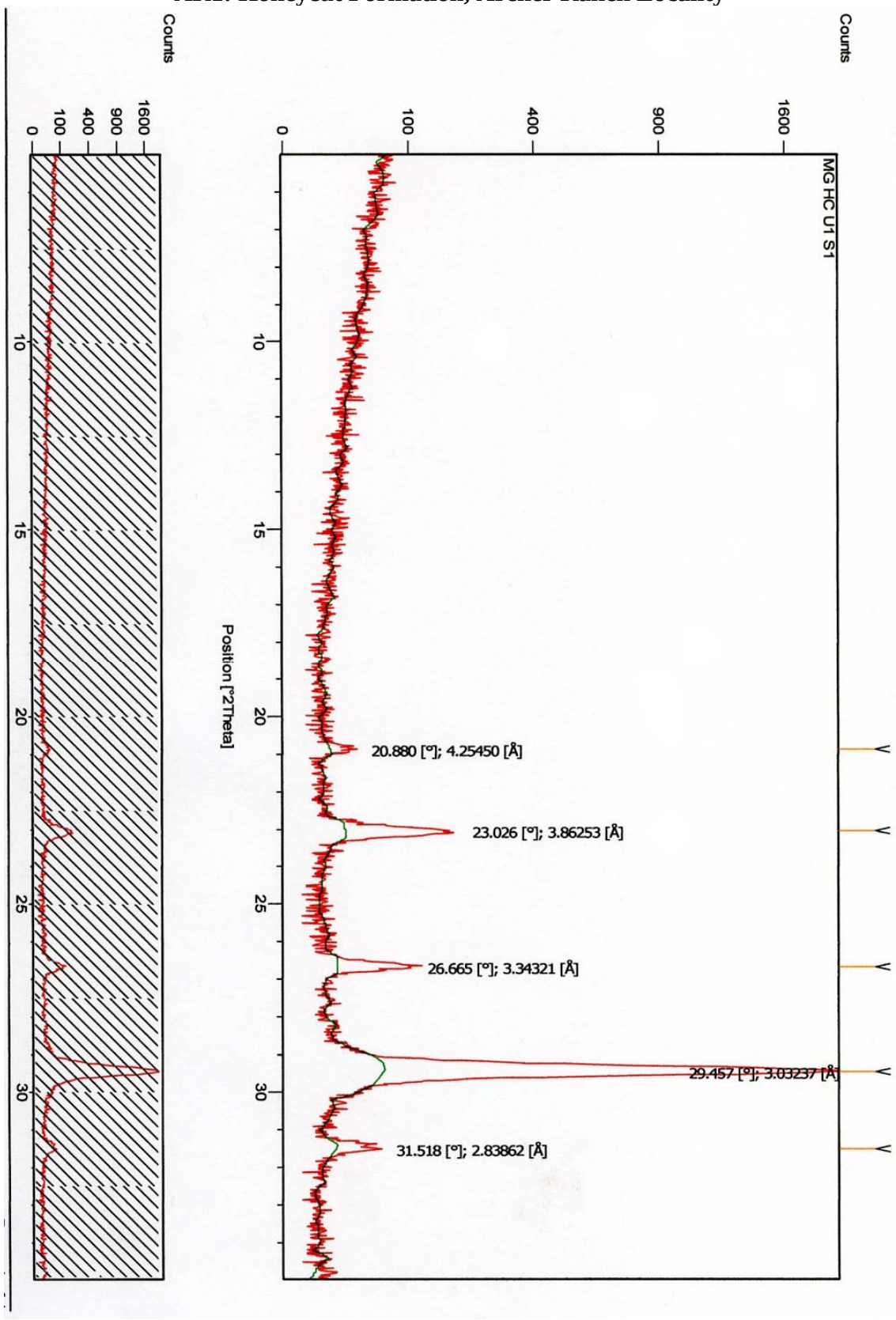

AR1: Honeycut Formation, Archer Ranch Locality

Location: 30° 16' 39.64" N; 98° 19' 28.28" W

2Θ	d-Spacing	Mineral
20.880	4.25450	Quartz
23.026	3.86253	Calcite
26.665	3.34321	Quartz
29.457	3.03237	Calcite
31.518	2.83862	Dolomite

Dominant Peaks from X-Ray diffraction and interpretations

Location of sample for XRD (Thinly bedded & highly fractured)

AR2: Honeycut Formation, Archer Ranch Locality

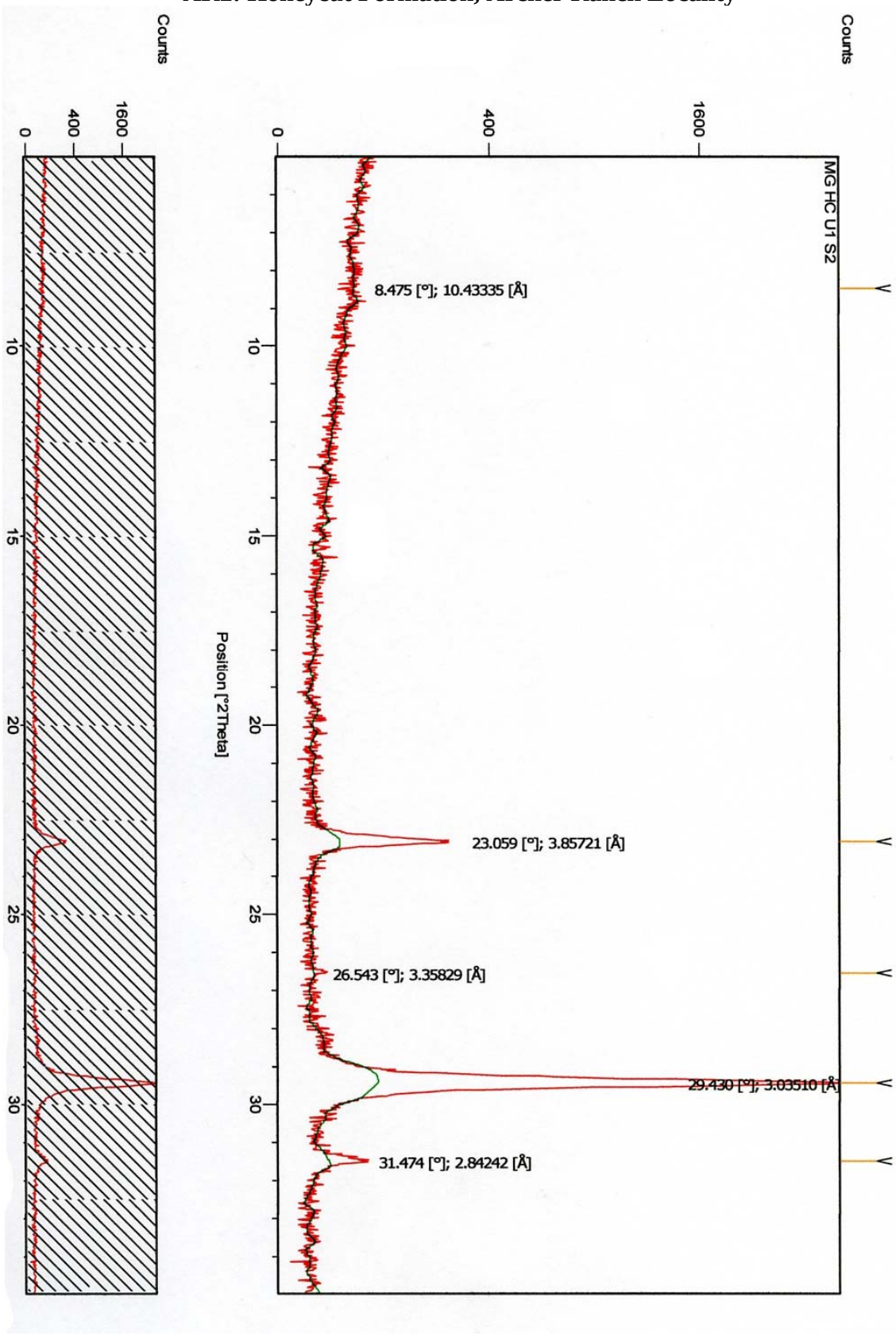

AR2: Honeycut Formation, Archer Ranch Locality

Location: 30° 16' 39.64" N; 98° 19' 28.28" W

2Θ	d-Spacing	Mineral
8.475	10.43335	Illite
23.059	3.85721	Calcite
26.543	3.35829	Quartz
29.430	3.03510	Calcite
31.474	2.84242	Dolomite

Dominant Peaks from X-Ray diffraction and interpretations

Location of sample for XRD (Thick bedded & lower fracture intensity then AR1)

AR3: Marble Falls Limestone, Archer Ranch Locality

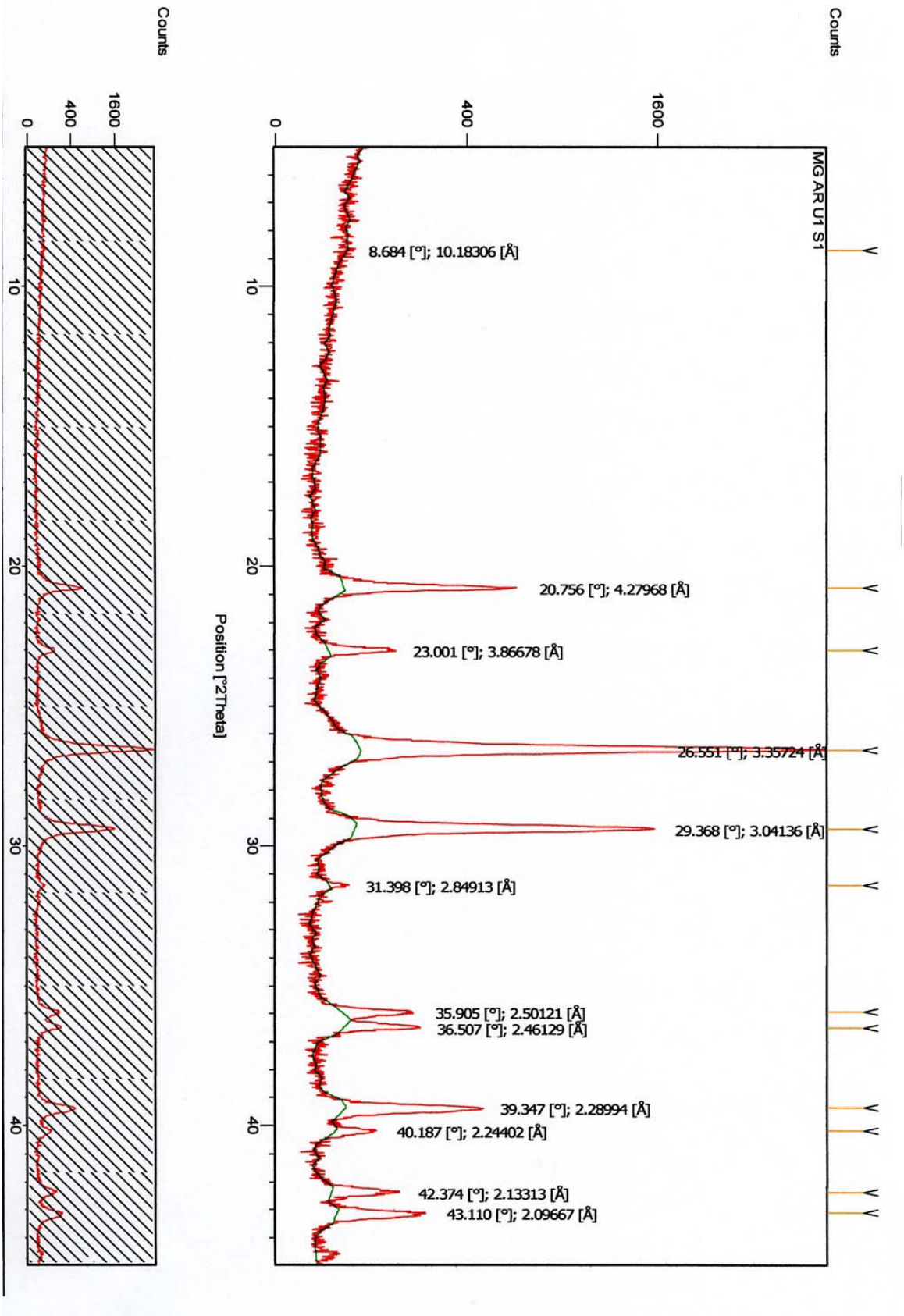

AR3: Marble Falls Limestone, Archer Ranch Locality

Location: 30° 16' 39.64" N; 98° 19' 28.28" W

2Θ	d-Spacing	Mineral
8.684	10.18306	Illite
20.756	4.27968	Quartz
23.001	3.86678	Calcite
26.551	3.35724	Quartz
29.368	3.04136	Calcite
31.398	2.84913	Kaolinite
35.905	2.50121	Calcite
36.507	2.46129	Quartz
39.347	2.28994	Calcite
40.187	2.24402	Quartz
42.374	2.13313	Quartz
43.110	2.09667	Calcite

Dominant peaks from X-Ray diffraction and interpretations

Location of sample for XRD

AR4: Marble Falls Limestone, Archer Ranch Locality

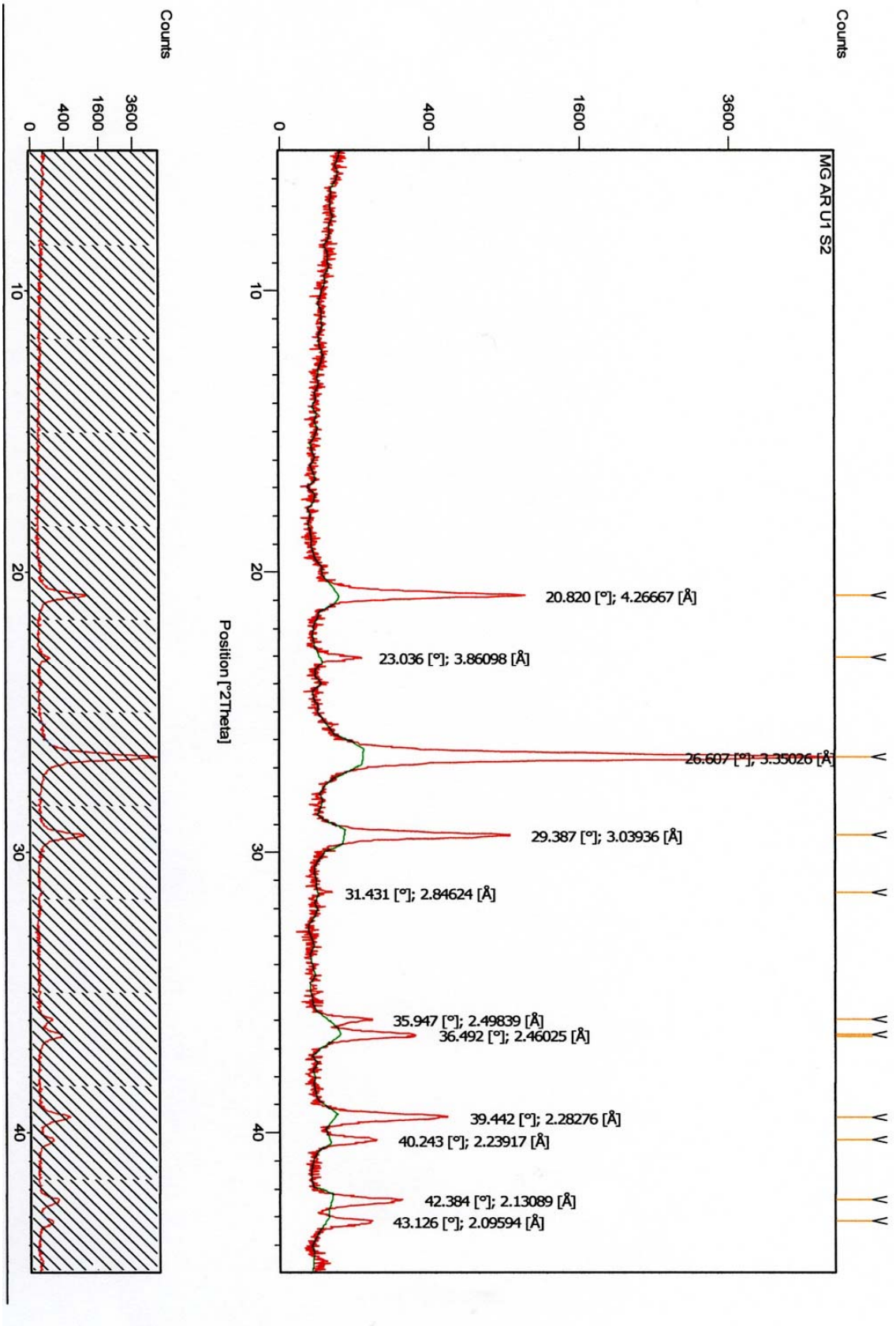

AR4: Marble Falls Limestone, Archer Ranch Locality

Location: 30° 16' 39.64" N; 98° 19' 28.28" W

2Θ	d-Spacing	Mineral
20.820	4.26667	Quartz
23.036	3.86098	Calcite
26.607	3.35026	Quartz
29.387	3.03936	Calcite
31.431	2.84624	Kaolinite
35.947	2.49839	Calcite
36.492	2.46025	Quartz
39.442	2.28276	Calcite
40.243	2.23917	Quartz
42.384	2.13089	Quartz
43.126	2.09594	Calcite

Dominant Peaks from X-Ray diffraction and interpretations

Location of sample for XRD

AR5: Marble Falls Limestone, Archer Ranch Locality

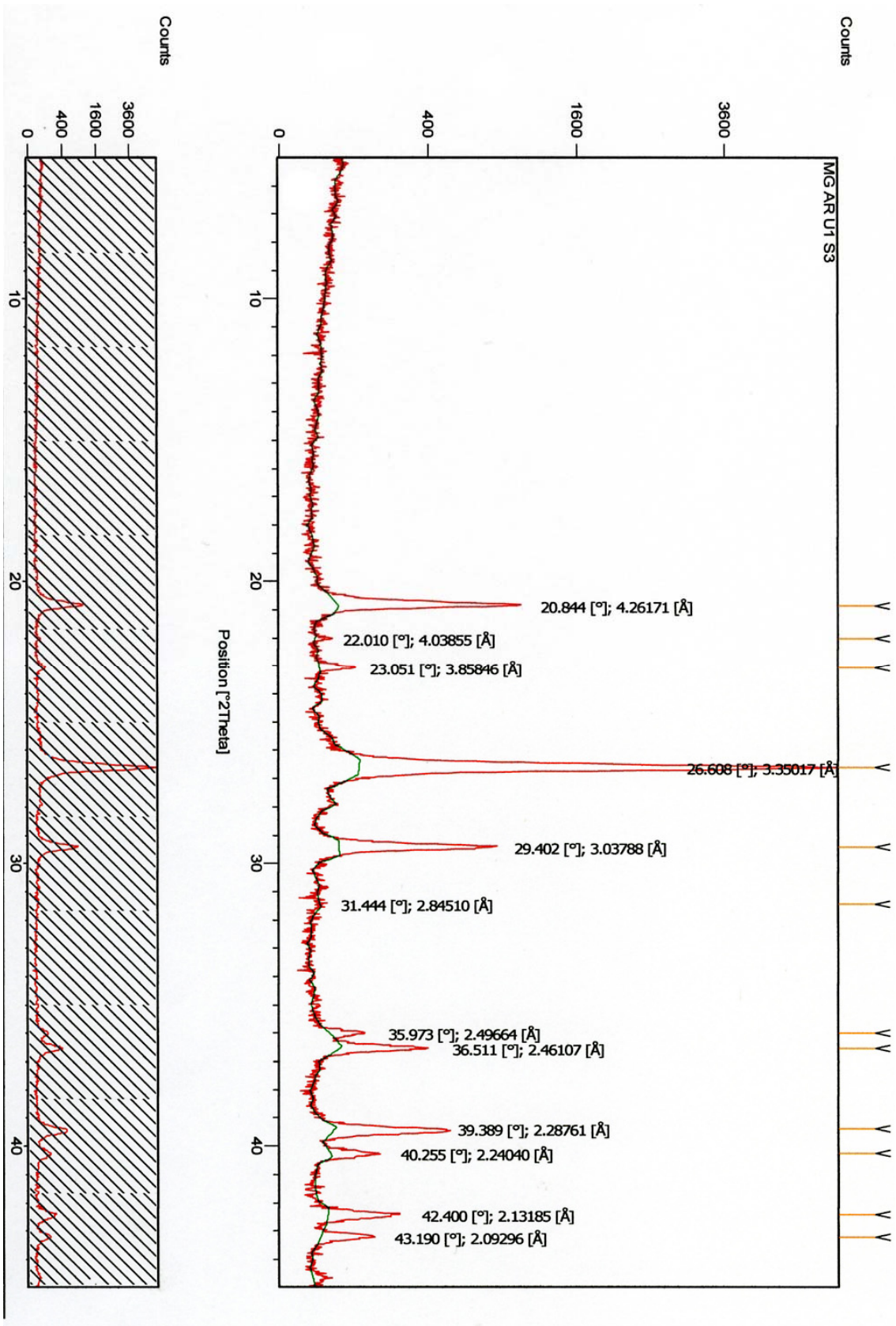

AR5: Marble Falls Limestone, Archer Ranch Locality

Location: 30° 16' 39.64" N; 98° 19' 28.28" W

2Θ	d-Spacing	Mineral
20.844	4.26171	Quartz
22.010	4.03855	Plagioclase
23.051	3.85846	Calcite
26.608	3.35017	Quartz
29.402	3.03788	Calcite
31.444	2.84510	Kaolinite
35.973	2.49664	Calcite
36.511	2.46107	Quartz
39.389	2.28761	Calcite
40.255	2.24040	Quartz
42.400	2.13185	Quartz
43.190	2.09296	Calcite

Dominant peaks from X-Ray diffraction and interpretations

Location of sample for XRD (Thinly bedded & unfractured)

AR6: Marble Falls Limestone, Archer Ranch Locality

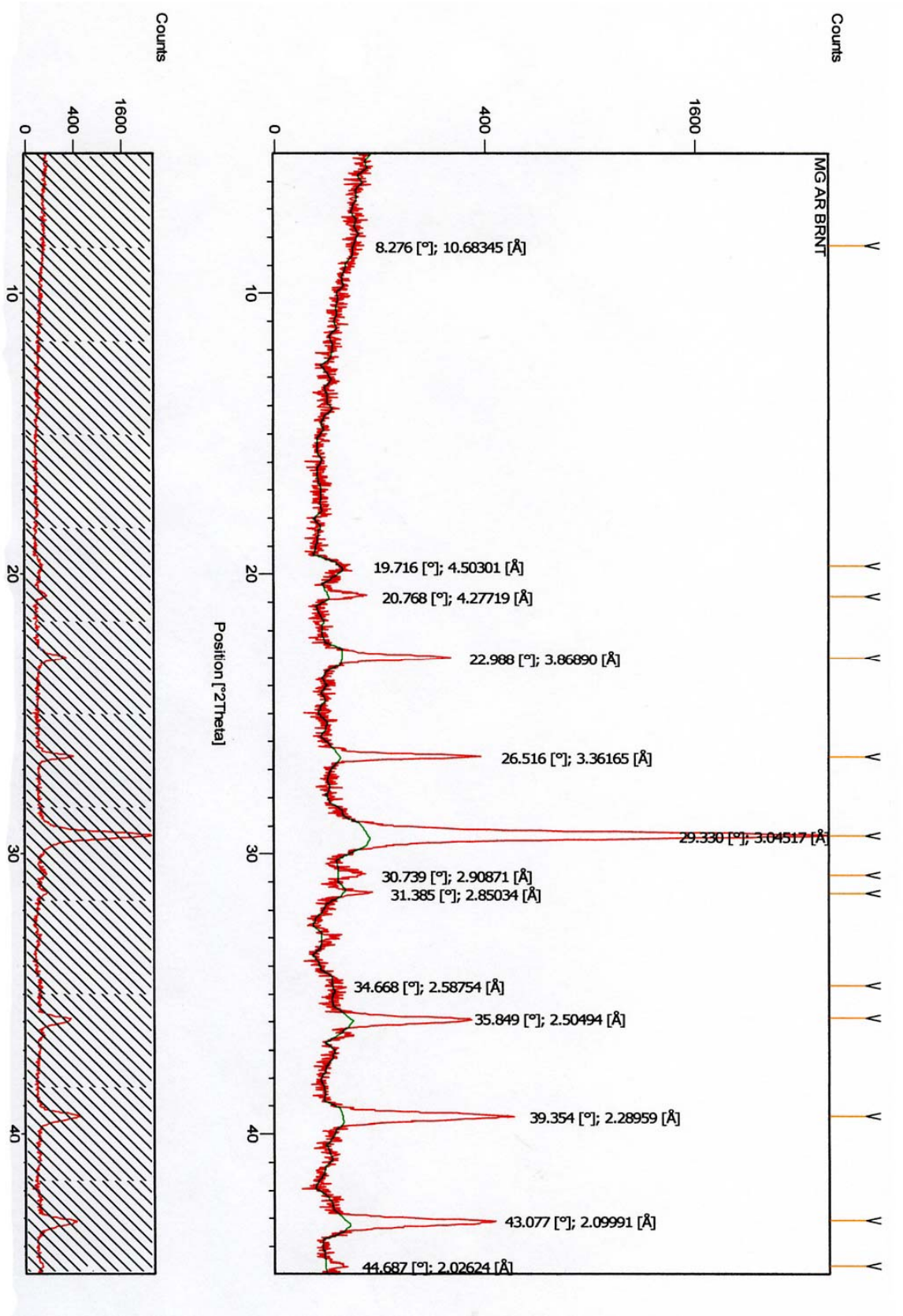

AR6: Marble Falls Limestone, Archer Ranch Locality

Location: 30° 16' 39.64" N; 98° 19' 28.28" W

2Θ	d-Spacing	Mineral
8.276	10.68345	Illite
19.716	4.50301	Kaolinite
20.768	4.27719	Quartz
22.988	3.86890	Calcite
26.516	3.36165	Quartz
29.330	3.04517	Calcite
30.739	2.90871	??
31.385	2.85024	Kaolinite
34.668	2.58754	??
35.849	2.50494	Calcite
39.354	2.28959	Quartz
43.077	2.09991	Calcite
44.687	2.02624	Dolomite

Dominant peaks from X-Ray diffraction and interpretations

Location of sample for XRD (Black shale base of Marble Falls)

APPENDIX B: RESULTS OF CLAY MINERAL EXTRACTION

Bend River Locality

BR4: Marble Falls/Smithwick Contact, Bend River Locality - Clay Extraction

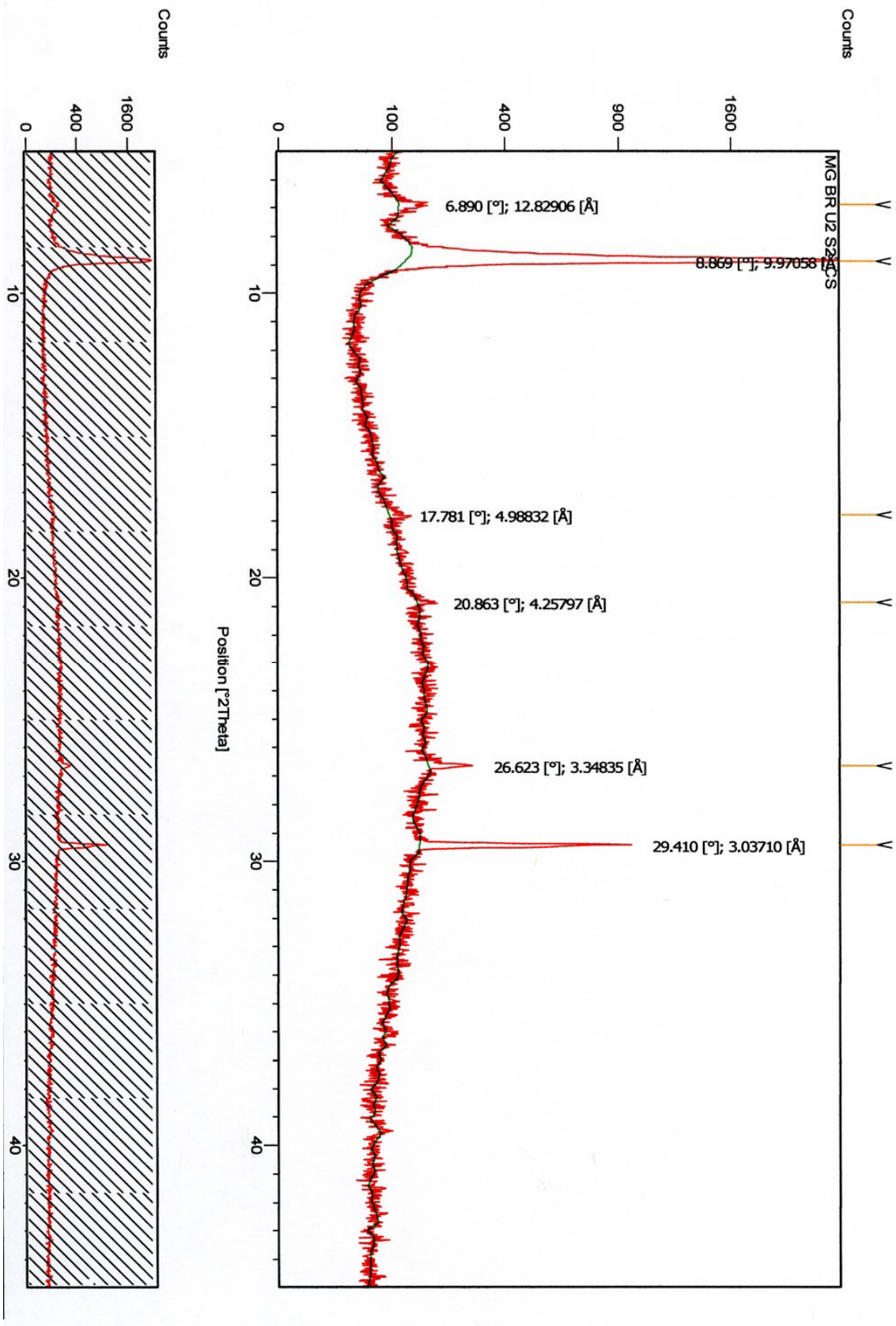

BR4: Marble Falls/Smithwick Contact, Bend River Locality - Clay Extraction

2Θ	d-Spacing	Mineral
6.890	12.82906	Unidentified Clay Mineral
8.869	9.97058	Illite
17.781	4.98832	Unidentified Clay Mineral
20.863	4.25797	Quartz
26.623	3.34835	Quartz
29.410	3.03710	Calcite

Dominant peaks from X-Ray diffraction and interpretations

BR5: Marble Falls/Smithwick Contact, Bend River Locality - Clay Extraction

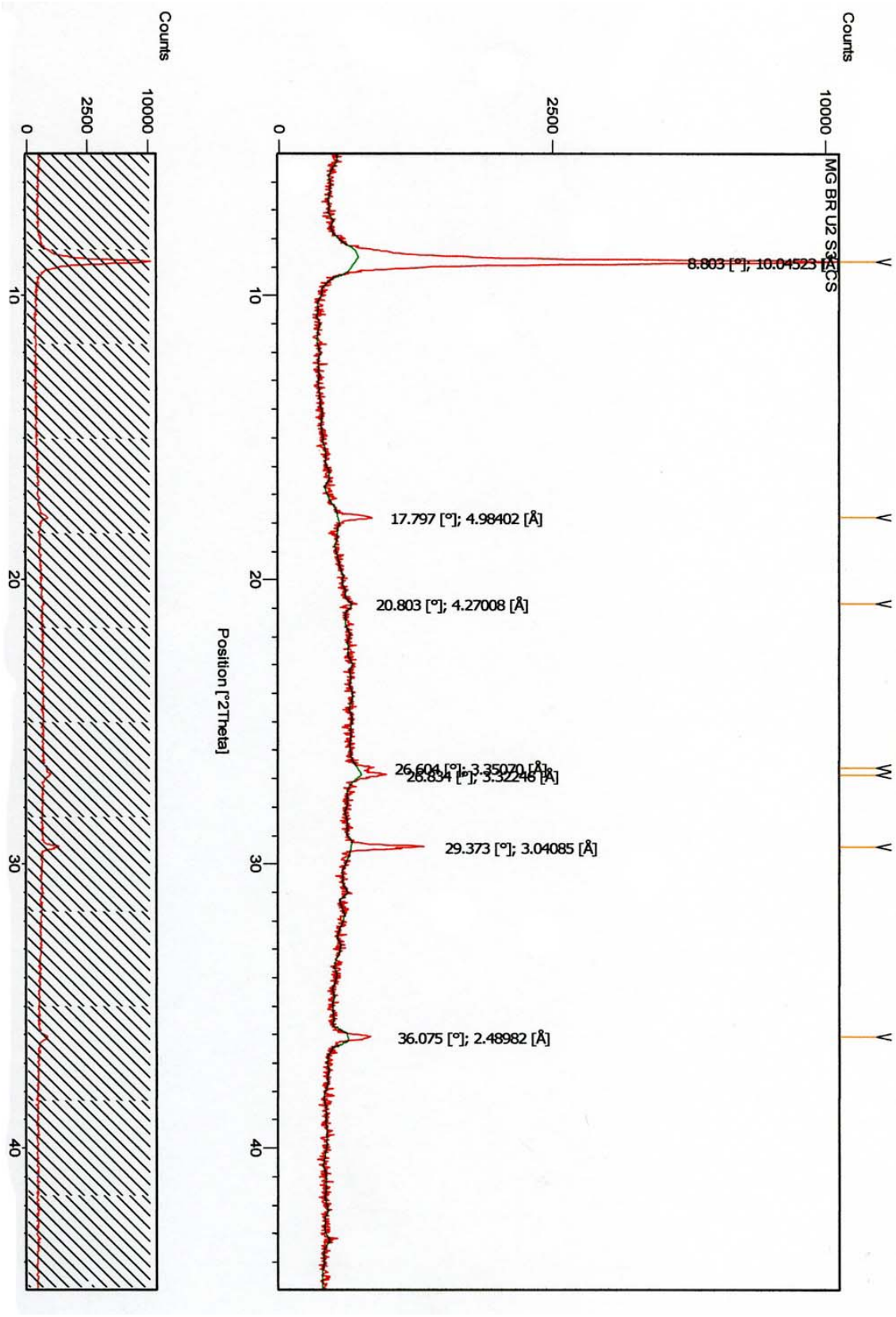

BR5: Marble Falls/Smithwick Contact, Bend River Locality - Clay Extraction

2Θ	d-Spacing	Mineral
8.803	10.04523	Illite
17.797	4.98402	Unidentified Clay Mineral
20.803	4.27008	Quartz
26.604	3.35070	Quartz
26.834	3.32246	Feldspar?
29.373	3.04085	Calcite
36.075	2.48982	Calcite

Dominant peaks from X-Ray diffraction and interpretations

Archer Ranch Locality

AR1: Honeycut Formation, Archer Ranch Locality - Clay Extraction

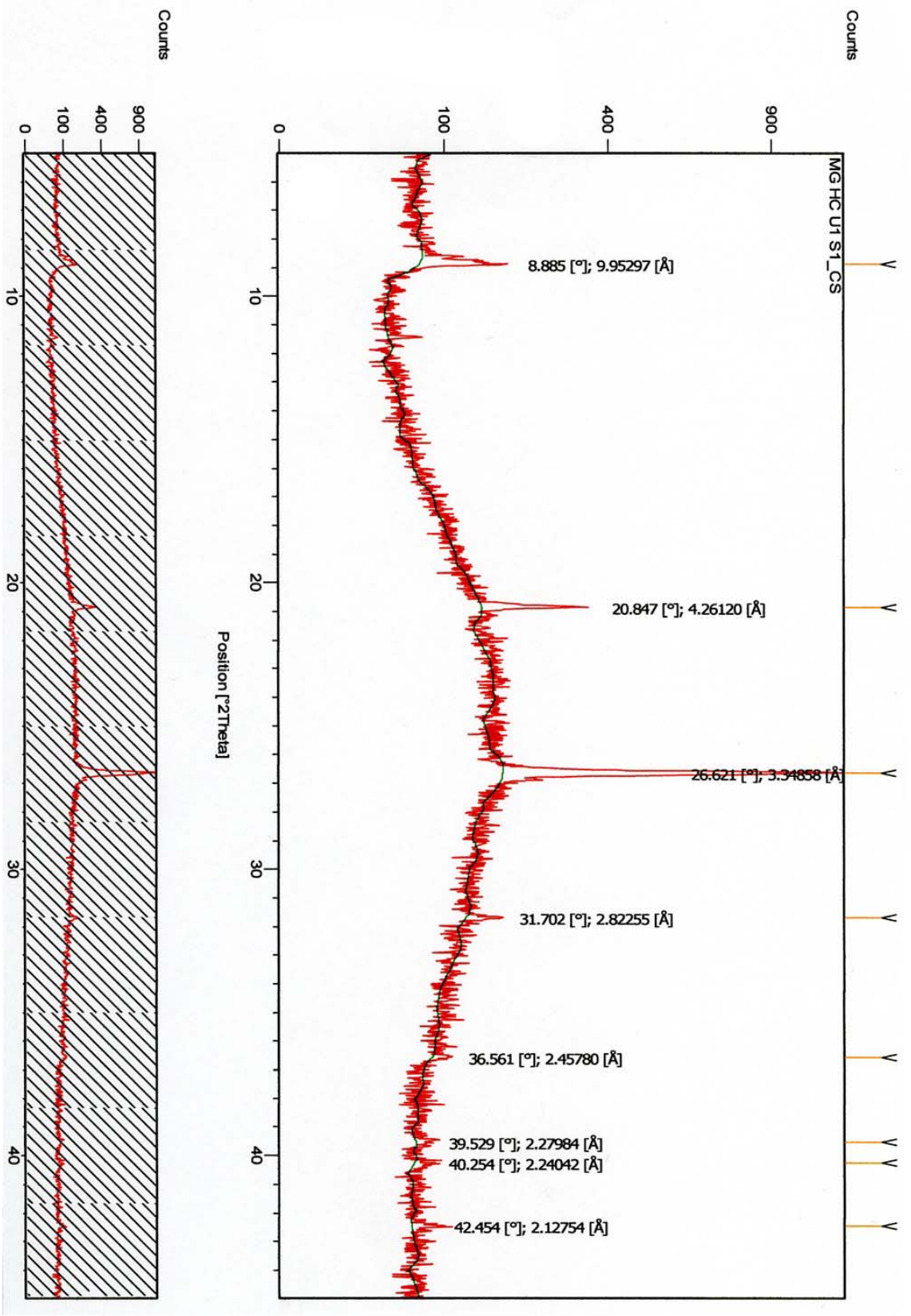

AR1: Honeycut Formation, Archer Ranch Locality - Clay Extraction

2Θ	d-Spacing	Mineral
8.885	9.95297	Illite
20.847	4.26120	Quartz
26.621	3.34858	Quartz
31.702	2.28226	Illite
36.561	2.45780	Quartz
39.529	2.27984	Quartz
40.254	2.24042	Quartz
42.454	2.12754	Quartz

AR2: Honeycut Formation, Archer Ranch Locality - Clay Extraction

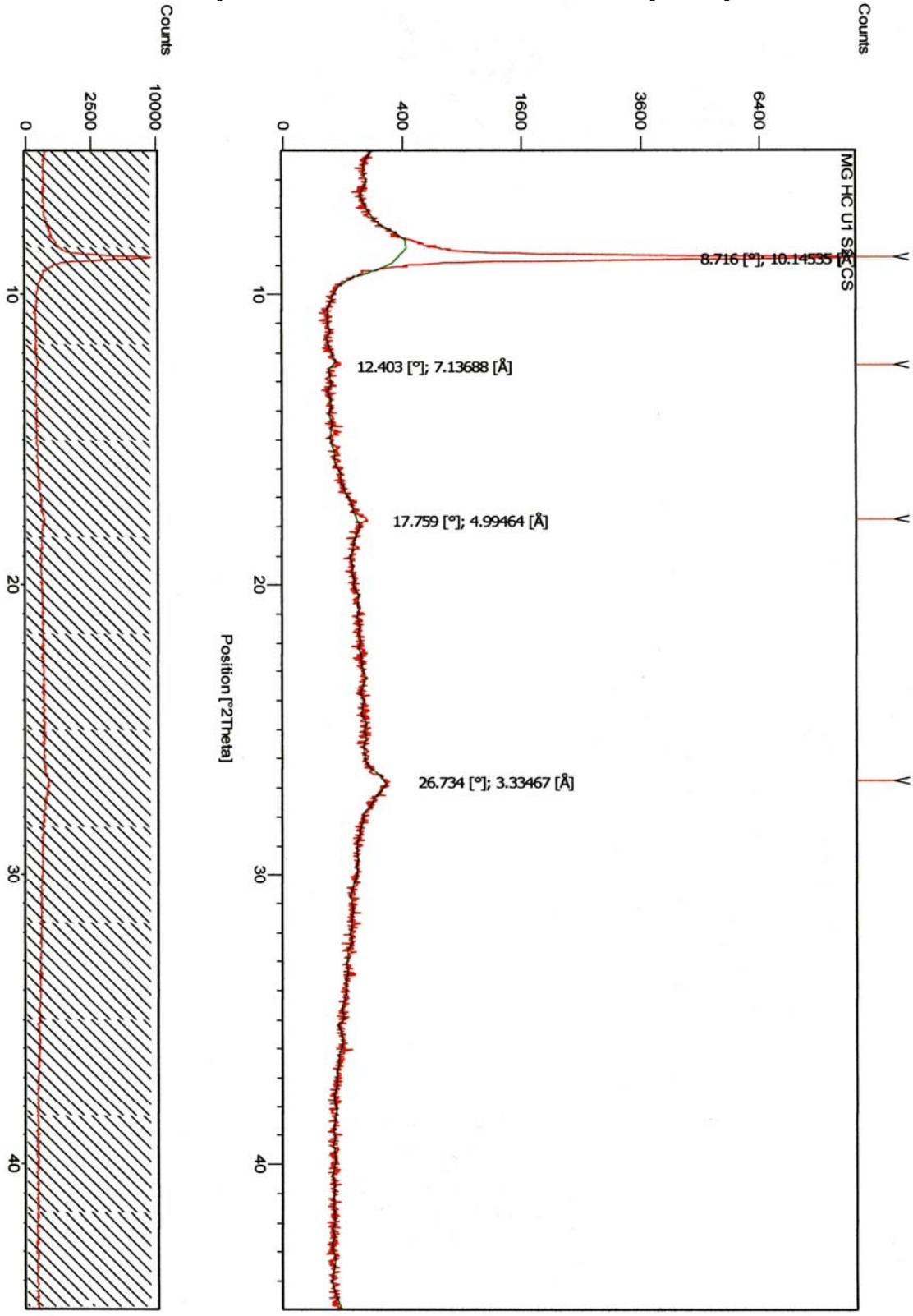

AR2: Honeycut Formation, Archer Ranch Locality - Clay Extraction

2Θ	d-Spacing	Mineral
8.716	10.14535	Illite
12.403	7.13688	Unidentified Clay Mineral
17.759	4.99464	Unidentified Clay Mineral
26.734	3.33467	Quartz

Surface Measurements

Surface to Subsurface Correlation

Fractures Related to Compression

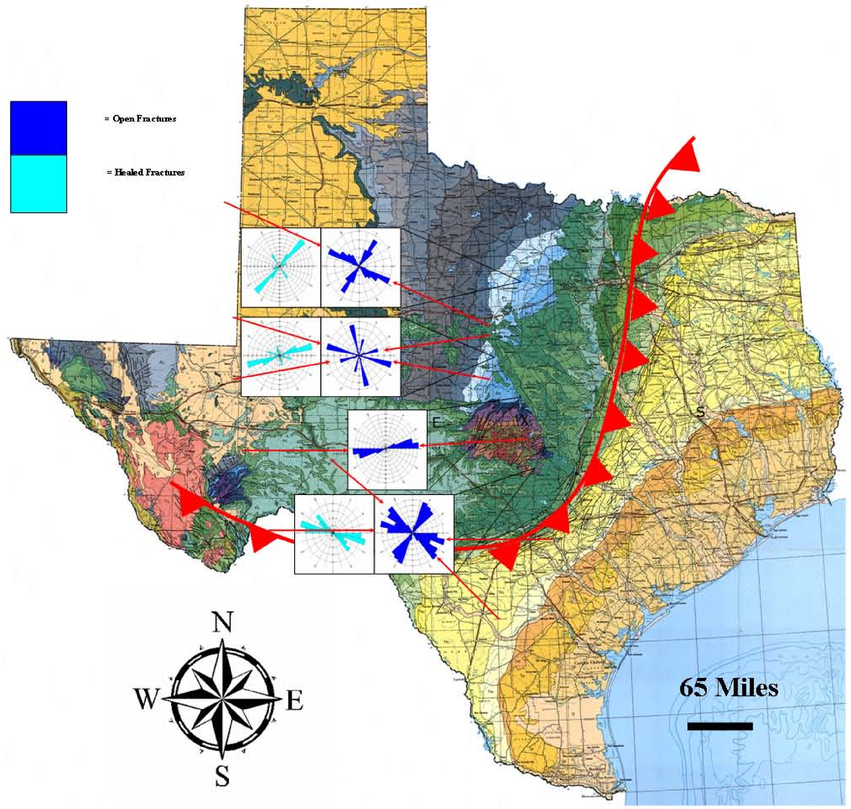

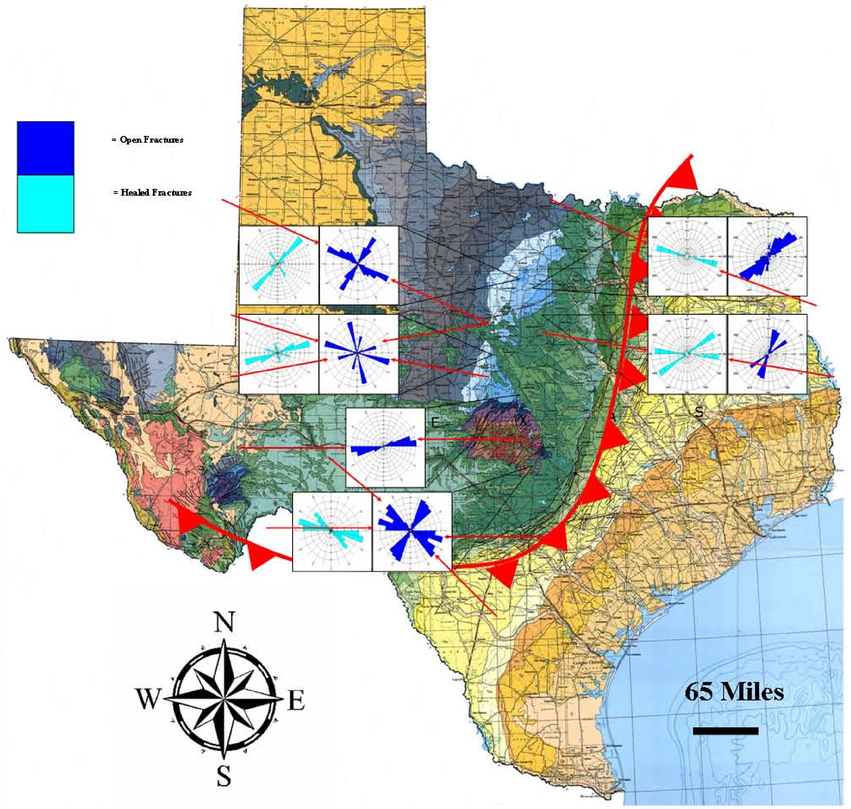

Fractures Related to Extension

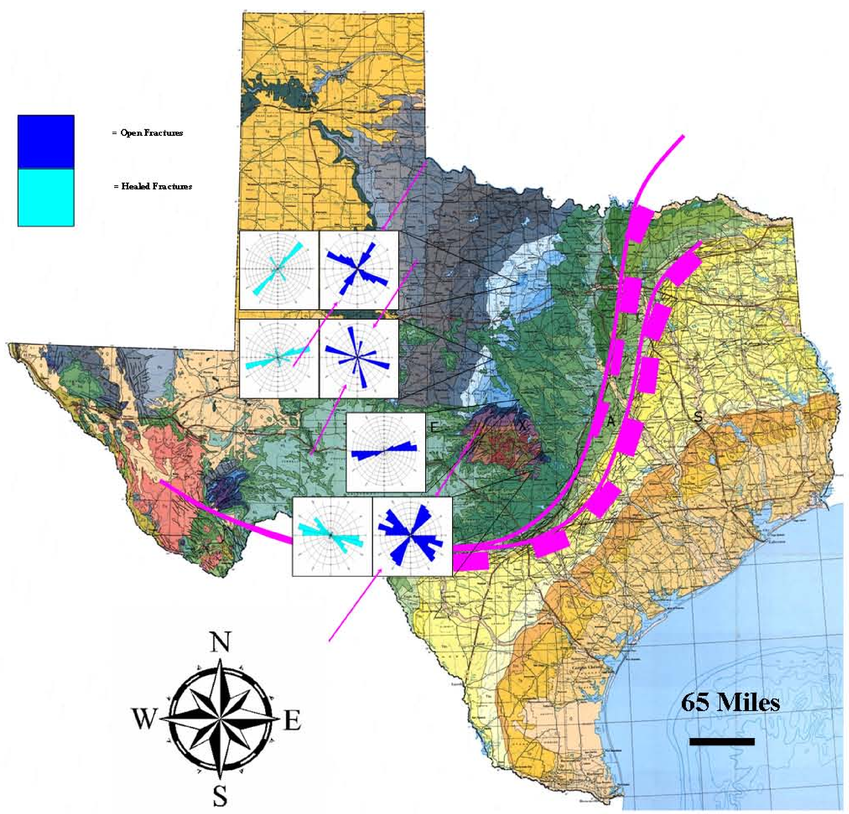

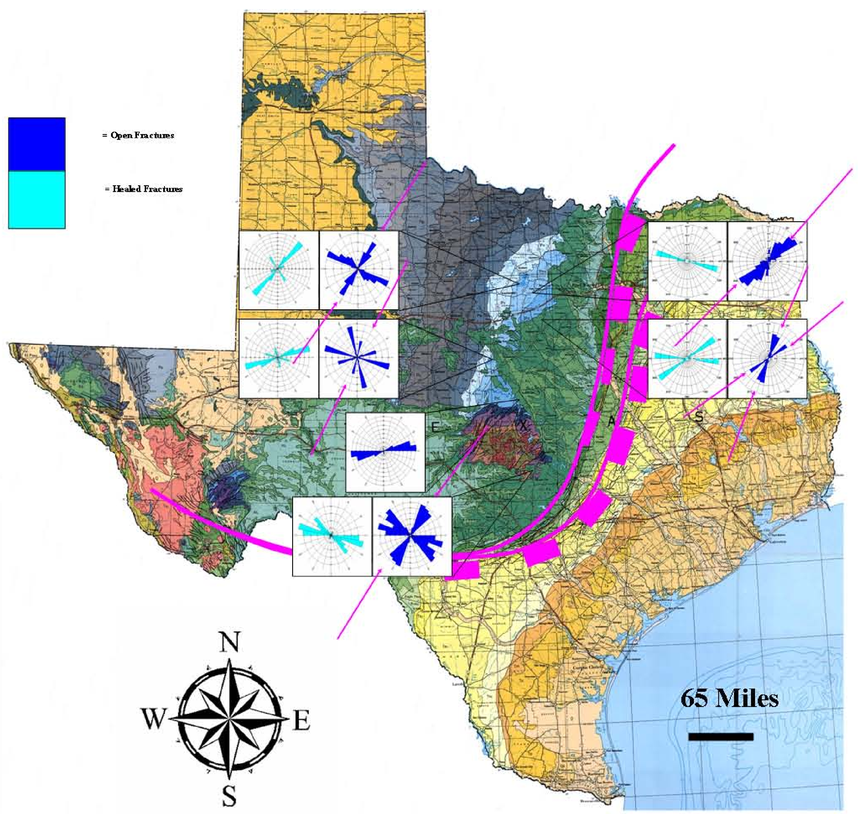

VITA

Matthew Russell Garrison

Candidate for the Degree of

Master of Science

Thesis: SURFACE TO SUBSURFACE CORRELATION OF NATURAL FRACTURES IN PALEOZOIC ROCKS IN SELECTED AREAS OF CENTRAL AND NORTH-CENTRAL TEXAS

Major Field: Geology

Biographical:

Personal Data:

Born December 18, 1981 in Metairie, LA
Parents: Robert and Loretta Garrison
Married to Ashley Lorene Garrison

Education:

B.S. Texas A & M University, College Station, TX in May 2005
M.S. Oklahoma State University, Stillwater, OK in May 2007

Experience:

Summer Internships:

1. Summer '03: EOG Resources, Tyler Division
2. Summer '05: EOG Resources, Fort Worth Division
3. Summer '06: EOG Resources, Fort Worth Division

Name: Matthew R. Garrison Date of Degree: May, 2007

Institution: Oklahoma State University Location: Stillwater, Oklahoma

Title of Study: SURFACE TO SUBSURFACE CORRELATION OF NATURAL FRACTURES IN PALEOZOIC ROCKS IN SELECTED AREAS OF CENTRAL AND NORTH-CENTRAL TEXAS

Pages in Study 168 Candidate for the Degree of Master of Science

Major Field: Geology

Scope and Method of Study:

This study is aimed at gaining a better understanding of the complexity of natural fracture systems within the orogenic foreland of the Ouachita thrust belt. To do this, four localities, in central and north Texas, within the Ordovician-Pennsylvanian limestone units were chosen to study the fractures in the surface using classic field methods. They are (1) Possum Kingdom Lake; (2) Lake Brownwood Spillway; (3) Bend River; (4) Archer Ranch.

Findings and Conclusions:

Two prominent sets were found: (1) an east-west set attributed to Ouachita tectonism, and (2) a northeast-southwest set attributed to the opening of the Gulf of Mexico. Fracture orientations obtained from outcrop were compared to subsurface data from Formation Micro Imaging logs. Orientations from both fracture sets were similar, and therefore correlative in regards to their origin and cross-cutting relationships. This correlation will help in understanding the complexity and regional extent of fracture systems formed by both compressive and extensional forces.

ADVISER'S APPROVAL: Dr. Ibrahim Cemen